ACCSCIENCE PUBLISHING

An International Journal of Optimization and Control: Theories & Applications
ISSN: 2146-0957 eISSN: 2146-5703
Vol.16, No.6, pp.2288-2327 (2026)
https://doi.org/10.36922/IJOCTA026290159

IJOCTA

RESEARCH ARTICLE

Threshold dynamics and optimal vaccination in a fractional stochastic SEIR model with delay

Jameelah Alotaibi*

Department of Mathematics, College of Science At Zulfi, Majmaah University, Al Majmaah, Saudi Arabia
js.alotaibi@mu.edu.sa

ARTICLE INFO

Article History:
Received: July 13, 2026
Revised: August 27, 2026
Accepted: September 8, 2026
Published Online: November 11, 2026

Keywords:
Caputo fractional derivative
Stochastic SEIR model
Time delay
Basic reproduction number
Global stability
Almost-sure extinction
Optimal vaccination control

MSC 2020:
34A08, 92D30, 34K18, 49J15

ABSTRACT

This paper presents a Caputo fractional-order SEIR epidemic model of order $\alpha \in (\frac{1}{2}, 1]$ in which the latent period enters as a discrete delay in the incidence, environmental variability acts as multiplicative white noise on the infectious class, and a time-dependent vaccination effort is applied to the susceptible class. The model is written in its stochastic Volterra form, and the restriction $\alpha > \frac{1}{2}$, under which the stochastic convolution against the singular kernel has finite variance, is shown to govern both the well-posedness of the model and the mean-square convergence of its discretisation. Local existence and uniqueness are obtained by a contraction argument; the solution is then continued globally by the method of steps, which exploits the fact that the delayed incidence is linear on each delay window, and the moments of the total population are controlled through a Mittag-Leffler resolvent representation, so that the demographic balance law holds in expectation. Positivity of the noisy compartment is proved for the deterministic model and for the classical order, and is adopted as an explicit hypothesis, supported by numerical evidence, for the fractional stochastic case. The basic reproduction number R_0 is derived from the next-generation matrix. When $R_0 < 1$, the disease-free equilibrium of the deterministic skeleton is globally asymptotically stable and the infected classes of the stochastic model vanish in the mean, for every delay and every noise intensity. When $R_0 > 1$, a unique endemic equilibrium exists, is globally asymptotically stable in the absence of delay and, by a modulus estimate on the characteristic quasi-polynomial, remains locally asymptotically stable for every delay, so that latency alone cannot destabilise the endemic state through a Hopf bifurcation. For the classical order, an explicit noise threshold depending on the delay is derived, beyond which the infection dies out almost surely at an exponential rate. An optimal vaccination problem is formulated, the existence of an optimal control is proved, and the optimal policy is characterised through a maximum principle whose adjoint system is a backward Volterra equation carrying a time-advanced term. A fractional predictor-corrector scheme with a fractional Euler-Maruyama step is described, its convergence orders are verified through error tables, and simulations quantify the influence of the fractional order, the delay, the noise intensity, the transmission rate and the vaccination policy on the course of the epidemic.

CC BY

1. Introduction

Mathematical models remain one of the most reliable instruments for understanding how infectious diseases propagate through a population and for weighing the interventions meant to contain them. Within the compartmental tradition, the susceptible-exposed-infectious-recovered (SEIR) structure is the natural description of diseases that carry a latent phase, during which an individual is infected but not yet infectious. Classical SEIR formulations, however, rest on three idealisations that are increasingly difficult to de-

*Corresponding Author

fend when the model is asked to reproduce real outbreaks: the dynamics are local in time and therefore memoryless, they are deterministic and so blind to the randomness of contact and environment, and they treat the transition between infection and infectiousness as instantaneous. Each of these simplifications has prompted a distinct line of generalisation, and the present work is concerned with combining all three in a single, rigorously analysed model that also accommodates a vaccination control.

The first refinement replaces the integer-order derivative by a fractional one, and the reasons for doing so deserve to be spelled out. The Caputo derivative of order $\alpha \in (0,1)$ weights the whole past of a state through the power-law kernel $(t-s)^{-\alpha}$, so that the rate of change at time t depends on the history of the epidemic rather than on its present state alone; the foundational treatments of Podlubny,[1] Kilbas, Srivastava and Trujillo[2] and Diethelm[3] develop the corresponding calculus. Three features of infectious-disease dynamics call for this kind of memory. Residence times in the exposed and infectious classes are not exponentially distributed, and a power-law kernel produces the heavy-tailed waiting times that are observed; immunity, behaviour and reporting adapt to the past course of an outbreak, which makes the transmission process hereditary; and the order α furnishes one additional, epidemiologically interpretable parameter with which incidence curves can be fitted without enlarging the compartmental structure. Diethelm[4] showed on dengue data that a fractional model reproduces an outbreak more faithfully than its integer-order counterpart, Almeida[5] analysed a fractional SEIR model with treatment, Rihan *et al.*[6] combined fractional memory with delay and nonlinear incidence, and Naik, Zu and Owolabi[7] carried out a global stability and optimal control analysis of a fractional HIV model. More recent contributions include fractional SEIR models with general incidence,[8,9] fractional SVEIR models with vaccination and optimal control,[10,11] and fractional SEIJR models with nonlinear transmission.[12] Fractional-order dynamics have also been developed for systems far from epidemiology; for delayed fractional-order complex-valued neural networks, Yazhini, Samidurai and Shang[13] established global Mittag-Leffler synchronisation under event-triggered control by means of fractional Lyapunov-Krasovskii functionals and Razumikhin-type arguments, with an application to image encryption. The analytical toolkit of that work, Mittag-Leffler stability, Lyapunov functionals and the location of characteristic roots, overlaps with the one used here, but the epidemic setting differs in three respects that shape the analysis below: the state lives in a positive cone whose dynamics are organised by a threshold quantity rather than by a synchronisation manifold, the delay enters a bilinear incidence term rather than a linear coupling, and the noise is multiplicative on a single compartment, so that population conservation can only hold in expectation.

The second refinement injects randomness. Real epidemics unfold in fluctuating environments, and the demographic and environmental stochasticity that the deterministic theory ignores can change the qualitative outcome entirely, most strikingly by extinguishing an infection that would otherwise persist. The probabilistic foundations are by now classical;[14,15] the stochastic SIS model of Gray *et al.*[16] and the stochastic SEIR model of Liu *et al.*[17] are representative of a large literature on persistence and extinction thresholds for white-noise perturbations of epidemic systems. The synthesis of fractional memory with stochastic forcing is more delicate and more recent. Existence theory for Caputo fractional stochastic differential equations was developed by Sakthivel, Revathi and Ren,[18] a variation of constants formula was obtained by Anh, Doan and Huong,[19] asymptotic separation of solutions was studied in,[20] the Euler-Maruyama scheme was analysed by Doan *et al.*,[21] and well-posedness and numerical schemes for the delayed case were treated in.[22,23] On the modelling side, fractal-fractional epidemic models with Lévy noise and vaccination,[24] fractional stochastic multi-compartment models on switching networks[25] and existence theory for stochastic fractional SEIR systems[26] have begun to chart this territory, while exposing the analytical subtleties that arise when a singular memory kernel meets a Brownian driver.

The third refinement is the explicit incorporation of time delay. Because the latent period has positive duration, the force of infection acting today reflects the infectious population of some earlier time, which is most economically modelled by a discrete delay in the transmission term. The qualitative theory of delay differential equations is well developed,[27–29] and its fractional extension rests on the stability criterion of Matignon[30] and its delayed version due to Deng, Li and Lü.[31] A recurring theme in this literature is that delay can destabilise an equilibrium and give rise to sustained oscillations through a Hopf bifurcation, a phenomenon documented for SEIRS models with two delays by Cooke and van den Driessche,[32] for fractional models with nonlinear incidence,[6] for delayed fractional neural networks,[33] for a fractional delayed model with waning immunity and

control,[34] and for a tuberculosis model with distributed latency kernels and vaccination, where the latency delay crossing a critical value produces periodic solutions.[35] Whether such delay-induced oscillations occur in a given model is, however, a structural question that must be settled case by case rather than assumed.

Alongside these structural extensions runs the practical question of control. Vaccination is the most direct lever on the susceptible pool, and optimal-control formulations of fractional and stochastic epidemic models have been used to design intervention schedules that balance the burden of infection against the cost of the intervention.[7,10,12,36,37] The deterministic fractional maximum principle goes back to Agrawal[38] and was extended to delayed arguments by Jarad, Abdeljawad and Baleanu;[39] the stochastic maximum principle of Peng[40] and Yong and Zhou[41] was extended to delayed diffusions by Chen and Wu[42] and by Øksendal, Sulem and Zhang,[43] where time-advanced backward equations appear, and to controlled stochastic Volterra equations through the backward stochastic Volterra integral equations of Yong,[44,45] the Malliavin approach of Agram and Øksendal,[46] the linear-quadratic theory of Wang,[47] and the maximum principles of Hamaguchi for Volterra equations with delay[48] and with singular kernels.[49] The analysis of any of these models ultimately relies on accurate numerical integration of fractional systems, for which the predictor-corrector method of Diethelm, Ford and Freed,[50,51] its delayed variant[52] and the monograph of Li and Zeng[53] provide the standard tools.

Despite this rich and active literature, the four ingredients above, fractional memory, multiplicative noise, a transmission delay and a vaccination control, have rarely been treated together within one model and with the same analytical care. **Table 1** places the present work among the studies closest to it. Several recurring gaps stand out. First, the well-posedness of a Caputo system driven by Brownian motion is frequently asserted rather than established; the stochastic convolution against the singular kernel $(t-s)^{\alpha-1}$ has finite variance only when $\alpha > \frac{1}{2}$, a threshold that conditions the entire theory and is often left implicit. Second, when the noise is placed in a single compartment the total population becomes a random process, so the almost-sure boundedness routinely claimed for the deterministic skeleton does not hold and must be replaced by a statement in the mean; the same placement raises the question of whether the positive cone remains invariant, which is settled here for the deterministic and for the classical stochastic case and is examined numerically for the fractional stochastic case. Third, delay-induced Hopf analyses are sometimes carried out at an equilibrium where a bifurcation cannot in fact occur, and extinction thresholds are sometimes derived from heuristic bounds. Fourth, necessary conditions for optimal control are often written down formally without indicating which maximum principle supports them, although the presence of memory and delay changes the adjoint structure. The present paper is motivated by the wish to close these gaps within a single coherent framework.

The model studied here is a Caputo fractional-order SEIR system of order $\alpha \in (\frac{1}{2}, 1]$ in which the latent period enters as a discrete delay τ in the incidence, environmental fluctuation enters as a multiplicative noise on the infectious compartment, and a time-dependent vaccination control acts on the susceptibles. The contributions are the following.

- The model is cast in its stochastic Volterra form and the condition $\alpha > \frac{1}{2}$ is identified as the one under which the stochastic condition, and hence the model, is well-posed. Local existence and uniqueness are proved by a contraction argument, and the solution is continued globally by the method of steps, which exploits the fact that the delayed incidence is linear on each delay window; a Mittag-Leffler resolvent representation of the total population gives the demographic balance law in expectation together with second-moment bounds. Positivity of the noisy compartment is proved for the deterministic model and for the classical order and is stated as an explicit hypothesis, examined numerically, for the fractional stochastic case, under which the stochastic results for $\alpha < 1$ are formulated.
- The basic reproduction number R_0 is derived through the next-generation matrix. The notions of stability in the mean, in mean square and almost surely are distinguished, and it is proved that for $R_0 < 1$ the infected classes vanish in the mean for every delay, every order and every noise intensity (under the positivity hypothesis when $\alpha < 1$), which for the deterministic skeleton is the global asymptotic stability of the disease-free equilibrium. For $R_0 > 1$ a unique endemic equilibrium exists and is globally asymptotically stable in the absence of delay.
- By a modulus estimate on the characteristic quasi-polynomial at the endemic equilibrium it

is shown that this equilibrium is locally asymptotically stable for every delay $\tau \geq 0$; the frequency equation that would signal a Hopf bifurcation has no positive root, so no delay-induced Hopf bifurcation occurs in this structure.

- For the classical order an explicit threshold on the noise intensity, depending on the delay, is derived beyond which the infection becomes extinct almost surely at an exponential rate, and the scope of this result relative to the fractional case is stated precisely.
- An optimal vaccination problem is formulated, existence of an optimal control is proved, and the optimal policy is characterised by a maximum principle whose adjoint system is a backward Volterra equation with a time-advanced term; the sources of each step of the derivation are identified.
- A fractional predictor-corrector scheme with a fractional Euler-Maruyama step is described, its convergence orders are verified through error tables against closed-form and reference solutions, and an extensive set of simulations quantifies the influence of the order, the delay, the noise, the transmission rate and the vaccination policy.

Table 1. Related SEIR-type models and the features they establish. The abbreviations F, D, N and C stand for fractional memory, transmission delay, white noise and control.

Reference	F	D	N	C	Main results
Almeida[5]	✓				stability of a fractional SEIR model with treatment
Rihan *et al.*[6]	✓	✓			stability and Hopf bifurcation, nonlinear incidence
Gacem *et al.*[8]	✓	✓			global stability, general incidence
Majee *et al.*[34]	✓	✓		✓	Hopf bifurcation and optimal control, waning immunity
Suganya *et al.*[10]	✓			✓	fractional SVEIR model with optimal control
Liu *et al.*[17]			✓		stationary distribution and extinction, classical order
Sabbar *et al.*[24]	✓		✓		fractal-fractional model with Lévy jumps and vaccination
Ren *et al.*[25]	✓		✓		fractional stochastic SPEIQR model on a switching network
Tamimi *et al.*[26]	✓		✓		existence theory for a stochastic fractional SEIR system
Huong and The[22]	✓	✓	✓		well-posedness of Caputo stochastic delay equations
Doan *et al.*[21]	✓		✓		Euler-Maruyama scheme for Caputo stochastic equations
This work	✓	✓	✓	✓	well-posedness with $\alpha > \frac{1}{2}$, balance law in the mean, delay-independent endemic stability, delay-dependent noise threshold, maximum principle, verified convergence orders

The fractional stochastic framework adopted here has advantages and limitations that should be stated at the outset. Its advantages are the ability to represent memory and heavy-tailed residence times with a single additional parameter, the possibility of treating noise, delay and control within one set of equations, and the fact that the threshold quantities it produces, R_0 and the noise threshold, are explicit in the parameters. Its limitations are equally concrete: the fractional order changes the physical dimension of the rate constants and calls for a convention to reconcile them; the solution operator of a Caputo system is not a semigroup, so invariance arguments that are routine for ordinary differential equations require care; the Itô formula has no elementary counterpart for the Caputo stochastic convolution, which restricts the pathwise stochastic analysis to the classical order; the positivity of a noisy compartment is not implied by the boundary behaviour of the coefficients when memory is present; and the memory integral makes the cost of a simulation quadratic in the number of time steps. These points are addressed in the corresponding sections.

The paper is organised as follows. Section 2 formulates the model, discusses the placement of the noise and the dimensional convention, and collects the fractional-calculus tools that are used later. Section 3 establishes local and global well-posedness, invariance of the positive cone and moment bounds. Section 4 derives R_0, defines the notions of stability for the stochastic model and proves the threshold result for the disease-free equilibrium. Section 5 treats the endemic equilibrium, its global stability without delay and the noise-induced extinction threshold. Section 6 proves that the endemic equilibrium is stable

for every delay. Section 7 is devoted to the optimal vaccination problem. Section 8 describes the numerical scheme, verifies its convergence and reports the simulations, whose findings are interpreted in Section 9. Section 10 concludes.

2. Model formulation and preliminaries

2.1. Model formulation

Throughout, the host population is partitioned into four mutually exclusive compartments, and $S(t)$, $E(t)$, $I(t)$ and $R(t)$ denote, respectively, the numbers of susceptible, exposed (latently infected), infectious and recovered individuals at time t. Two features distinguish the present model from the classical SEIR template. First, the disease memory is encoded through a Caputo fractional derivative of order α, which captures the non-local, history-dependent nature of contagion and immune response. Second, the erratic environment in which an epidemic unfolds is represented by a multiplicative white-noise perturbation acting on the infectious class, while a time-dependent vaccination effort $u(t)$ is applied to the susceptible class. The flow diagram in **Figure 1** summarises the structure.

Collecting these ingredients, the dynamics are governed by the Caputo fractional stochastic delay differential system

$$\begin{cases} {}^{C}D_t^{\alpha} S(t) = \Lambda - \beta S(t)\, I(t-\tau) - \mu S(t) - u(t) S(t), \\ {}^{C}D_t^{\alpha} E(t) = \beta S(t)\, I(t-\tau) - (\kappa+\mu) E(t), \\ {}^{C}D_t^{\alpha} I(t) = \kappa E(t) - (\gamma+\mu) I(t) + \sigma I(t)\, \dot{W}(t), \\ {}^{C}D_t^{\alpha} R(t) = \gamma I(t) - \mu R(t) + u(t) S(t), \end{cases} \tag{1}$$

where ${}^{C}D_t^{\alpha}$ is the Caputo fractional derivative of order $\alpha \in (\frac{1}{2}, 1]$ (the lower bound $\alpha > \frac{1}{2}$ being dictated by the square-integrability of the stochastic convolution, see **Remark 4**), and $W(t)$ is a one-dimensional standard Brownian motion defined on a filtered probability space $(\widehat{\Omega}, \mathcal{F}, \{\mathcal{F}_t\}_{t\geq 0}, \mathbb{P})$ whose filtration satisfies the usual conditions. The notation $\sigma I \dot{W}$ is understood, as customary, in the Itô sense through the integral formulation of Section 3.

System (1) is supplemented with the history

$$\begin{aligned} &\big(S(\theta), E(\theta), I(\theta), R(\theta)\big) = \\ &\big(\phi_1(\theta), \phi_2(\theta), \phi_3(\theta), \phi_4(\theta)\big), \\ &\theta \in [-\tau, 0], \end{aligned} \tag{2}$$

where each $\phi_i \in C\big([-\tau, 0]; \mathbb{R}_+\big)$ is continuous and nonnegative.

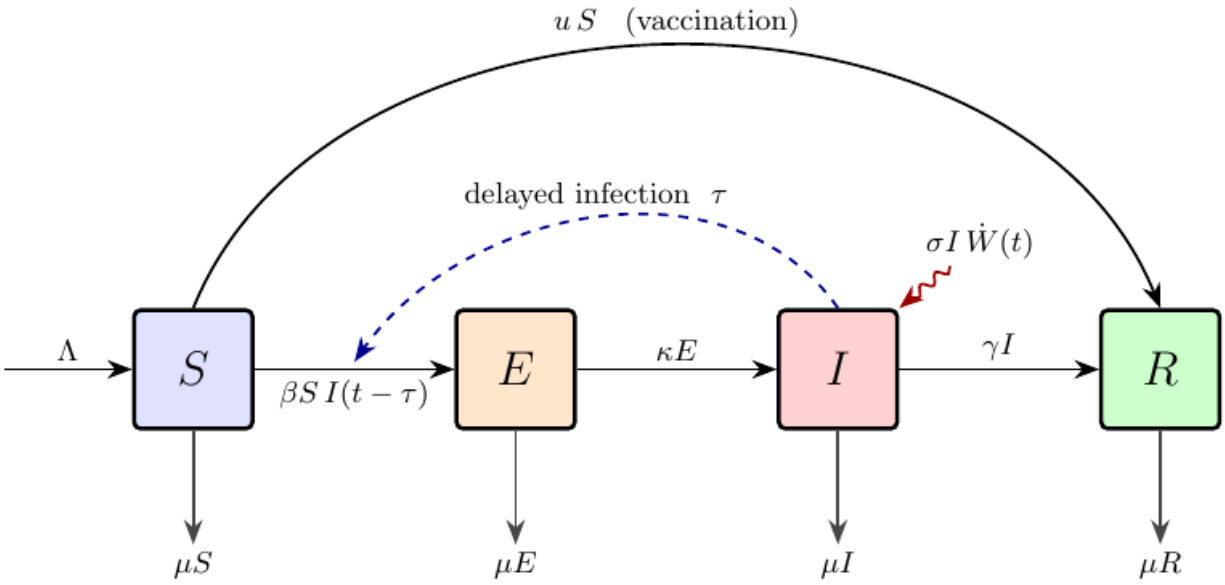


Figure 1. Compartmental flow diagram of the fractional stochastic delayed SEIR model with vaccination. Solid arrows are deterministic flows; the dashed arrow marks the delayed transmission coupling $\beta S\, I(t-\tau)$, and the wavy arrow the environmental perturbation $\sigma I\, \dot{W}(t)$ acting on the infectious class.

The biological meaning of the parameters is as follows: $\Lambda > 0$ is the constant recruitment rate, $\beta > 0$ the transmission coefficient, $\mu > 0$ the natural mortality rate, $\kappa > 0$ the rate at which exposed individuals become infectious, $\gamma > 0$ the recovery rate, $\tau > 0$ the latent (incubation) delay, and $\sigma \geq 0$ the intensity of the environmental noise. The control $u(\cdot)$ is measurable with $0 \leq u(t) \leq 1$, the bounds corresponding to no vaccination and maximal immunisation effort, respectively.

Remark 1. *The perturbation $\sigma I\dot{W}$ corresponds to the proportional white-noise formulation $\sigma_i X_i \dot{W}_i$, applied to every compartment in,[17] restricted here to the infectious class alone. Three considerations motivate this choice. Infectious individuals are the ones most exposed to environmental variability: fluctuations in isolation, treatment capacity, care-seeking behaviour and case ascertainment change the size of the infectious pool directly, whereas the susceptible and recovered pools respond to them only indirectly. Concentrating the fluctuation in one compartment isolates its effect on transmission through a single parameter σ, so that the extinction threshold of* ***Theorem 8*** *is explicit. Finally, the placement keeps the susceptible equation free of noise, which is what makes the pathwise bound $S(t) \le \Lambda/\mu$ available and drives the extinction analysis. The price is that the total population $N = S + E + I + R$ is no longer conserved along sample paths: the noise represents an exchange of infectious individuals with the outside, such as importation and exportation of cases or misclassification, and Section 3 shows that the demographic balance then holds in expectation. If pathwise conservation is preferred, the fluctuation can instead be attached to the transmission coefficient, $\beta \mapsto \beta + \sigma\dot{W}$, as in;[16]* ***Remark 7*** *indicates how the results change under that alternative.*

Remark 2. *The Caputo derivative of order α has the physical dimension $(time)^{-\alpha}$, so* ***(1)*** *is dimensionally consistent only when every rate constant carries the same dimension. Two conventions reconcile the model with rates measured in $(time)^{-1}$: either each rate p in* ***(1)*** *is read as p^{α}, as proposed in,[4] or the fractional derivative is multiplied by an auxiliary constant of dimension $(time)^{1-\alpha}$. The first convention is adopted here, so that the parameter values of Section 8 are understood as already raised to the power α; the noise intensity then has dimension $(time)^{\frac{1}{2}-\alpha}$ and the control u, which multiplies S, has the dimension of a rate. The threshold quantities derived below, R_0 in* ***(16)*** *and the control reproduction number R_v of* ***Remark 8****, are ratios of products of rates and are dimensionless under either convention, and none of the qualitative results depends on the convention chosen.*

Remark 3. *For linear compartmental models with time-varying rates, Lie-algebraic techniques of Wei-Norman type produce closed-form solutions: Shang obtained analytical solutions in this way for a susceptible-infected-susceptible epidemic,[54] for a biological population model,[55] for an in-host viral infection model with time-inhomogeneous rates[56] and for an affinity-based information diffusion process on social networks.[57] The method requires the generator of the dynamics to belong to a finite-dimensional Lie algebra, which is the case for linear, or linearisable, systems. In* ***(1)*** *the bilinear incidence $\beta S\, I(t-\tau)$, the delayed argument, the non-local Caputo operator and the multiplicative noise place the system outside this class, and no closed-form solution should be expected. The linear components of the analysis below do admit explicit expressions: the total population and its mean are given by Mittag-Leffler formulas (****Lemma 7****), and the mean dynamics near the disease-free equilibrium reduce to a linear fractional delay system (Section 4). It is for such linear subsystems, particularly when the rates are allowed to vary in time, that a Lie-algebraic treatment would be the natural complement to the qualitative results obtained here.*

2.2. Preliminaries

We recall the fractional-calculus tools used below; for proofs and a systematic treatment we refer to the monographs of Podlubny,[1] Kilbas *et al.*[2] and Diethelm.[3] The probabilistic notions employed in the stochastic analysis, the Itô integral, the Itô isometry and the Burkholder-Davis-Gundy inequality, are standard and may be found in Mao,[15] while a focused introduction to stochastic epidemic modelling is given by Allen.[14]

Definition 1. *For $\alpha \in (0,1)$ and an absolutely continuous function f, the Caputo fractional derivative of order α is*

$$ {}^{C}D_t^{\alpha} f(t) = \frac{1}{\Gamma(1-\alpha)} \int_0^t \frac{f'(s)}{(t-s)^{\alpha}}\, ds, $$

with ${}^{C}D_t^{1} f = f'$ understood in the limit $\alpha \to 1$.

Definition 2. *For $\alpha > 0$, the (left) fractional integral of order α is*

$$ I_t^{\alpha} f(t) = \frac{1}{\Gamma(\alpha)} \int_0^t (t-s)^{\alpha-1} f(s)\, ds. $$

On a bounded interval $[0,T]$ the right fractional integral and the right Riemann-Liouville derivative, which govern the adjoint equations of Section 7, are

$$ I_{T-}^{\alpha} f(t) = \frac{1}{\Gamma(\alpha)} \int_t^T (s-t)^{\alpha-1} f(s)\, ds, $$

$$ {}_{t}D_T^{\alpha} f(t) = -\frac{d}{dt}\, I_{T-}^{1-\alpha} f(t). $$

The two-parameter Mittag-Leffler function $E_{\alpha,\beta}(z) = \sum_{k\ge 0} z^k/\Gamma(\alpha k + \beta)$, with the shorthand $E_{\alpha}(z) := E_{\alpha,1}(z)$, plays the role of the fractional exponential. For $\alpha \in (0,1]$ and $x \ge 0$

the functions $E_\alpha(-x)$ and $E_{\alpha,\alpha}(-x)$ are positive and nonincreasing in x, with $E_\alpha(-x) \in (0,1]$ and $E_{\alpha,\alpha}(-x) \le 1/\Gamma(\alpha)$.[2] Throughout, we write

$$k(t) := \frac{t^{\alpha-1}}{\Gamma(\alpha)}, \qquad k_c(t) := t^{\alpha-1}E_{\alpha,\alpha}(-c\,t^\alpha), \quad c \ge 0,\ t > 0, \tag{3}$$

for the memory kernel and for the Mittag-Leffler resolvent kernel; the latter satisfies the resolvent identity $k_c = k - c\,k * k_c$, where $*$ denotes convolution on $[0,\infty)$, together with

$$\int_0^t k_c(r)\,dr = \frac{1 - E_\alpha(-c\,t^\alpha)}{c} \le \frac{1}{c}, \qquad c > 0. \tag{4}$$

Lemma 1. *Let $v(t) \ge 0$ be continuous on $[0,T]$ and suppose*

$$v(t) \le a + b\int_0^t (t-s)^{\alpha-1} v(s)\,ds, \qquad t \in [0,T],$$

for some constants $a \ge 0$, $b \ge 0$ and $\alpha > 0$. Then

$$v(t) \le a\,E_\alpha\big(b\,\Gamma(\alpha)\,t^\alpha\big), \qquad t \in [0,T].$$

Lemma 2. *Let $x \in C([0,T];\mathbb{R})$ admit a continuous Caputo derivative of order $\alpha \in (0,1)$. If $x(t) \ge 0$ on $[0,t^*]$ and $x(t^*) = 0$ for some $t^* \in (0,T]$, then ${}^C\!D_t^\alpha x(t^*) \le 0$, with equality only if $x \equiv 0$ on $[0,t^*]$. Moreover, if ${}^C\!D_t^\alpha x(t) \le \Lambda - \mu x(t)$ with $x(0) = x_0$, then $x(t) \le x_0 E_\alpha(-\mu t^\alpha) + \frac{\Lambda}{\mu}\big(1 - E_\alpha(-\mu t^\alpha)\big)$.*

The first part follows from the generalised mean value theorem of Odibat and Shawagfeh:[58] integrating by parts in the definition of the Caputo derivative at t^* gives $\Gamma(1-\alpha)\,{}^C\!D_t^\alpha x(t^*) = -x(0)(t^*)^{-\alpha} - \alpha\int_0^{t^*} x(s)(t^*-s)^{-\alpha-1}ds \le 0$. The second part is the standard fractional comparison estimate obtained from **Lemma 1**. The next lemma treats linear Caputo equations with measurable coefficients, which is the form in which the equations of **(1)** appear once the delayed argument is regarded as known; it is the tool used in Section 3 for positivity and comparison.

Lemma 3. *Let $T > 0$, let $a : [0,T] \to [0,c]$ be measurable, let $f \in L^\infty(0,T)$ and $x_0 \in \mathbb{R}$. The Volterra equation*

$$x(t) = x_0 + \int_0^t k(t-s)\big(f(s) - a(s)x(s)\big)\,ds, \qquad t \in [0,T], \tag{5}$$

has a unique continuous solution, and this solution satisfies

$$x(t) = x_0 E_\alpha(-c\,t^\alpha) + \int_0^t k_c(t-s)\big(f(s) + (c - a(s))x(s)\big)\,ds. \tag{6}$$

Consequently:

(i) *if $x_0 \ge 0$ and $f \ge 0$, then $x \ge 0$ on $[0,T]$;*

(ii) *if in addition $a \ge \mu > 0$ and $f \le \Lambda$, then $x(t) \le x_0 E_\alpha(-\mu t^\alpha) + \frac{\Lambda}{\mu}\big(1 - E_\alpha(-\mu t^\alpha)\big) \le \max\{x_0, \Lambda/\mu\}$;*

(iii) *if $a \equiv \mu > 0$ and $f(t) \to 0$ as $t \to \infty$ (with $T = \infty$), then $x(t) \to 0$.*

Proof. Writing **(5)** as $x = h - c\,k * x$ with $h := x_0 + k * f + k * ((c-a)x)$ and applying the resolvent identity gives $x = h - c\,k_c * h$, which is **(6)** after using **(4)** for the constant term. The map $y \mapsto k_c * ((c-a)y)$ is a contraction on $C[0,T]$ with constant $c\int_0^T k_c \le 1 - E_\alpha(-cT^\alpha) < 1$, so **(6)**, and hence **(5)**, has a unique continuous solution, obtained as the limit of the Picard iterates $x_{n+1} = x_0 E_\alpha(-c\,t^\alpha) + k_c * (f + (c-a)x_n)$ started from $x_{-1} \equiv 0$. Since $k_c > 0$, $c - a \ge 0$ and $f \ge 0$, every iterate is nonnegative when $x_0 \ge 0$, which proves (i). For (ii) let w be the solution of **(5)** with $a \equiv \mu$ and $f \equiv \Lambda$, which is the Mittag-Leffler expression displayed; the difference $d = w - x$ solves $d = k * \big((\Lambda - f) + (a-\mu)x - \mu d\big)$, so by **(6)** with $c = \mu$, $d = k_\mu * \big((\Lambda - f) + (a-\mu)x\big) \ge 0$ because $x \ge 0$ by (i). For (iii), **(6)** with $c = \mu$ reads $x(t) = x_0 E_\alpha(-\mu t^\alpha) + \int_0^t k_\mu(t-s)f(s)ds$; the first term tends to zero, and splitting the integral at $t/2$ and using $k_\mu \in L^1(0,\infty)$ together with $f(s) \to 0$ shows that the second term tends to zero as well. □

The same argument applies componentwise to linear systems with a Metzler matrix, which is the setting of the comparison arguments of Section 4.

Lemma 4. *Let $A \in \mathbb{R}^{n\times n}$ be a Metzler matrix (nonnegative off-diagonal entries), let $B \in \mathbb{R}^{n\times n}$ have nonnegative entries, let $r : [0,\infty) \to \mathbb{R}^n_+$ be locally bounded and measurable, and let $\psi \in C([-\tau,0];\mathbb{R}^n_+)$. Then the solution of*

$$x(t) = \psi(0) + \int_0^t k(t-s)\big(Ax(s) + Bx(s-\tau) + r(s)\big)\,ds, \qquad x|_{[-\tau,0]} = \psi,$$

satisfies $x(t) \ge 0$ componentwise for all $t \ge 0$.

Proof. Choose $c \ge \max_i(-A_{ii})$ so that $A + cI$ has nonnegative entries. Applying the resolvent identity componentwise, exactly as in the proof of **Lemma 3**, gives $x(t) = \psi(0)E_\alpha(-c\,t^\alpha) + \int_0^t k_c(t-s)\big((A+cI)x(s) + Bx(s-\tau) + r(s)\big)ds$. The Picard iterates of this equation started from the nonnegative history are nonnegative and nondecreasing in n; they are bounded on every bounded interval by **Lemma 1**, hence converge to the unique solution, which is therefore nonnegative. The result is a special case of the theory of positive fractional systems with delays in.[59] □

Finally we record the stability criterion for linear fractional systems with a delay, due to Deng, Li and Lü,[31] which for $\tau = 0$ reduces to the sector criterion of Matignon.[30]

Lemma 5. *Consider* ${}^{C}D_t^{\alpha} x(t) = Ax(t) + Bx(t-\tau)$ *with* $\alpha \in (0,1]$ *and* $A, B \in \mathbb{R}^{n\times n}$. *If every root* λ *of the characteristic equation* $\det\big(\lambda^{\alpha} I - A - Be^{-\lambda\tau}\big) = 0$ *(principal branch of* λ^{α}*) satisfies* $\operatorname{Re}\lambda < 0$, *then the zero solution is asymptotically stable. For* $\tau = 0$ *the condition is equivalent to* $|\arg\nu| > \alpha\pi/2$ *for every eigenvalue* ν *of* A.

3. Well-posedness: existence, uniqueness, positivity and boundedness

3.1. Equivalent integral formulation

Because Brownian sample paths are nowhere differentiable, the noisy equation in **(1)** is given precise meaning through its Volterra integral form, which is the object on which all subsequent analysis is carried out. Writing $X(t) = (S(t), E(t), I(t), R(t))^{\top}$ and applying the fractional integral operator to **(1)** yields, for $t \geq 0$,

$$S(t) = S(0) + \frac{1}{\Gamma(\alpha)} \int_0^t (t-s)^{\alpha-1} \big(\Lambda - \beta S(s) I(s-\tau) - \mu S(s) - u(s) S(s)\big)\, ds, \tag{7}$$

$$E(t) = E(0) + \frac{1}{\Gamma(\alpha)} \int_0^t (t-s)^{\alpha-1} \big(\beta S(s) I(s-\tau) - (\kappa+\mu) E(s)\big)\, ds, \tag{8}$$

$$I(t) = I(0) + \frac{1}{\Gamma(\alpha)} \int_0^t (t-s)^{\alpha-1} \big(\kappa E(s) - (\gamma+\mu) I(s)\big)\, ds + \frac{\sigma}{\Gamma(\alpha)} \int_0^t (t-s)^{\alpha-1} I(s)\, dW(s), \tag{9}$$

$$R(t) = R(0) + \frac{1}{\Gamma(\alpha)} \int_0^t (t-s)^{\alpha-1} \big(\gamma I(s) - \mu R(s) + u(s) S(s)\big)\, ds, \tag{10}$$

together with $X(\theta) = \Phi(\theta) := (\phi_1, \phi_2, \phi_3, \phi_4)^{\top}(\theta)$ on $[-\tau, 0]$. The last integral in **(9)** is an Itô integral against a singular kernel.

Remark 4. *The restriction* $\alpha > \frac{1}{2}$ *is not cosmetic. By the Itô isometry, the variance of the stochastic convolution in* ***(9)*** *is controlled by* $\int_0^t (t-s)^{2\alpha-2}\, \mathbb{E}\, I(s)^2\, ds$, *and the kernel* $(t-s)^{2\alpha-2}$ *is integrable at* $s = t$ *if and only if* $2\alpha - 2 > -1$, *that is,* $\alpha > \frac{1}{2}$. *For* $\alpha \leq \frac{1}{2}$ *the noisy compartment ceases to have finite second moment, and the model is ill-posed in* L^2. *The deterministic subsystem (*$\sigma = 0$*) remains well-posed on the whole range* $\alpha \in (0, 1]$.

3.2. Standing assumptions

(A1) $\Lambda, \beta, \mu, \kappa, \gamma > 0$, $\sigma \geq 0$ and $\tau > 0$.
(A2) $\alpha \in (\frac{1}{2}, 1]$.
(A3) $u : [0, \infty) \to [0, 1]$ is Lebesgue measurable.
(A4) $\phi_i \in C([-\tau, 0]; \mathbb{R}_+)$, $i = 1, \ldots, 4$, is a deterministic history.

We work in the Banach space

$$\mathcal{H}_T := \Big\{ X : [-\tau, T] \to \mathbb{R}^4 \ \{\mathcal{F}_t\}\text{-adapted},$$

$$\mathbb{P}\text{-a.s. continuous},\ X|_{[-\tau,0]} = \Phi,\ \|X\|_{\mathcal{H}_T} < \infty \Big\},$$

endowed with the norm $\|X\|_{\mathcal{H}_T}^2 := \sup_{-\tau \leq t \leq T} \mathbb{E}\, |X(t)|^2$. The biologically relevant state space is the closed cone

$$\Omega := \Big\{ (S, E, I, R) \in \mathbb{R}_+^4 :\ S + E + I + R \leq \tfrac{\Lambda}{\mu} \Big\}.$$

The positivity of the noisy compartment plays a special role. It is proved below for the deterministic model and for the classical order $\alpha = 1$; for $\alpha \in (\frac{1}{2}, 1)$ with $\sigma > 0$ it is adopted as a hypothesis, whose status is discussed in **Remark 6**.

(H) The infectious class of the solution satisfies $I(t) \geq 0$ for all $t \geq 0$ almost surely.

Every statement of this paper concerning the stochastic model with $\alpha \in (\frac{1}{2}, 1)$ is understood under (H); when $\sigma = 0$ or $\alpha = 1$, (H) is a consequence of (A1)-(A4) by **Theorem 2**, and no additional hypothesis is involved.

3.3. Local existence and uniqueness

Theorem 1. *Under* (A1)-(A4) *there exists* $T > 0$ *such that the system* ***(7)-(10)*** *possesses a unique adapted, a.s. continuous solution* $X \in \mathcal{H}_T$.

Proof. Denote by $b(t, X)$ the drift vector field and by $g(X) = (0, 0, \sigma I, 0)^{\top}$ the diffusion vector in **(1)**. On any ball $B_R = \{x \in \mathbb{R}^4 : |x| \leq R\}$ the only nonlinearity, the bilinear term $\beta S\, I(t-\tau)$, is Lipschitz; hence there is $L_R > 0$ with

$$|b(t,x) - b(t,y)| \leq L_R\, |x - y|,$$
$$|g(x) - g(y)| = \sigma |x_3 - y_3| \leq \sigma |x - y|, \qquad x, y \in B_R,$$

uniformly in t and in the (bounded) delayed argument, because the delayed component $I(s-\tau)$ for $s \leq \tau$ is the prescribed history ϕ_3 and for $s > \tau$ is bounded by the same ball. Replace b and g

by their compositions with the radial projection π_R onto B_R; the truncated coefficients are globally Lipschitz with the constants L_R and σ, the argument below produces a unique solution of the truncated system, and since the truncated and the original coefficients coincide on B_R this solution solves the original system up to its first exit time from B_R. Letting $R \to \infty$ gives the maximal local solution; the global continuation is the object of **Theorem 2**, whose construction does not rely on the present argument.

Define the operator $\mathcal{T} : \mathcal{H}_T \to \mathcal{H}_T$ by setting $(\mathcal{T}X)(t) = \Phi(t)$ for $t \in [-\tau, 0]$ and, for $t \in [0, T]$, by the right-hand sides of **(7)**-**(10)**. Let X, Y lie in the closed ball of $\mathcal{H}_T$ of radius R around the constant history. Using the elementary inequality $|a+b|^2 \le 2|a|^2 + 2|b|^2$ we split the drift and diffusion contributions.

By the Cauchy-Schwarz inequality applied to the kernel,

$$\begin{aligned}&\Big|\tfrac{1}{\Gamma(\alpha)}\int_0^t (t-s)^{\alpha-1}\big(b(s,X)-b(s,Y)\big)ds\Big|^2\\ &\le \frac{1}{\Gamma(\alpha)^2}\Big(\int_0^t (t-s)^{\alpha-1}ds\Big)\\ &\qquad\times\int_0^t (t-s)^{\alpha-1}\big|b(s,X)-b(s,Y)\big|^2 ds.\end{aligned}$$

Since $\int_0^t (t-s)^{\alpha-1}ds = t^\alpha/\alpha$, taking expectations and using the Lipschitz bound gives, for $0 \le t \le T$,

$$\begin{aligned}\mathbb{E}\Big|\cdots\Big|^2 &\le \frac{L_R^2}{\Gamma(\alpha)^2}\,\frac{t^\alpha}{\alpha}\int_0^t (t-s)^{\alpha-1}\|X-Y\|_{\mathcal{H}_T}^2\,ds\\ &\le \frac{L_R^2\,T^{2\alpha}}{\Gamma(\alpha+1)^2}\,\|X-Y\|_{\mathcal{H}_T}^2.\end{aligned}$$

Only **(9)** carries noise. By the Itô isometry and the Lipschitz property of g,

$$\begin{aligned}&\mathbb{E}\Big|\tfrac{\sigma}{\Gamma(\alpha)}\int_0^t (t-s)^{\alpha-1}\big(I_X(s)-I_Y(s)\big)dW(s)\Big|^2\\ &= \frac{\sigma^2}{\Gamma(\alpha)^2}\int_0^t (t-s)^{2\alpha-2}\,\mathbb{E}\big|I_X(s)-I_Y(s)\big|^2 ds.\end{aligned}$$

Here the hypothesis $\alpha > \frac{1}{2}$ enters decisively, for $\int_0^t (t-s)^{2\alpha-2}ds = t^{2\alpha-1}/(2\alpha-1) < \infty$, whence

$$\mathbb{E}\Big|\cdots\Big|^2 \le \frac{\sigma^2\,T^{2\alpha-1}}{\Gamma(\alpha)^2\,(2\alpha-1)}\,\|X-Y\|_{\mathcal{H}_T}^2.$$

Combining the two bounds,

$$\|\mathcal{T}X-\mathcal{T}Y\|_{\mathcal{H}_T}^2 \le \Theta(T)\,\|X-Y\|_{\mathcal{H}_T}^2,$$

$$\Theta(T) := 2\frac{L_R^2\,T^{2\alpha}}{\Gamma(\alpha+1)^2} + 2\frac{\sigma^2\,T^{2\alpha-1}}{\Gamma(\alpha)^2(2\alpha-1)}.$$

Since $2\alpha > 1$, we have $\Theta(T) \to 0$ as $T \downarrow 0$; choosing T small enough that $\Theta(T) < 1$ (and that $\mathcal{T}$ maps the ball into itself, which follows from the same estimates with Y replaced by the constant history) makes $\mathcal{T}$ a contraction. The Banach fixed-point theorem produces a unique $X \in \mathcal{H}_T$ with $\mathcal{T}X = X$, which is the desired solution; a standard Kolmogorov argument based on the Burkholder-Davis-Gundy inequality yields the a.s. continuous modification. □

The local result gives no information on how far the solution can be continued. The following lemma shows that the linear stochastic equation satisfied by the infectious class, once the exposed class is regarded as a known process, is well-posed on every bounded interval; it is the stochastic counterpart of **Lemma 3**.

Lemma 6. *Let $T > 0$, $a \ge 0$, $\sigma \ge 0$, $\alpha \in (\frac{1}{2}, 1]$, let $I_0 \ge 0$ be deterministic and let f be an adapted, a.s. continuous process with $\sup_{t\le T}\mathbb{E}f(t)^2 < \infty$. Then the equation*

$$\begin{aligned}I(t) = I_0 + \int_0^t k(t-s)\big(f(s) - aI(s)\big)ds +\\ \sigma\int_0^t k(t-s)I(s)\,dW(s), \qquad t \in [0,T],\end{aligned} \tag{11}$$

has a unique adapted, a.s. continuous solution with $\sup_{t\le T}\mathbb{E}I(t)^2 < \infty$. If $\alpha = 1$ and $f \ge 0$, the solution is given by

$$\begin{aligned}I(t) &= \Xi(t)\Big(I_0 + \int_0^t \Xi(s)^{-1}f(s)\,ds\Big),\\ \Xi(t) &:= \exp\Big(\sigma W(t) - \big(a + \tfrac{\sigma^2}{2}\big)t\Big),\end{aligned} \tag{12}$$

*and is therefore nonnegative; if $\sigma = 0$ and $f \ge 0$, it is nonnegative by **Lemma 3**.*

Proof. For $\lambda > 0$ consider the norm $\|Z\|_\lambda^2 := \sup_{t\le T} e^{-\lambda t}\mathbb{E}Z(t)^2$ on adapted processes and the map $\mathcal{S}$ defined by the right-hand side of **(11)**. For two processes Z_1, Z_2 with difference Z, the weighted Cauchy-Schwarz inequality gives

$$\begin{aligned}e^{-\lambda t}\,\mathbb{E}\Big|\int_0^t k(t-s)\,a\,Z(s)\,ds\Big|^2 &\le a^2\Big(\int_0^t k(r)e^{-\lambda r}dr\Big)\\ &\Big(\int_0^t k(r)\,dr\Big)\|Z\|_\lambda^2 \le \frac{a^2T^\alpha\lambda^{-\alpha}}{\Gamma(\alpha+1)}\,\|Z\|_\lambda^2,\end{aligned}$$

and the Itô isometry gives

$$\begin{aligned}e^{-\lambda t}\,\mathbb{E}\Big|\sigma\int_0^t k(t-s)Z(s)\,dW(s)\Big|^2 \le\\ \sigma^2\Big(\int_0^\infty k(r)^2e^{-\lambda r}dr\Big)\|Z\|_\lambda^2 = \frac{\sigma^2\,\Gamma(2\alpha-1)\,\lambda^{1-2\alpha}}{\Gamma(\alpha)^2}\,\|Z\|_\lambda^2,\end{aligned}$$

where the last integral is finite precisely because $\alpha > \frac{1}{2}$. Both constants tend to zero as $\lambda \to \infty$, so $\mathcal{S}$ is a contraction on the Banach space of adapted processes with finite $\|\cdot\|_\lambda$ for λ large, which gives existence and uniqueness with $\sup_{t\le T}\mathbb{E}I(t)^2 < \infty$; a.s. continuity follows as in **Theorem 1**. For $\alpha = 1$, **(11)** is the linear Itô

equation $dI = (f - aI)dt + \sigma I\, dW$, whose solution is **(12)** by the variation of constants formula [Chapter 3].[15] □

3.4. Global existence, uniqueness and invariance of the cone

Global existence is usually obtained by stopping the solution at the exit times of large balls and controlling a Lyapunov function. For a Volterra equation this route is delicate, because a stopped process no longer solves the stopped equation. The delayed structure of **(1)** offers a more direct path: on each window $[(j-1)\tau, j\tau]$ the delayed factor $I(t-\tau)$ is already known, so every equation of the system becomes linear in its own unknown, and the linear theory of **Lemmas 3** and **6** applies.

Theorem 2. *Assume* (A1)-(A4) *and let* $\bar{S} := \max\{\phi_1(0), \Lambda/\mu\}$.

(i) *If* $\sigma = 0$, *or if* $\alpha = 1$, *the system* ***(7)-(10)*** *has a unique adapted, a.s. continuous solution on* $[-\tau, \infty)$. *Its components are nonnegative for all* $t \geq 0$ *almost surely,* $S(t) \leq \bar{S}$ *for all* $t \geq 0$, *and* $\sup_{t \leq T} \mathbb{E}|X(t)|^2 < \infty$ *for every* $T > 0$. *In particular* (H) *holds.*

(ii) *If* $\alpha \in (\frac{1}{2}, 1)$ *and* $\sigma > 0$, *then under* (H) *the same conclusions hold: the system has a unique adapted, a.s. continuous solution on* $[-\tau, \infty)$, *all four components are nonnegative,* $S(t) \leq \bar{S}$ *for all* $t \geq 0$ *almost surely, and* $\sup_{t \leq T} \mathbb{E}|X(t)|^2 < \infty$ *for every* $T > 0$.

Proof. We construct the solution on $[0, j\tau]$ by induction on $j \geq 1$; the induction hypothesis is that a unique adapted continuous solution exists on $[-\tau, (j-1)\tau]$, with $I \geq 0$ and finite second moments there. For $j = 1$ the hypothesis is (A4). In case (ii) the nonnegativity of I on each window is supplied by (H); in case (i) it is proved along the way. The sign of I is used only to obtain the bounds $a \geq \mu$ and $S \leq \bar{S}$ below; the linear equations of each window are uniquely solvable for bounded measurable coefficients of either sign, so it is the moment bounds, not the existence of the solution, that depend on (H).

The susceptible class. On $[0, j\tau]$ the process $a(t) := \beta I(t-\tau) + \mu + u(t)$ is known, adapted, measurable, locally bounded along each sample path because I is continuous on $[-\tau, (j-1)\tau]$, and $a \geq \mu$ because $I \geq 0$ there. **Equation (7)** is therefore, pathwise, the linear equation **(5)** with $f \equiv \Lambda$ and coefficient a, and **Lemma 3** (with $c = \sup_{[0,j\tau]} a$, finite for each path) yields a unique continuous solution on $[0, j\tau]$ with $0 \leq S(t) \leq \bar{S}$; by uniqueness it coincides on $[0, (j-1)\tau]$ with the solution constructed before, and it is adapted because the Picard iterates are.

The exposed class. **Equation (8)** is **(5)** with $a \equiv \kappa + \mu$ and the known nonnegative forcing $f = \beta S\, I(\cdot - \tau)$, so **Lemma 3** gives a unique nonnegative continuous adapted solution on $[0, j\tau]$. Since a is constant, **(6)** reduces to $E(t) = \phi_2(0) E_\alpha(-(\kappa+\mu)t^\alpha) + \int_0^t k_{\kappa+\mu}(t-s) f(s) ds$, and the Cauchy-Schwarz inequality with the kernel as weight together with **(4)** gives

$$\sup_{t \leq j\tau} \mathbb{E}\, E(t)^2 \leq 2\phi_2(0)^2 + \frac{2\beta^2 \bar{S}^2}{(\kappa+\mu)^2} \sup_{t \leq (j-1)\tau} \mathbb{E}\, I(t)^2 < \infty.$$

The infectious class. **Equation (9)** is **(11)** with $a = \gamma + \mu$ and $f = \kappa E$, and **Lemma 6** provides a unique adapted continuous solution on $[0, j\tau]$ with finite second moments. When $\sigma = 0$ or $\alpha = 1$ the solution is nonnegative by the same lemma, which propagates the positivity of I to the next window in case (i).

The recovered class. **Equation (10)** is **(5)** with $a \equiv \mu$ and the nonnegative forcing $\gamma I + uS$, whose second moments are finite; the solution exists, is unique, is nonnegative, and its second moments are bounded exactly as those of E.

The induction closes. On each $[0, j\tau]$ the solution is the unique one in $\mathcal{H}_{j\tau}$, because each component is the unique solution of a linear equation with known coefficients, and it therefore extends the solution of **Theorem 1**. This proves all assertions of (i) and (ii). □

Remark 5. *Several results below are stated for* $\tau = 0$ *as a limiting case. There the delayed factor is not known in advance and the step argument does not apply, but the classical theory covers the two unconditional cases: for* $\sigma = 0$ *the solution of the deterministic fractional system exists globally and remains in* Ω *by* ***Lemma 2*** *applied at a first exit time, and for* $\alpha = 1$ *the positivity of I follows from* ***(12)*** *with* $f = \kappa E$ *while global existence follows from the linear growth of the drift on the cone [Chapter 2].*[15]

Remark 6. *The heuristic that a diffusion coefficient vanishing at* $I = 0$ *prevents the noise from pushing I across zero is rigorous for* $\alpha = 1$, *where the explicit formula* ***(12)*** *shows that I stays positive, and it does not require any argument for* $\sigma = 0$. *For* $\alpha \in (\frac{1}{2}, 1)$ *the stochastic convolution retains the memory of past increments, so the increment of I over a short interval after a time at which I is small is not solely governed by the current value of the diffusion coefficient, and the argument of the classical case does not transfer. Invariance results for stochastic Volterra equations*

*with the fractional kernel are available for certain autonomous coefficients,[60] but the delayed and non-autonomous structure of **(9)**, whose forcing κE depends on the past of the whole system, is not covered, and a proof of (H) for $\alpha < 1$ is left open. Three pieces of evidence support the hypothesis. The increment of the stochastic convolution over $[t_0, t_0 + \Delta]$ has a conditional standard deviation of order $\sigma\Delta^{\alpha-1/2}$ times the values of I over a neighbourhood of t_0 of length comparable to Δ, so that by continuity it is proportional to the local level of I, exactly as in the classical multiplicative case. In the simulations of Section 8 the discrete solution leaves the cone only through the finite step-size kick of the explicit Euler-Maruyama step, and the proportion of paths doing so decreases under mesh refinement (**Table 2**), as expected for a finite-step effect of the explicit noise treatment. And in the endemic regime, where I stays away from zero, no path of the fractional stochastic model left the cone in any of the runs reported below.*

Table 2. Proportion of sample paths in which the discrete infectious class becomes negative on $[0, 60]$ (near-critical regime, $\tau = 0$, 300 paths), with the step-size indicator κ_h of **(43)** in parentheses.

α	σ	$h = 0.05$	$h = 0.02$	$h = 0.01$
0.9	0.5	0 (0.16)	0 (0.11)	0 (0.08)
0.9	0.9	0.097 (0.28)	0 (0.20)	0 (0.15)
0.8	0.5	0.003 (0.22)	0 (0.17)	0 (0.13)
0.8	0.9	0.993 (0.39)	0.607 (0.30)	0.110 (0.24)
0.7	0.5	0.363 (0.30)	0.117 (0.25)	0.023 (0.22)
0.7	0.9	1.000 (0.54)	1.000 (0.45)	1.000 (0.39)

3.5. Moment bounds and the balance law in expectation

Because the noise enters the I-equation, the total population $N(t) = S(t) + E(t) + I(t) + R(t)$ is a random process; summing the four equations of **(1)** gives

$$ {}^{C}D_t^{\alpha} N(t) = \Lambda - \mu N(t) + \sigma I(t)\, \dot{W}(t). $$

The demographic balance law therefore holds in expectation, and the resolvent kernel k_μ of **(3)** gives an explicit representation of the fluctuation around the mean.

Lemma 7. *Assume* (A1)-(A4) *and, if $\alpha < 1$ and $\sigma > 0$, also* (H). *Then, for every $t \geq 0$,*

$$ \begin{aligned} N(t) &= m(t) + \sigma \int_0^t k_\mu(t-s)\, I(s)\, dW(s), \\ m(t) &:= N(0)\, E_\alpha(-\mu t^\alpha) + \frac{\Lambda}{\mu}\big(1 - E_\alpha(-\mu t^\alpha)\big), \end{aligned} \tag{13} $$

where $N(0) = \sum_i \phi_i(0)$. Consequently $\mathbb{E}\, N(t) = m(t) \leq \max\{N(0), \Lambda/\mu\}$, $\lim_{t\to\infty} \mathbb{E}\, N(t) = \Lambda/\mu$, and

$$ \mathbb{E}\, N(t)^2 = m(t)^2 + \sigma^2 \int_0^t k_\mu(t-s)^2\, \mathbb{E}\, I(s)^2\, ds. \tag{14} $$

Proof. Summing **(7)**-**(10)** gives $N = h - \mu\, k * N$ with $h := N(0) + \Lambda\,(1 * k) + Z$, where $Z(t) := \sigma \int_0^t k(t-s) I(s) dW(s)$ is a well-defined square-integrable process because $\alpha > \frac{1}{2}$ and $\sup_{s\leq t} \mathbb{E} I(s)^2 < \infty$ (**Theorem 2**). The resolvent identity gives $N = h - \mu\, k_\mu * h$. For the deterministic part of h this is the Mittag-Leffler solution m of the linear Caputo problem ${}^{C}D_t^{\alpha} m = \Lambda - \mu m$, $m(0) = N(0)$. For the stochastic part, the stochastic Fubini theorem, applicable since $k, k_\mu \in L^2(0,t)$, yields $(k_\mu * Z)(t) = \sigma \int_0^t (k_\mu * k)(t-s) I(s) dW(s)$, so that $Z - \mu k_\mu * Z = \sigma \int_0^t (k - \mu k_\mu * k)(t-s) I(s) dW(s) = \sigma \int_0^t k_\mu(t-s) I(s) dW(s)$ by the resolvent identity once more. This is **(13)**. Taking expectations annihilates the Itô integral and gives $\mathbb{E} N = m$; the bound and the limit follow from $E_\alpha(-\mu t^\alpha) \in (0, 1]$ and $E_\alpha(-\mu t^\alpha) \to 0$. Finally **(14)** is the Itô isometry applied to **(13)**. □

Theorem 3. *Assume* (A1)-(A4) *and, if $\alpha < 1$ and $\sigma > 0$, also* (H). *Then:*

(i) *for every $T > 0$,*

$$ \sup_{t\leq T} \mathbb{E}\, N(t)^2 \leq \max\{N(0), \Lambda/\mu\}^2\, E_{2\alpha-1} \Big(\frac{\sigma^2\, \Gamma(2\alpha-1)}{\Gamma(\alpha)^2}\, T^{2\alpha-1}\Big) < \infty; $$

(ii) *if $\sigma^2 \Lambda_2 < 1$, where $\Lambda_2 := \int_0^\infty k_\mu(r)^2\, dr < \infty$, then*

$$ \sup_{t\geq 0} \mathbb{E}\, N(t)^2 \leq \frac{\max\{N(0), \Lambda/\mu\}^2}{1 - \sigma^2 \Lambda_2}. $$

For $\alpha = 1$ one has $\Lambda_2 = 1/(2\mu)$, and the condition reads $\sigma^2 < 2\mu$.

Proof. Under the assumptions all compartments are nonnegative, so $0 \leq I \leq N$ and **(14)** gives $y(t) := \mathbb{E} N(t)^2 \leq m(t)^2 + \sigma^2 \int_0^t k_\mu(t-s)^2 y(s) ds$. Since $0 < E_{\alpha,\alpha}(-x) \leq 1/\Gamma(\alpha)$ for $x \geq 0$, we have $k_\mu(r)^2 \leq r^{2\alpha-2}/\Gamma(\alpha)^2$, and **Lemma 1** with the exponent $2\alpha - 1 > 0$ gives (i). For (ii), $k_\mu(r)^2$ is integrable at $r = 0$ because $2\alpha - 2 > -1$ and at infinity because $E_{\alpha,\alpha}(-x) = O(x^{-2})$ as $x \to \infty$ for $\alpha < 1$,[2] so that $k_\mu(r)^2 = O(r^{-2\alpha-2})$; for $\alpha = 1$, $k_\mu(r) = e^{-\mu r}$ and $\Lambda_2 = 1/(2\mu)$. The inequality $y \leq \bar{m}^2 + \sigma^2 k_\mu^2 * y$ with $\bar{m} := \sup m$ and a nonnegative kernel of total mass $\sigma^2 \Lambda_2 < 1$ implies, by iteration, $y \leq \bar{m}^2 \sum_{n\geq 0} (\sigma^2 \Lambda_2)^n$, which is the stated bound. □

Corollary 1. *Under the assumptions of* ***Theorem 3****, if* $X(0) \in \Omega$ *then* $\mathbb{E}\,X(t) \in \Omega$ *for every* $t \geq 0$*; in particular* $\mathbb{E}\,N(t) \leq \Lambda/\mu$*. The nonnegativity part of the invariance holds pathwise (****Theorem 2****).*

Proof. Nonnegativity of $\mathbb{E}\,X(t)$ is immediate from **Theorem 2**, and the population bound is **Lemma 7** evaluated at $N(0) \leq \Lambda/\mu$. □

Remark 7. *If one prefers the total population to satisfy* ${}^{C}D_t^{\alpha} N = \Lambda - \mu N$ *pathwise (so that* Ω *is invariant almost surely rather than only in the mean), it suffices to model the environmental fluctuation as a perturbation of the transmission rate,* $\beta \mapsto \beta + \sigma \dot{W}$*, as in.*[16] *The noise then appears as* $-\sigma SI(t-\tau)\dot{W}$ *in the S-equation and as* $+\sigma SI(t-\tau)\dot{W}$ *in the E-equation, cancelling in the sum, and* $N(t) \leq \max\{N(0), \Lambda/\mu\}$ *along every path. The construction of* ***Theorem 2*** *goes through with the roles of the compartments exchanged, the susceptible class now carrying the linear stochastic equation of* ***Lemma 6*** *on each window; the disease-free analysis of Section 4 is unchanged because the diffusion still vanishes at the disease-free equilibrium, whereas the extinction threshold of* ***Theorem 8*** *takes a different form, since the noise then acts on the incidence rather than on the infectious period. The formulation* ***(1)*** *is retained here because it attributes the fluctuation directly to the infectious dynamics, as discussed in* ***Remark 1****.*

4. Basic reproduction number and the disease-free equilibrium

4.1. Disease-free equilibrium and reproduction numbers

In the absence of disease ($E = I = 0$) and of vaccination ($u \equiv 0$) the deterministic skeleton of **(1)** admits the disease-free equilibrium (DFE)

$$\mathcal{E}_0 = (S_0, 0, 0, 0), \qquad S_0 = \frac{\Lambda}{\mu}. \tag{15}$$

We compute the basic reproduction number R_0 by the next-generation matrix method of van den Driessche and Watmough.[61] With $x = (E, I)^{\top}$ collecting the infected compartments, the inflow of new infections and the remaining transfers are

$$\mathcal{F}(x) = \begin{pmatrix} \beta S\, I(t-\tau) \\ 0 \end{pmatrix},$$

$$\mathcal{V}(x) = \begin{pmatrix} (\kappa+\mu)E \\ (\gamma+\mu)I - \kappa E \end{pmatrix}.$$

Linearising at $\mathcal{E}_0$ (where the equilibrium value $I(t-\tau) = I$ makes the delay immaterial for the steady-state Jacobian) gives

$$F = \begin{pmatrix} 0 & \beta S_0 \\ 0 & 0 \end{pmatrix}, \qquad V = \begin{pmatrix} \kappa+\mu & 0 \\ -\kappa & \gamma+\mu \end{pmatrix},$$

$$V^{-1} = \frac{1}{(\kappa+\mu)(\gamma+\mu)} \begin{pmatrix} \gamma+\mu & 0 \\ \kappa & \kappa+\mu \end{pmatrix}.$$

The next-generation matrix $K = FV^{-1}$ has spectral radius

$$\begin{aligned} R_0 = \rho(FV^{-1}) &= \frac{\beta S_0\, \kappa}{(\kappa+\mu)(\gamma+\mu)} \\ &= \frac{\beta \Lambda\, \kappa}{\mu(\kappa+\mu)(\gamma+\mu)}. \end{aligned} \tag{16}$$

The factor $\kappa/(\kappa+\mu)$ is the probability that an exposed individual survives latency to become infectious, $1/(\gamma+\mu)$ is the mean infectious period, and βS_0 is the rate of new infections produced near the DFE; their product is the expected number of secondary cases.

Remark 8. *When a constant vaccination effort* $u(t) \equiv \bar{u} \in [0,1]$ *is applied, the disease-free susceptible level shifts to* $S_0^{\bar{u}} = \Lambda/(\mu+\bar{u})$ *and the corresponding control (effective) reproduction number becomes*

$$R_v = \frac{\beta\, \kappa\, \Lambda}{(\mu+\bar{u})(\kappa+\mu)(\gamma+\mu)} = \frac{\mu}{\mu+\bar{u}}\, R_0 \leq R_0,$$

so vaccination lowers the reproduction number monotonically, and $R_v < 1$ *as soon as* $\bar{u} > \mu(R_0 - 1)$*.*

4.2. Notions of stability for the stochastic model

For the stochastic model the word stability admits several meanings, which respond to the noise in different ways and are kept apart throughout.

Definition 3. *Let* $\alpha \in (\frac{1}{2}, 1]$ *and let* (E, I) *denote the infected classes of the solution of* ***(1)****. The disease-free equilibrium is said to be*

(a) *globally attractive in the mean if* $\mathbb{E}\,E(t) + \mathbb{E}\,I(t) \to 0$ *as* $t \to \infty$ *for every history satisfying (A4) with* $\Phi(0) \in \Omega$*;*
(b) *mean-square attractive if* $\mathbb{E}\,E(t)^2 + \mathbb{E}\,I(t)^2 \to 0$*;*
(c) *almost surely exponentially attractive if* $\limsup_{t\to\infty} t^{-1} \ln\big(E(t) + I(t)\big) < 0$ *almost surely.*

The three notions are not related by implication in general, and they depend on σ in opposite directions. The Itô isometry adds a nonnegative term to every second moment, so mean-square attractivity can only be expected under a smallness condition on σ; the almost-sure notion, on the contrary, is favoured by large noise, because

the Itô correction $-\frac{1}{2}\sigma^2$ in the logarithm of the infected mass is negative. The results of this section concern notion (a), which is accessible for every fractional order, since the mean of the stochastic convolution vanishes; the almost-sure notion (c) is treated in Section 5 for $\alpha = 1$, where the Itô formula is available. No mean-square statement is claimed in this paper.

4.3. The linearised mean dynamics

Linearising **(1)** about $\mathcal{E}_0$ and writing the susceptible perturbation $s = S - S_0$, one finds ${}^{C}D_t^{\alpha} s = -\mu s - \beta S_0 I(t-\tau) + \text{h.o.t.}$, so s is slaved to the infected variables. After taking expectations (the multiplicative noise $\sigma I \dot{W}$ has zero mean and vanishes at $I = 0$), the infected subsystem reduces to the deterministic fractional delay system

$$ {}^{C}D_t^{\alpha} E(t) = \beta S_0\, I(t-\tau) - (\kappa+\mu)E(t), \quad (17)$$

$$ {}^{C}D_t^{\alpha} I(t) = \kappa E(t) - (\gamma+\mu)I(t), \quad (18)$$

where E and I now stand for the means. Seeking solutions proportional to $e^{\lambda t}$ produces the characteristic equation

$$ \big(\lambda^{\alpha}+\kappa+\mu\big)\big(\lambda^{\alpha}+\gamma+\mu\big) - \kappa\beta S_0\, e^{-\lambda\tau} = 0, \quad (19)$$

in which λ^{α} is the principal branch. By **Lemma 5** the zero solution of **(17)**-**(18)** is asymptotically stable when every root of **(19)** has negative real part; for $\tau = 0$ this is the sector condition $|\arg z| > \alpha\pi/2$ on the roots $z = \lambda^{\alpha}$ of the resulting quadratic.

Theorem 4. *Let $\alpha \in (\frac{1}{2}, 1]$.*

(i) *If $R_0 < 1$, then every root of **(19)** has negative real part for every $\tau \geq 0$, and the linearised mean system **(17)** and **(18)** is asymptotically stable for every delay.*

(ii) *If $R_0 > 1$, then **(19)** has a positive real root for every $\tau \geq 0$, and the linearised mean system is unstable.*

Proof. *(i)* Suppose that **(19)** has a root $\lambda \neq 0$ with $\operatorname{Re}\lambda \geq 0$, so that $|\arg\lambda| \leq \pi/2$ and $|e^{-\lambda\tau}| = e^{-\tau \operatorname{Re}\lambda} \leq 1$ for all $\tau \geq 0$. Put $z = \lambda^{\alpha}$; then $|\arg z| = \alpha|\arg\lambda| \leq \alpha\pi/2 \leq \pi/2$, hence $\operatorname{Re} z \geq 0$. For $a > 0$ this gives the elementary lower bound $|z+a| \geq \operatorname{Re}(z+a) = \operatorname{Re} z + a \geq a$. Taking moduli in **(19)**,

$$\begin{aligned}(\kappa+\mu)(\gamma+\mu) &\leq |z+\kappa+\mu|\,|z+\gamma+\mu| \\ &= \kappa\beta S_0\,|e^{-\lambda\tau}| \leq \kappa\beta S_0,\end{aligned}$$

that is, $R_0 \geq 1$, which contradicts $R_0 < 1$. The case $\lambda = 0$ is excluded because substituting $z = 0$ into **(19)** forces $(\kappa+\mu)(\gamma+\mu) = \kappa\beta S_0$, i.e. $R_0 = 1$. Hence every root has negative real part, for every $\tau \geq 0$, and **Lemma 5** gives the asymptotic stability.

(ii) For real $\lambda \geq 0$ set $F(\lambda) := (\lambda^{\alpha}+\kappa+\mu)(\lambda^{\alpha}+\gamma+\mu) - \kappa\beta S_0 e^{-\lambda\tau}$. Then $F(0) = (\kappa+\mu)(\gamma+\mu)(1-R_0) < 0$, while $F(\lambda) \to +\infty$ as $\lambda \to \infty$ because $e^{-\lambda\tau} \leq 1$. By the intermediate value theorem F has a positive real root λ_+ for every $\tau \geq 0$, and the mode $e^{\lambda_+ t}$ grows without bound. □

4.4. Extinction in the mean below the threshold

The linear analysis above is local. The comparison structure of the model turns it into a global statement in the mean, valid for every order, every delay and every noise intensity.

Theorem 5. *Assume* (A1)-(A4), *$u \equiv 0$, $\Phi(0) \in \Omega$ and, if $\alpha < 1$ and $\sigma > 0$, also* (H). *If $R_0 < 1$, then for every $\tau \geq 0$*

$$\lim_{t\to\infty} \mathbb{E}\,E(t) = \lim_{t\to\infty} \mathbb{E}\,I(t) = 0,$$

$$\lim_{t\to\infty} \mathbb{E}\,S(t) = S_0, \qquad \lim_{t\to\infty} \mathbb{E}\,R(t) = 0,$$

so $\mathcal{E}_0$ is globally attractive in the mean. If $\sigma = 0$, the disease-free equilibrium of the deterministic fractional delayed system is globally asymptotically stable in Ω for every $\tau \geq 0$.

Proof. Let $m_E := \mathbb{E}\,E$ and $m_I := \mathbb{E}\,I$. Taking expectations in **(8)** and **(9)**, which is legitimate since all processes have finite second moments and the stochastic convolution has zero mean, gives

$$\begin{aligned} m_E(t) &= \phi_2(0) + \int_0^t k(t-s)\big(\beta S_0\, m_I(s-\tau) - \\ &\qquad (\kappa+\mu)m_E(s) - r(s)\big)ds, \\ m_I(t) &= \phi_3(0) + \int_0^t k(t-s)\big(\kappa\, m_E(s) - (\gamma+\mu) \\ &\qquad m_I(s)\big)ds, \end{aligned}$$

with $r(s) := \beta\,\mathbb{E}\big[(S_0 - S(s))I(s-\tau)\big] \geq 0$, because $S \leq S_0$ pathwise (**Theorem 2** with $\phi_1(0) \leq S_0$) and $I \geq 0$. Let (w_E, w_I) be the solution of the linear system **(17)** and **(18)** with the same history (ϕ_2, ϕ_3). The difference $d := (w_E - m_E,\, w_I - m_I)$ vanishes on $[-\tau, 0]$ and satisfies $d(t) = \int_0^t k(t-s)\big(Ad(s) + Bd(s-\tau) + (r(s), 0)^{\top}\big)ds$ with

$$A = \begin{pmatrix} -(\kappa+\mu) & 0 \\ \kappa & -(\gamma+\mu) \end{pmatrix}, \qquad B = \begin{pmatrix} 0 & \beta S_0 \\ 0 & 0 \end{pmatrix}.$$

Since A is Metzler, $B \geq 0$ and $r \geq 0$, **Lemma 4** gives $d \geq 0$, that is, $0 \leq m_E \leq w_E$ and $0 \leq m_I \leq w_I$. By **Theorem 4(i)** and **Lemma 5**, $(w_E, w_I) \to 0$, hence $m_E, m_I \to 0$. For the susceptible mean, taking expectations in **(7)** gives ${}^{C}D_t^{\alpha}\,\mathbb{E}S = \Lambda - \mu\,\mathbb{E}S - \varphi$ with $\varphi := \beta\,\mathbb{E}[S\,I(\cdot-\tau)] \in [0, \beta S_0\, m_I(\cdot-\tau)]$, so $\varphi(t) \to 0$, and **Lemma 3(iii)** applied to $\mathbb{E}S - S_0$ gives $\mathbb{E}S \to S_0$; the same lemma applied to **(10)** gives $\mathbb{E}R \to 0$. When $\sigma = 0$ all quantities are deterministic, so the argument shows that every solution in Ω converges

to $\mathcal{E}_0$; Lyapunov stability follows from the same comparison, because $(E, I) \le (w_E, w_I)$ and the solution w of the asymptotically stable linear system is small whenever its history is small, while $S - S_0$ and R are then bounded, through **(6)** with $c = \mu$ and **(4)**, by their initial values and by μ^{-1} times the supremum of their forcing terms, which are small. □

Remark 9. ***Theorem 5*** *is an attractivity statement for the first moment of the infected classes; it holds irrespective of σ, because the noise disappears upon averaging, and it is global rather than local, because the comparison argument does not linearise the incidence but bounds it from above. Mean-square attractivity would require, in addition, a smallness condition on σ of the type discussed in* ***Theorem 3(ii)****, and it is not pursued here. Conversely, when $R_0 > 1$* ***Theorem 4(ii)*** *shows that the linearised mean dynamics at $\mathcal{E}_0$ are unstable for every delay, so the threshold $R_0 = 1$ is sharp for the linear analysis of the mean.*

5. Endemic equilibrium, global stability and noise-induced extinction

5.1. The uncontrolled deterministic skeleton

To isolate the threshold dynamics in their classical form, we switch off the vaccination effort by setting $u(t) \equiv 0$ and examine the deterministic drift system underlying **(1)**, in which the delay acts solely through the force of infection:

$$
\begin{aligned}
{}^{C}D_t^{\alpha} S(t) &= \Lambda - \beta S(t) I(t-\tau) - \mu S(t), && (20)\\
{}^{C}D_t^{\alpha} E(t) &= \beta S(t) I(t-\tau) - (\kappa+\mu) E(t), && (21)\\
{}^{C}D_t^{\alpha} I(t) &= \kappa E(t) - (\gamma+\mu) I(t), && (22)\\
{}^{C}D_t^{\alpha} R(t) &= \gamma I(t) - \mu R(t). && (23)
\end{aligned}
$$

Because R is absent from the first three equations, the epidemiologically decisive dynamics live in the (S, E, I) subsystem, and R is recovered by quadrature.

Theorem 6. *If $R_0 > 1$, then system* ***(20)-(23)*** *possesses a unique endemic equilibrium $\mathcal{E}^* = (S^*, E^*, I^*, R^*)$ with strictly positive coordinates, given by*

$$
\begin{aligned}
S^* &= \frac{(\kappa+\mu)(\gamma+\mu)}{\beta\kappa} = \frac{S_0}{R_0},\\
I^* &= \frac{\kappa\Lambda}{(\kappa+\mu)(\gamma+\mu)}\Big(1 - \frac{1}{R_0}\Big),
\end{aligned}
\qquad (24)
$$

$$
E^* = \frac{\gamma+\mu}{\kappa}\, I^*, \qquad R^* = \frac{\gamma}{\mu}\, I^*. \qquad (25)
$$

If $R_0 \le 1$, no positive equilibrium exists and the disease-free equilibrium is the only steady state in Ω.

Proof. At a steady state the delayed argument satisfies $I(t-\tau) = I^*$, so the delay is immaterial. **Equation (22)** gives $\kappa E^* = (\gamma+\mu) I^*$, whence $E^* = \frac{\gamma+\mu}{\kappa} I^*$. Substituting into **(21)**, $\beta S^* I^* = (\kappa+\mu) E^* = \frac{(\kappa+\mu)(\gamma+\mu)}{\kappa} I^*$; if $I^* > 0$ this forces $S^* = \frac{(\kappa+\mu)(\gamma+\mu)}{\beta\kappa}$, and comparison with **(16)** yields $S^* = S_0/R_0$. Inserting S^* into the equilibrium version of **(20)**, $\beta S^* I^* = \Lambda - \mu S^*$, gives $I^* = (\Lambda - \mu S^*)/(\beta S^*)$; a direct computation reduces this to the expression in **(24)**, and $R^* = \gamma I^*/\mu$ follows from **(23)**. Since S^* is fixed and the remaining coordinates are then determined, the equilibrium is unique. Positivity of I^* is equivalent to $1 - 1/R_0 > 0$, that is, $R_0 > 1$. □

We record a fractional differential inequality that will drive the global-stability proof; it is the Caputo counterpart of the elementary identity $\frac{d}{dt}(x - x^* \ln x) = (1 - x^*/x)\dot{x}$, and it was established by Vargas-De-León[62] on the basis of the quadratic inequality of Aguila-Camacho, Duarte-Mermoud and Gallegos.[63]

Lemma 8. *For every $x \in C^1((0,\infty);(0,\infty))$ and every $x^* > 0$,*

$$
{}^{C}D_t^{\alpha}\Big(x(t) - x^* - x^* \ln \frac{x(t)}{x^*}\Big) \le \Big(1 - \frac{x^*}{x(t)}\Big) {}^{C}D_t^{\alpha} x(t), \qquad \alpha \in (0,1).
$$

5.2. Global stability of the endemic equilibrium for $\tau = 0$

Theorem 5 settles the behaviour below the threshold for every delay. Above the threshold, the natural companion result is that, in the absence of delay, supercritical transmission leads to a globally attracting endemic state rather than to oscillations; Section 6 then shows that the delay does not change the local picture.

Theorem 7. *Let $\tau = 0$ and $u \equiv 0$. If $R_0 > 1$, then the endemic equilibrium $\mathcal{E}^*$ is globally asymptotically stable in the interior* $\operatorname{int}\Omega = \{(S, E, I, R) \in \Omega : S, E, I > 0\}$.

Proof. Consider the Volterra-Goh functional, restricted to the driving (S, E, I) block,

$$
V = \Big(S - S^* - S^* \ln \tfrac{S}{S^*}\Big) + \Big(E - E^* - E^* \ln \tfrac{E}{E^*}\Big) + \frac{\kappa+\mu}{\kappa}\Big(I - I^* - I^* \ln \tfrac{I}{I^*}\Big),
$$

which is positive definite about $\mathcal{E}^*$ and radially unbounded on $\operatorname{int}\Omega$. Applying **Lemma 8** term by term,

$$
{}^{C}D_t^{\alpha} V \le \Big(1-\tfrac{S^*}{S}\Big)\,{}^{C}D_t^{\alpha} S + \Big(1-\tfrac{E^*}{E}\Big)\,{}^{C}D_t^{\alpha} E + \frac{\kappa+\mu}{\kappa}\Big(1-\tfrac{I^*}{I}\Big)\,{}^{C}D_t^{\alpha} I.
$$

Using the equilibrium identities $\Lambda = \beta S^* I^* + \mu S^*$, $(\kappa+\mu)E^* = \beta S^* I^*$ and $(\gamma+\mu)I^* = \kappa E^*$ to eliminate the parameters, the cross terms telescope and one obtains, after collecting,

$$
{}^{C}D_t^{\alpha} V \le -\mu\frac{(S-S^*)^2}{S} + \beta S^* I^*\Big[3 - \frac{S^*}{S} - \frac{S\,I\,E^*}{S^*\,I^*\,E} - \frac{E\,I^*}{E^*\,I}\Big].
$$

The first term is manifestly nonpositive. For the bracket, the arithmetic-geometric mean inequality applied to the three positive ratios, whose product equals 1, gives

$$
\frac{S^*}{S} + \frac{S\,I\,E^*}{S^*\,I^*\,E} + \frac{E\,I^*}{E^*\,I} \ge 3,
$$

so the bracket is ≤ 0. Consequently ${}^{C}D_t^{\alpha} V \le 0$, with equality precisely when $S = S^*$ and the three ratios are simultaneously unity, i.e. on the ray $\{S = S^*,\ (E,I) = c\,(E^*, I^*),\ c > 0\}$. On that ray **(20)** gives ${}^{C}D_t^{\alpha} S = \beta S^* I^* (1-c)$, which vanishes only for $c = 1$, so the largest invariant subset of $\{{}^{C}D_t^{\alpha} V = 0\}$ is $\{\mathcal{E}^*\}$. The invariance principle for Caputo systems, in the form of [64, Lemma 4.6], whose rigorous foundation is given by Gallegos and Duarte-Mermoud,[65] then yields global asymptotic stability of $\mathcal{E}^*$ in $\operatorname{int}\Omega$. □

5.3. Noise-induced extinction

We now make precise the intuition that environmental fluctuations can extinguish an outbreak that would persist deterministically. The analysis exploits a feature of the model that is easy to overlook: since the noise sits only in the I-equation, the susceptible equation is pathwise comparable to a linear equation, so $S(t) \le S_0$ holds along every path when $S(0) \le S_0$, not merely in mean. For the logarithmic estimate we work in the classical regime $\alpha = 1$, where Itô calculus is available; the scope of the result relative to the fractional case is discussed in **Remark 11**. The delay is handled through a Lyapunov functional that stores the infectious history over one latent period, which produces a threshold depending explicitly on τ.

Theorem 8. *Let $\alpha = 1$, $u \equiv 0$, $\tau \ge 0$, and let the history satisfy (A4) with $\Phi(0) \in \Omega$ and $\phi_2(0) + \phi_3(0) > 0$. Define*

$$
\Theta_\tau := \max_{0\le p\le 1}\Big\{-\mu + \big(\beta S_0 e^{\mu\tau} - \gamma\big)\,p - \tfrac{\sigma^2}{2}\,p^2\Big\}. \tag{26}
$$

If $\Theta_\tau < 0$, then

$$
\limsup_{t\to\infty} \frac{1}{t}\ln\big(E(t)+I(t)\big) \le \Theta_\tau < 0 \quad a.s.,
$$

so the exposed and infectious classes decay exponentially and the disease becomes extinct almost surely. Explicitly, with $c_\tau := \beta S_0 e^{\mu\tau} - \gamma$,

$$
\Theta_\tau = \begin{cases} -\mu, & c_\tau \le 0, \\ -\mu + \dfrac{c_\tau^2}{2\sigma^2}, & 0 < c_\tau < \sigma^2, \\ -\mu + c_\tau - \dfrac{\sigma^2}{2}, & c_\tau \ge \sigma^2, \end{cases} \tag{27}
$$

so that $\Theta_\tau < 0$ holds for every $\sigma > 0$ when $c_\tau \le \mu$ (and also for $\sigma = 0$ when $c_\tau < \mu$), and otherwise if and only if $\sigma > \sigma_\tau^*$, where

$$
\sigma_\tau^* := \begin{cases} \sqrt{2(c_\tau - \mu)}, & \mu < c_\tau < 2\mu, \\ c_\tau/\sqrt{2\mu}, & c_\tau \ge 2\mu. \end{cases} \tag{28}
$$

Proof. By **Theorem 2** the solution is global, positive, and $S(t) \le S_0$ for all $t \ge 0$, because $\dot S \le \Lambda - \mu S$ and $S(0) \le S_0$. Define the weighted history integral and the functional

$$
J(t) := \int_{t-\tau}^{t} e^{\mu(\tau - t + s)}\, I(s)\, ds,
$$
$$
V(t) := E(t) + I(t) + \beta S_0\, J(t),
$$

so that $V \ge E + I$ and $V(0) > 0$. Since I is continuous, J is absolutely continuous with $\dot J = -\mu J + e^{\mu\tau} I(t) - I(t-\tau)$, and V is a semimartingale whose martingale part is that of I. From **(1)**,

$$
\begin{aligned}
dV &= \Big[\beta S\, I(t-\tau) - \mu E - (\gamma+\mu) I + \beta S_0\big(-\mu J \\
&\quad + e^{\mu\tau} I - I(t-\tau)\big)\Big]\,dt + \sigma I\, dW \\
&= \Big[-\mu\big(E + I + \beta S_0 J\big) + \big(\beta S_0 e^{\mu\tau} - \gamma\big) I - \\
&\quad \beta\big(S_0 - S\big) I(t-\tau)\Big]\,dt + \sigma I\, dW \\
&\le \big[-\mu V + c_\tau I\big]\,dt + \sigma I\, dW,
\end{aligned}
$$

where the cancellation $-(\kappa+\mu)E + \kappa E = -\mu E$ and the bound $S \le S_0$ have been used. By Itô's formula, with $p := I/V \in [0,1]$,

$$
\begin{aligned}
d\ln V = \frac{dV}{V} - \frac{\sigma^2 I^2}{2V^2}\,dt &\le \Big[-\mu + c_\tau\, p - \tfrac{\sigma^2}{2} p^2\Big]dt + \\
&\quad \sigma p\, dW \le \Theta_\tau\, dt + \sigma p\, dW.
\end{aligned}
$$

Integrating, $\ln V(t) \le \ln V(0) + \Theta_\tau t + M(t)$ with $M(t) = \int_0^t \sigma p(s)\, dW(s)$. The martingale M has quadratic variation $\langle M\rangle_t = \sigma^2 \int_0^t p(s)^2 ds \le \sigma^2 t$, so by the strong law of large numbers for local martingales [Theorem 1.3.4],[15] $M(t)/t \to 0$ a.s. Dividing by t and letting $t \to \infty$ gives $\limsup_t t^{-1} \ln V(t) \le \Theta_\tau$, and $E + I \le V$ concludes. The piecewise formula **(27)** is obtained by maximising the concave quadratic $p \mapsto -\mu + c_\tau p - \frac{\sigma^2}{2} p^2$ over $[0,1]$, the unconstrained maximiser

being $p^\star = c_\tau/\sigma^2$. Since Θ_τ is nonincreasing in σ, the threshold **(28)** is obtained by solving $\Theta_\tau = 0$: at $\sigma^2 = c_\tau$ one has $\Theta_\tau = c_\tau/2 - \mu$, so the zero lies in the third regime of **(27)** when $c_\tau < 2\mu$ and in the second when $c_\tau \geq 2\mu$. □

Remark 10. *In every regime an increase in σ lowers Θ_τ, so stronger environmental fluctuations enlarge the extinction set; this is the rigorous content of the statement that noise can suppress transmission. For $\tau = 0$ the threshold reduces to $\Theta_0 = \max_p\{-\mu+(\beta S_0-\gamma)p-\sigma^2p^2/2\}$. The criterion is a sufficient condition. For $\tau > 0$ the factor $e^{\mu\tau}$ measures the cost of storing the infectious history over one latent period in the functional V, which makes the condition more conservative as τ grows, and the simulations of Section 8 indicate that the actual extinction threshold moves only slightly with the delay. In the deterministic limit $\sigma \to 0$ the criterion reduces to $\beta S_0 e^{\mu\tau} < \gamma + \mu$, a conservative sufficient condition, the sharp deterministic threshold being $R_0 < 1$ from **Theorem 5**.*

Remark 11. ***Theorem 8*** *is a statement about the classical order. For $\alpha \in (\frac{1}{2}, 1)$ the logarithmic computation is not available, because the stochastic convolution with the singular kernel is not a semimartingale and Itô's formula has no elementary Caputo counterpart; what is available for every order is the mean threshold of **Theorem 5**, which is independent of σ, and the moment bounds of **Theorem 3**. An almost-sure extinction threshold for the fractional model therefore remains an open problem, and the simulations of Section 8 explore it numerically: for $\alpha = 0.9$ the infected mass at a fixed horizon decreases with σ in the same way as for $\alpha = 1$, but the decay is algebraic rather than exponential, in keeping with the Mittag-Leffler relaxation of fractional systems.*

6. Delay-independent stability of the endemic equilibrium

6.1. Characteristic equation at $\mathcal{E}^*$

When $R_0 > 1$ the disease-free equilibrium is unstable (it carries a positive real characteristic root for every delay, by **Theorem 4**), so it cannot be the seat of delay-induced oscillations; the relevant object is the endemic equilibrium $\mathcal{E}^*$, which is globally stable in the absence of delay (**Theorem 7**). The purpose of this section is to show that $\mathcal{E}^*$ retains its local stability for every delay, so that the transmission delay, although it reshapes the transient, cannot produce a Hopf bifurcation in this model. We linearise **(20)**-**(22)** about $\mathcal{E}^*$. Writing (s, e, i) for the perturbations and linearising the incidence $\beta S(t)I(t-\tau)$ as $\beta I^* s(t) + \beta S^* i(t-\tau)$, the variational system is

$$\begin{aligned} {}^{C}D_t^\alpha s &= -(\mu + \beta I^*)s - \beta S^* i(t-\tau), \\ {}^{C}D_t^\alpha e &= \beta I^* s + \beta S^* i(t-\tau) - (\kappa+\mu)e, \\ {}^{C}D_t^\alpha i &= \kappa e - (\gamma+\mu)i. \end{aligned}$$

Seeking solutions proportional to $e^{\lambda t}$ and writing $m = \lambda^\alpha$ (principal branch), the determinantal condition reduces, after using $\kappa\beta S^* = (\kappa+\mu)(\gamma+\mu)$ from **(24)**, to the transcendental equation

$$\begin{aligned} &\underbrace{(m+\mu+\beta I^*)(m+\kappa+\mu)(m+\gamma+\mu)}_{=:P(m)} \\ &\quad - \underbrace{(m+\mu)(\kappa+\mu)(\gamma+\mu)}_{=:Q(m)}\, e^{-\lambda\tau} = 0. \end{aligned} \tag{29}$$

By **Lemma 5**, $\mathcal{E}^*$ is locally asymptotically stable whenever every root λ of **(29)** has negative real part. A delay-induced loss of stability would require a root to cross the imaginary axis as τ increases, that is, a purely imaginary root $\lambda = i\omega$ for some τ; the standard machinery of Hopf analysis (see[66] and, for fractional systems,[33]) consists in locating such roots through the frequency function

$$\Psi(\omega) := |P\big((i\omega)^\alpha\big)|^2 - |Q\big((i\omega)^\alpha\big)|^2, \qquad \omega > 0, \tag{30}$$

whose positive zeros are the candidate crossing frequencies. We show that no such frequency exists.

6.2. Stability at zero delay

Proposition 1. *Let $R_0 > 1$. At $\tau = 0$, equation **(29)** becomes the cubic $m^3 + a_2m^2 + a_1m + a_0 = 0$ in $m = \lambda^\alpha$ with*

$$\begin{aligned} a_2 &= \beta I^* + \kappa + \gamma + 3\mu, \\ a_1 &= (\beta I^* + \mu)(\kappa + \gamma + 2\mu), \\ a_0 &= \beta I^*(\kappa+\mu)(\gamma+\mu). \end{aligned}$$

The Routh-Hurwitz conditions $a_2 > 0$, $a_0 > 0$, $a_2a_1 > a_0$ hold for every admissible parameter set, so every root m has negative real part and $\mathcal{E}^*$ is locally asymptotically stable when $\tau = 0$.

Proof. Writing $k = \kappa + \mu$, $g = \gamma + \mu$ and $b = \beta I^* > 0$, at $\tau = 0$ the left side of **(29)** is

$$\begin{aligned} &(m+\mu+b)(m+k)(m+g) - (m+\mu)kg = m^3 + \\ &\quad (b+\mu+k+g)m^2 + (\mu+b)(k+g)\,m + b\,kg, \end{aligned}$$

which gives the stated coefficients. All three are positive, and

$$\begin{aligned} a_2a_1 &= (b+\mu+k+g)(\mu+b)(k+g) \geq (k+g) \\ &\quad b\,(k+g) = b\,(k+g)^2 \geq 4bkg > bkg = a_0. \end{aligned}$$

Hence every root m satisfies $\mathrm{Re}\, m < 0$, so $|\arg m| > \pi/2$, and the corresponding $\lambda = m^{1/\alpha}$

satisfies $|\arg\lambda| = |\arg m|/\alpha > \pi/(2\alpha) \geq \pi/2$, that is, $\operatorname{Re}\lambda < 0$; roots m with $|\arg m| > \alpha\pi$ correspond to no λ at all, and $|\arg m| = \alpha\pi$ corresponds to a negative real λ. **Lemma 5** concludes. □

6.3. Stability for every delay

Theorem 9. *Let $R_0 > 1$ and $\alpha \in (\frac{1}{2}, 1]$. Then every root of **(29)** has negative real part for every $\tau \geq 0$, so the endemic equilibrium $\mathcal{E}^*$ of **(20)**-**(23)** is locally asymptotically stable for every delay. In particular the frequency function **(30)** is positive on $(0, \infty)$, no characteristic root ever reaches the imaginary axis, and the system admits no Hopf bifurcation with respect to τ.*

Proof. Suppose, for contradiction, that for some $\tau \geq 0$ equation **(29)** has a root λ with $\operatorname{Re}\lambda \geq 0$. Then $|e^{-\lambda\tau}| \leq 1$, and $|\arg m| = \alpha|\arg\lambda| \leq \alpha\pi/2 \leq \pi/2$ for $m = \lambda^\alpha$, so $\operatorname{Re} m \geq 0$. Writing $m = x + iy$ with $x \geq 0$ and comparing moduli,

$$\frac{|P(m)|}{|Q(m)|} = \frac{|m+\mu+\beta I^*|}{|m+\mu|} \cdot \frac{|m+\kappa+\mu|}{\kappa+\mu} \cdot \frac{|m+\gamma+\mu|}{\gamma+\mu}.$$

For $x \geq 0$ and $a > 0$ one has $|m+a| \geq \operatorname{Re}(m+a) = x + a \geq a$, so the last two factors are at least 1; and since $(x+\mu+\beta I^*)^2 > (x+\mu)^2$ the first factor exceeds 1. Therefore $|P(m)| > |Q(m)| \geq |Q(m)e^{-\lambda\tau}|$, contradicting **(29)**. Hence every root has negative real part for every $\tau \geq 0$, and Lemma 5 gives the local asymptotic stability. The same modulus computation at $m = (i\omega)^\alpha$, for which $\operatorname{Re} m = \omega^\alpha \cos(\alpha\pi/2) \geq 0$, gives $|P(m)| > |Q(m)|$, i.e. $\Psi(\omega) > 0$ for every $\omega > 0$, so **(30)** has no positive root and no purely imaginary characteristic root exists for any τ; a Hopf bifurcation, which requires a pair of roots to cross the imaginary axis transversally, is therefore excluded. □

Remark 12. *The mechanism is the cascade structure of the SEIR flow together with the delay entering only the incidence: in the right half-plane the gain polynomial P dominates the delay polynomial Q in modulus, whatever the phase $e^{-\lambda\tau}$ contributes, because each factor of P is at least as large as the corresponding factor of Q and the first one is strictly larger. The argument does not use the fractional order beyond the inclusion $\operatorname{Re}\lambda \geq 0 \Rightarrow \operatorname{Re}\lambda^\alpha \geq 0$, so the conclusion holds already in the integer-order case $\alpha = 1$, and the fractional memory only reinforces the damping of the transient. Sustained oscillations require a different feedback geometry: two delays as in the SEIRS model of Cooke and van den Driessche,[32] a delayed nonlinear incidence as in,[6] waning immunity as in,[34] or distributed latency kernels acting on both the exposed and the infectious classes as in the tuberculosis model of,[35] where the latency delay crossing a critical value does produce periodic solutions. Under the present formulation, larger τ produces a slower rise and a lower, later peak, and the transient settles at $\mathcal{E}^*$ in every case computed, as **Figure 2** illustrates.*

Remark 13. *For the stochastic model the endemic equilibrium is not an equilibrium of the mean dynamics, because $\mathbb{E}[S\,I(t-\tau)] \neq \mathbb{E}S \cdot \mathbb{E}I(t-\tau)$; **Theorem 9** therefore concerns the deterministic skeleton. The simulations of Section 8 show that, for moderate noise, the sample paths of the stochastic model fluctuate in a neighbourhood of $\mathcal{E}^*$ whose size grows with σ, without developing oscillations of their own.*

7. Optimal vaccination control

7.1. Formulation

We reinstate the vaccination control in the stochastic model **(1)** and seek to drive the infection down at acceptable cost over a fixed horizon $[0, T]$. Vaccination campaigns are planned in advance and cannot react to the unobservable environmental noise, so the admissible controls are open-loop schedules,

$$\mathcal{U} = \big\{u \in L^\infty(0,T) : \ 0 \leq u(t) \leq 1 \text{ for a.e. } t\big\},$$

and the cost functional, balancing the burden of infection against the expense of vaccination, is

$$J(u) = \mathbb{E}\left[\int_0^T \big(A\,I(t)^2 + B\,u(t)^2\big)\,dt\right], \qquad A, B > 0. \tag{31}$$

The control problem is to find $u^* \in \mathcal{U}$ with $J(u^*) = \min_{u\in\mathcal{U}} J(u)$. Throughout this section the standing assumptions (A1)-(A4) are in force, together with (H) when $\alpha < 1$ and $\sigma > 0$, so that for each $u \in \mathcal{U}$ **Theorem 2** provides a unique state X^u with $0 \leq S^u \leq \bar{S}$ and finite second moments on $[0, T]$; the map $u \mapsto X^u$ is the control-to-state map. We emphasise a structural feature that simplifies the analysis: the diffusion coefficient σI in **(1)** does not depend on u, so the control acts only through the drift, and it enters the drift linearly.

7.2. Existence of an optimal control

Theorem 10. *There exists an optimal control $u^* \in \mathcal{U}$ minimising **(31)**.*

Proof. The set $\mathcal{U}$ is convex, bounded and weakly-$*$ closed in $L^\infty(0,T)$, hence weakly-$*$ sequentially compact. Since $J \geq 0$, a minimising sequence $\{u_n\} \subset \mathcal{U}$ exists, and after extraction $u_n \rightharpoonup u^*$ weakly-$*$ in $L^\infty(0,T)$, equivalently weakly in $L^2(0,T)$, with $u^* \in \mathcal{U}$.

We claim that the states converge in $\mathcal{H}_T$: writing $X_n := X^{u_n}$ and $X^* := X^{u^*}$, we have $\sup_{t\le T}\mathbb{E}|X_n(t)-X^*(t)|^2 \to 0$. The key observation is that, for every bounded continuous function φ on $[0,T]$, the map $v \mapsto k*(v\varphi)$ is compact from $L^2(0,T)$ to $C[0,T]$, because the image of a bounded set is uniformly bounded and uniformly Hölder continuous of exponent $\alpha-\frac{1}{2}>0$ (Cauchy-Schwarz applied to the kernel); compact operators map weakly convergent sequences to strongly convergent ones, so $\|k*((u_n-u^*)\varphi)\|_\infty \to 0$, and the same holds with the resolvent kernel k_c in place of k, since $0<k_c\le k$ and k_c differs from k by a smooth bounded factor. We apply this pathwise with $\varphi = S^*(\omega,\cdot)$, which is bounded by $\bar{S}$, and use the ω-independent bound

$$\|k*((u_n-u^*)\varphi)\|_\infty \le \frac{2\bar{S}\,T^\alpha}{\Gamma(\alpha+1)}$$

to pass to expectations by dominated convergence.

On the first delay window the difference $d_n := S_n - S^*$ satisfies $d_n = k*\big(-a_n d_n - (u_n-u^*)S^*\big)$ with $a_n = \beta\phi_3(\cdot-\tau)+\mu+u_n \in [\mu,c]$, $c := \beta\|\phi_3\|_\infty+\mu+1$. By **(6)**, $d_n = k_c*\big((c-a_n)d_n - (u_n-u^*)S^*\big)$, and since the map $y\mapsto k_c*((c-a_n)y)$ has norm at most $(c-\mu)/c<1$ on $C[0,\tau]$, $\|d_n\|_\infty \le \frac{c}{\mu}\|k_c*((u_n-u^*)S^*)\|_\infty \to 0$ pathwise, hence in mean square. The exposed class is driven by the forcing $\beta S_n\phi_3(\cdot-\tau)$, which converges in mean square, so $E_n \to E^*$ in mean square by the linear estimate **(6)**; the infectious class then converges by the continuous dependence of **(11)** on its forcing, which is part of the contraction argument of **Lemma 6**; and the recovered class converges because its forcing $\gamma I_n + u_n S_n$ does, the product being handled through $u_nS_n - u^*S^* = u_n(S_n-S^*)+(u_n-u^*)S^*$. On the following windows the coefficient of the susceptible equation is $a_n = \beta I_n(\cdot-\tau)+\mu+u_n \ge \mu$, and subtracting the equations of S_n and S^* gives $d_n = k*(-a_nd_n+g_n)$ with $g_n := -\beta\big(I_n-I^*\big)(\cdot-\tau)\,S^* - (u_n-u^*)S^*$, in which the multiplier S^* is the same for all n. Applying **(6)** pathwise with $c=\sup a_n$, finite for each path, and comparing with the equation with coefficient μ as in the proof of **Lemma 3(ii)** gives $|d_n|\le k_\mu*|g_n|$, hence, by the Cauchy-Schwarz inequality with the kernel as weight and **(4)**, $\mathbb{E}|d_n(t)|^2 \le \mu^{-2}\sup_{s\le t}\mathbb{E}|g_n(s)|^2$. The two terms of g_n converge to zero in mean square, the first by the induction hypothesis and the boundedness of S^*, the second by the compactness argument. The remaining classes are handled as on the first window, and proceeding window by window gives the claim on $[0,T]$.

It follows that $\mathbb{E}\int_0^T A\,I_n^2\,dt \to \mathbb{E}\int_0^T A\,(I^*)^2\,dt$, while the term $\int_0^T B\,u^2\,dt$ is convex and strongly continuous on $L^2(0,T)$, hence weakly lower semicontinuous. Therefore $J(u^*)\le \liminf_n J(u_n) = \inf_{\mathcal{U}} J$, and u^* is optimal. □

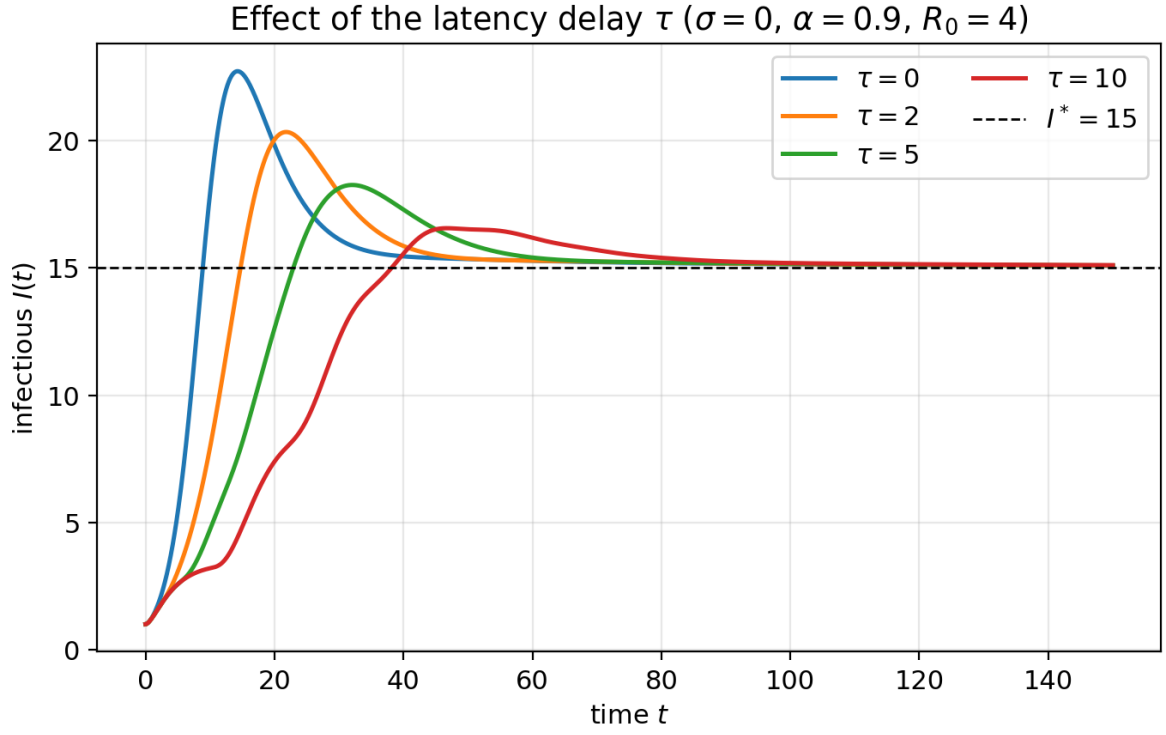


Figure 2. Influence of the delay τ on the infectious class of the deterministic skeleton ($\alpha=0.9$, $\sigma=0$). The endemic equilibrium is stable for all τ; the delay modulates only the transient, in agreement with **Theorem 9**.

7.3. Necessary conditions: the maximum principle

Because the noise coefficient is control-free and the control enters the drift linearly, the necessary conditions take a familiar projected form; what changes with respect to an ordinary differential equation is the adjoint equation, which must reflect the memory of the state through the kernel k and the delay through a time-advanced term. We first describe the structure in the deterministic skeleton, where the derivation is elementary, and then state the stochastic version.

Deterministic skeleton. Let $\sigma = 0$, and write $b(t, X, X_\tau, u)$ for the drift of **(1)**, with $X_\tau := X(t-\tau)$, and $\ell(X,u) := AI^2 + Bu^2$. For an admissible perturbation direction v (so that $u + \varepsilon v \in \mathcal{U}$ for small $\varepsilon > 0$), the first variation $Y := \frac{d}{d\varepsilon} X^{u+\varepsilon v}|_{\varepsilon=0}$ solves the linear delayed Volterra equation

$$\begin{aligned} Y(t) = \int_0^t k(t-s)\big(b_X(s)Y(s) + b_{X_\tau}(s) \\ Y(s-\tau) + b_u(s)v(s)\big)ds, \qquad Y|_{[-\tau,0]} = 0, \end{aligned} \tag{32}$$

where b_X, b_{X_τ}, b_u denote the partial Jacobians evaluated along (X^u, u), and $J'(u)v = \int_0^T \big(\ell_X(s)\cdot Y(s) + \ell_u(s)v(s)\big)ds$. Define the Hamiltonian

$$\begin{aligned} \mathcal{H}(t, X, X_\tau, u, p) := A\,I^2 + B\,u^2 + p_1\big(\Lambda - \beta S I_\tau - \mu S - \\ uS\big) + p_2\big(\beta S I_\tau - (\kappa+\mu)E\big) \\ + p_3\big(\kappa E - (\gamma+\mu)I\big) + \\ p_4\big(\gamma I - \mu R + uS\big), \end{aligned} \tag{33}$$

and let the adjoint $p = (p_1, \dots, p_4)$ be the solution of the backward Volterra equation

$$\begin{aligned} p(t) = \int_t^T k(s-t)\Big(\mathcal{H}_X(s) + \mathbf{1}_{[0,T-\tau]}(s) \\ \mathcal{H}_{X_\tau}(s+\tau)\Big)ds, \qquad t \in [0,T], \end{aligned} \tag{34}$$

where $\mathcal{H}_X(s)$ and $\mathcal{H}_{X_\tau}(s+\tau)$ are the gradients of **(33)** with respect to the current and the delayed state, evaluated along (X^u, u, p) at times s and $s+\tau$ respectively. **Equation (34)** is the integral form of ${}_tD_T^\alpha p = \mathcal{H}_X + \mathbf{1}_{[0,T-\tau]}\mathcal{H}_{X_\tau}(\cdot+\tau)$ with the terminal condition $p(T) = 0$, in agreement with the fractional maximum principle of Agrawal[38] and its delayed extension by Jarad, Abdeljawad and Baleanu;[39] it is a linear Volterra equation with the kernel $k(s-t)$ acting backward in time, and it has a unique continuous solution by the contraction argument of **Lemma 3** applied in reversed time, since the coefficients $\beta I(\cdot-\tau)$ and βS are bounded along the deterministic solution. Written out, with $\mathbf{1} := \mathbf{1}_{[0,T-\tau]}(t)$, the adjoint system reads

$$ {}_tD_T^\alpha p_1 = -p_1\big(\beta I(t-\tau) + \mu + u\big) + p_2\,\beta I(t-\tau) + p_4\,u, \tag{35}$$

$$ {}_tD_T^\alpha p_2 = -(\kappa+\mu)p_2 + \kappa p_3, \tag{36}$$

$$ {}_tD_T^\alpha p_3 = 2A\,I - (\gamma+\mu)p_3 + \gamma p_4 + \mathbf{1}\,\beta S(t+\tau)\big(p_2(t+\tau) - p_1(t+\tau)\big), \tag{37}$$

$$ {}_tD_T^\alpha p_4 = -\mu p_4, \qquad p_j(T) = 0, \quad j = 1,\dots,4. \tag{38}$$

Proposition 2. *Let $\sigma = 0$. For every admissible direction v,*

$$\begin{aligned} J'(u)v = \int_0^T \mathcal{H}_u(s)\,v(s)\,ds = \int_0^T \\ \big(2Bu(s) - (p_1(s) - p_4(s))S(s)\big)v(s)\,ds. \end{aligned}$$

Proof. Write $F := b_X Y + b_{X_\tau} Y_\tau + b_u v$ and $G := \ell_X + b_X^\top p + \mathbf{1}_{[0,T-\tau]}\, b_{X_\tau}(\cdot+\tau)^\top p(\cdot+\tau)$, so that **(32)** reads $Y = k * F$ and **(34)** reads $p(t) = \int_t^T k(s-t)G(s)ds$, because $\mathcal{H}_X = \ell_X + b_X^\top p$ and $\mathcal{H}_{X_\tau} = b_{X_\tau}^\top p$. By Fubini's theorem,

$$\begin{aligned} \int_0^T p(s)\cdot F(s)\,ds &= \int_0^T\!\!\int_s^T k(t-s)\,G(t)\cdot F(s)\,dt\,ds \\ &= \int_0^T G(t)\cdot\Big(\int_0^t k(t-s)F(s)ds\Big)dt \\ &= \int_0^T G\cdot Y\,dt. \end{aligned}$$

Expanding both sides and using $Y = 0$ on $[-\tau, 0]$ to write $\int_0^T p\cdot b_{X_\tau}Y_\tau\,ds = \int_0^{T-\tau}\big(b_{X_\tau}(t+\tau)^\top p(t+\tau)\big)\cdot Y(t)\,dt$, the terms containing b_X and b_{X_τ} cancel, and what remains is $\int_0^T \ell_X\cdot Y\,dt = \int_0^T (b_u^\top p)\,v\,ds$. Adding $\int_0^T \ell_u v\,ds$ gives the first equality, and $b_u = (-S, 0, 0, S)^\top$, $\ell_u = 2Bu$ give the second. □

Stochastic model. When $\sigma > 0$ the first variation Y carries the additional term $\sigma\int_0^t k(t-s)Y_3(s)\,dW(s)$, and the adjoint becomes a pair (λ, Z) solving a backward stochastic Volterra integral equation (BSVIE) in the sense of Yong:[44,45] with $G(\lambda)$ defined as above but with λ in place of p,

$$\begin{aligned} \lambda(t) = G(\lambda)(t) + \sigma\,\mathbf{e}_3\int_t^T k(s-t)\,Z_3(s,t)\,ds \\ - \int_t^T Z(t,s)\,dW(s), \\ p(t) := \int_t^T k(s-t)\lambda(s)\,ds, \end{aligned} \tag{39}$$

where $\mathbf{e}_3$ is the third unit vector, $Z(t,s)$ is adapted in s for each t, and the Hamiltonian adjoint p is the right fractional integral of λ. In the deterministic case $Z \equiv 0$, $\lambda = G(p)$, and p coincides with the solution of **(34)**. The duality relation of **Proposition 2** then holds in expectation, $J'(u)v = \int_0^T \mathbb{E}\big[\mathcal{H}_u(s)\big]v(s)\,ds$, with p given by **(39)**; this is the duality principle for stochastic Volterra integral equations [45, Section 5], extended to a delayed drift in[48] and to singular kernels of the type k in.[49] Existence and uniqueness of an adapted solution (λ, Z) with $\mathbb{E}\int_0^T |\lambda|^2 dt < \infty$ follow from the well-posedness theory of BSVIEs with Lipschitz generators,[45] the coefficients of G being the bounded process βS and the square-integrable process $\beta I(\cdot - \tau)$. Because the diffusion does not depend on u, the process Z does not enter $\mathcal{H}_u$, so it plays no role in characterising the optimal control and only the component p is needed below.

Theorem 11. *Let $u^* \in \mathcal{U}$ be optimal with state X^*, and let p^* be the Hamiltonian adjoint associated with (X^*, u^*), that is, the solution of **(34)** when $\sigma = 0$ and the process p of **(39)** when $\sigma > 0$. Then, for a.e. $t \in [0,T]$,*

$$u^*(t) = \min\left\{1,\ \max\left\{0,\ \frac{\mathbb{E}\big[(p_1^*(t) - p_4^*(t))S^*(t)\big]}{2B}\right\}\right\}, \quad (40)$$

the expectation being superfluous when $\sigma = 0$.

Proof. For any $u \in \mathcal{U}$ and $\varepsilon \in (0,1]$ the control $u^* + \varepsilon(u - u^*)$ is admissible by convexity, so optimality gives $J'(u^*)(u - u^*) \geq 0$. By **Proposition 2** and its stochastic version,

$$\int_0^T \Big(2Bu^*(t) - \mathbb{E}\big[(p_1^*(t) - p_4^*(t))S^*(t)\big]\Big) \big(u(t) - u^*(t)\big)dt \geq 0 \qquad \text{for all } u \in \mathcal{U}.$$

Since the integrand is affine in $u(t)$ and $u(t)$ ranges over the whole interval $[0,1]$ pointwise, the variational inequality is equivalent to the pointwise statement that $u^*(t)$ minimises the strictly convex function $w \mapsto Bw^2 - \mathbb{E}[(p_1^* - p_4^*)S^*](t)\,w$ over $[0,1]$ for a.e. t; the unconstrained minimiser is $w = \mathbb{E}[(p_1^* - p_4^*)S^*](t)/(2B)$, and its projection onto $[0,1]$ is **(40)**. □

The optimal triple (X^*, p^*, u^*) is thus the solution of the coupled forward state system **(1)** and backward adjoint system **(35)**-**(38)** (or **(39)**), closed by **(40)**.

Remark 14. *Since the cost does not involve R and the recovered class feeds back into no other equation, **(38)** with $p_4(T) = 0$ gives $p_4 \equiv 0$, so the control is governed by the susceptible adjoint alone, $u^* = \min\{1, \max\{0, \mathbb{E}[p_1 S]/(2B)\}\}$. The control switches on only when the marginal value of protecting a susceptible, measured by p_1, is positive, and its intensity scales with the susceptible stock S. A larger infection weight A raises p_3 through **(37)**, propagates into p_2 through **(36)** and into p_1 through the delayed incidence term of **(35)**, intensifying vaccination; a larger cost weight B flattens **(40)**, tempering it. The advanced term in **(37)** reflects that an infectious individual at time t infects susceptibles at time $t + \tau$, so the value of removing infection at t is assessed one latent period ahead; the indicator switches this term off in the last latent period before the horizon, where such infections no longer contribute to the cost. Finally, when $\sigma > 0$ the expectation in **(40)** averages the adjoint over the noise; replacing it by the adjoint of the deterministic skeleton is the certainty-equivalent approximation used in the computations of Section 8, whose performance on the noisy model is assessed there.*

Remark 15. *The optimality system is Lipschitz in (X, p) on the invariant region, and the terminal-initial split makes it a two-point boundary value problem in the fractional sense. A standard contraction argument then yields uniqueness of the optimal control provided the horizon T is sufficiently small, the smallness being dictated, as in the existence proof of the state system, by the singular kernel $(t-s)^{\alpha-1}$ and the magnitude of σ.*

8. Numerical simulations

The purpose of this section is threefold: to describe, in reproducible detail, the discretisation used to integrate the Caputo fractional stochastic delay system **(1)**; to verify its convergence quantitatively against closed-form and reference solutions; and to confront the qualitative predictions of Sections 3-7 with computation. All routines were written in Python 3 using `NumPy` for the array algebra, `SciPy` and `mpmath` for the special functions (Γ and the Mittag-Leffler evaluation), and `Matplotlib` for the figures. Each stochastic trajectory is one realisation of the noise; reported sample statistics (means, medians and one-standard-deviation envelopes) are Monte Carlo averages over M independent paths generated from a fixed seed, so that every figure can be regenerated bit-for-bit; the number M is stated with each experiment and is 2,000 in most of them, smaller values being used when the memory cost of the fractional scheme or the length of the horizon dictates it.

8.1. The numerical scheme

Fix a horizon T, a step $h = T/N$ and grid points $t_n = nh$. We assume the delay is commensurate

with the grid, $\tau = m_0 h$ for an integer $m_0 \geq 1$, and we store the prescribed history Φ on the auxiliary nodes $t_{-m_0}, \ldots, t_0$ so that a delayed value $I(t_n - \tau)$ is read off as I_{n-m_0}. Writing the system in the generic vector form

$$ {}^{C}D_t^{\alpha} X(t) = f\big(X(t), X(t-\tau)\big) + g\big(X(t)\big)\dot{W}(t), \qquad X = (S, E, I, R)^{\top}, $$

with $g(X) = (0, 0, \sigma I, 0)^{\top}$, the equivalent Volterra form **(7)-(10)** is discretised by combining the fractional Adams-Bashforth-Moulton (ABM) predictor-corrector method of Diethelm, Ford and Freed,[50,51] in the delayed form of Bhalekar and Daftardar-Gejji,[52] for the deterministic memory integral with a fractional Euler-Maruyama step, in the spirit of,[21,23] for the stochastic convolution.

Predictor (fractional Adams-Bashforth):

$$ X^{P}_{n+1} = X_0 + \frac{1}{\Gamma(\alpha)} \sum_{j=0}^{n} b_{j,n+1}\, f\big(X_j, X_{j-m_0}\big) + \frac{1}{\Gamma(\alpha)} \sum_{j=0}^{n} c_{j,n+1}\, g(X_j)\, \Delta W_j, \tag{41} $$

with predictor weights

$$ b_{j,n+1} = \frac{h^{\alpha}}{\alpha}\Big[(n+1-j)^{\alpha} - (n-j)^{\alpha}\Big]. $$

Corrector (fractional Adams-Moulton):

$$ X_{n+1} = X_0 + \frac{h^{\alpha}}{\Gamma(\alpha+2)}\Big[f\big(X^{P}_{n+1}, X_{n+1-m_0}\big) + \sum_{j=0}^{n} a_{j,n+1}\, f\big(X_j, X_{j-m_0}\big)\Big] + \frac{1}{\Gamma(\alpha)} \sum_{j=0}^{n} c_{j,n+1}\, g(X_j)\, \Delta W_j, \tag{42} $$

where the corrector weights are

$$ a_{j,n+1} = \begin{cases} n^{\alpha+1} - (n-\alpha)(n+1)^{\alpha}, & j = 0, \\ (n-j+2)^{\alpha+1} + (n-j)^{\alpha+1} - 2(n-j+1)^{\alpha+1}, & 1 \leq j \leq n. \end{cases} $$

The stochastic increments are $\Delta W_j = W(t_{j+1}) - W(t_j) \sim \mathcal{N}(0, h)$, independent across j, and the singular kernel in the diffusion convolution is replaced on each subinterval by its mean value,

$$ c_{j,n+1} = \frac{1}{h}\int_{t_j}^{t_{j+1}} (t_{n+1} - s)^{\alpha-1}\, ds = \frac{h^{\alpha-1}}{\alpha}\Big[(n+1-j)^{\alpha} - (n-j)^{\alpha}\Big], $$

which is the fractional analogue of the Euler-Maruyama rule; the same stochastic sum is used in the predictor and in the corrector, so that the noise is treated explicitly. When $\tau = 0$ the delayed argument X_{n+1-m_0} in the corrector is replaced by the predictor X^{P}_{n+1}. For $\alpha = 1$ the memory sums collapse to the trapezoidal rule and the scheme reduces to the classical Heun predictor-corrector with an Euler-Maruyama step; the long-horizon runs of Section 8.11 use this recursive form, whose cost is linear rather than quadratic in N. The procedure is summarised below.

8.2. Computational procedure

(1) Load the history $\{X_{-m_0}, \ldots, X_0\}$ from Φ and draw the increments $\{\Delta W_j\}$.
(2) For each $n = 0, 1, \ldots, N-1$: evaluate the drift over the past nodes, form the predictor X^{P}_{n+1} from **(41)**, then the corrector X_{n+1} from **(42)**, reading the delayed argument as X_{n+1-m_0}.
(3) Repeat over M realisations and average to obtain sample means and envelopes.

Remark 16. *Two features of the delayed problem deserve comment. First, the history is sampled at the auxiliary nodes and is required to be continuous at $t = 0$, with $\Phi(0) = X_0$; no discontinuity is therefore introduced at the start, and on the first window $[0, \tau]$ the delayed factor is a known function, so that the scheme integrates a fractional equation with a smooth forcing. Second, the solution of a delay equation has a derivative discontinuity at $t = \tau$ (the breaking point where the history is replaced by the computed solution), and the solution of a Caputo equation carries the singular term t^{α} at the origin. Both features are absorbed by the product-integration weights, which are exact for piecewise linear integrands: the convergence orders measured in Section 8.4 on the delayed problem, whose reference solution contains both singularities, show no degradation. The shape of the history does influence the early transient, as **Figure 3** shows for three histories sharing the same value at $t = 0$: a history that grows towards $t = 0$ (a rising epidemic before the observation window) delays the outbreak, a decaying history advances it, the curves differ by at most 1.3 infectious individuals during the rise, and the three trajectories are within $3 \cdot 10^{-3}$ of each other by $t = 60$, as the delay-independent stability of **Theorem 9** predicts.*

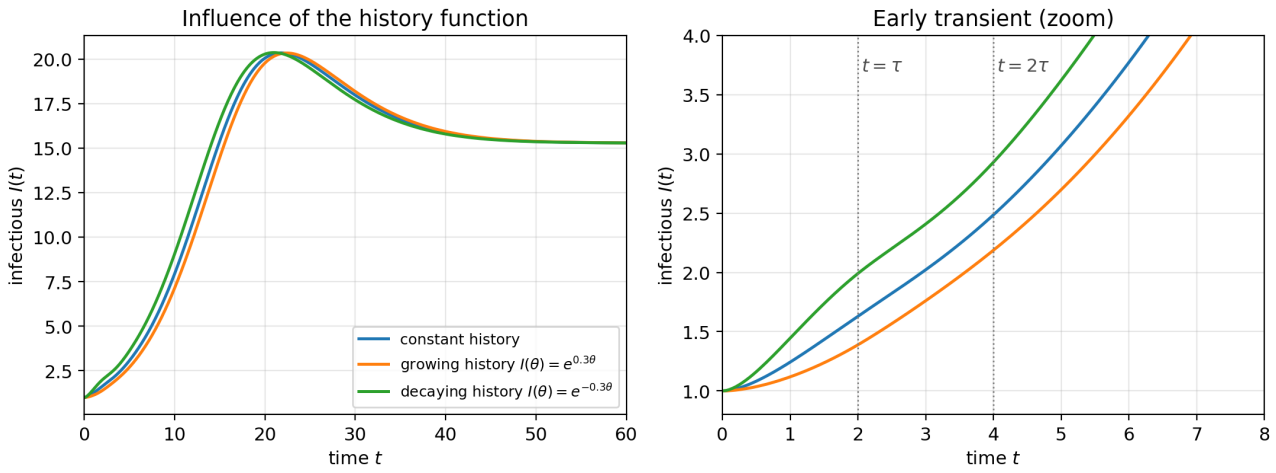


Figure 3. Influence of the history function on the infectious class ($\alpha = 0.9$, $\tau = 2$, $\sigma = 0$): constant history, exponentially growing history and exponentially decaying history, all with $I(0) = 1$. Right: zoom on the first latent periods; the dotted lines mark $t = \tau$ and $t = 2\tau$.

8.3. Convergence and structure preservation of the scheme

The numerical experiments rest on three guarantees: the deterministic memory is integrated to high order, the stochastic forcing is captured in mean square, and the discrete dynamics respect the conservation structure of the model. We make these precise.

Theorem 12. *Let $\sigma = 0$ and suppose the exact solution of **(1)** is twice continuously differentiable on $[0, T]$ and the drift f is Lipschitz on the invariant region Ω. Then the predictor-corrector scheme **(41)-(42)** converges, and*

$$\max_{0\le n\le N} \big|X(t_n) - X_n\big| = O\Big(h^{\min\{2,\,1+\alpha\}}\Big).$$

Sketch. The corrector is the product-integration (fractional trapezoidal) rule for the Volterra equation, whose local truncation error on a smooth integrand is $O(h^{1+\alpha})$ for $0 < \alpha < 1$ and $O(h^2)$ in the limit $\alpha \to 1$; the predictor (fractional rectangle rule) is one order lower and feeds the corrector without degrading its order. Subtracting the exact product-integration identity from **(42)**, bounding the drift differences by the Lipschitz constant and absorbing the convolution through the discrete fractional Gronwall inequality propagates the local error to the stated global rate; the delayed argument is handled window by window exactly as in **Theorem 2**, see.[51,52] The smoothness hypothesis is the usual one; if the solution carries the typical weak singularity t^α at the origin, the order is reduced, as quantified in,[51] and can be recovered by correction terms in the starting weights. □

Theorem 13. *Let $\alpha \in (\frac{1}{2}, 1]$ and assume f, g are globally Lipschitz with linear growth on Ω. Then the fractional Euler-Maruyama scheme **(41)** and **(42)** is mean-square convergent,*

$$\max_{0\le n\le N} \mathbb{E}\big|X(t_n) - X_n\big|^2 \longrightarrow 0 \qquad (h \to 0),$$

*and, for sufficiently regular coefficients, the rate is of order $h^{2\alpha-1}$ in mean square, that is, of order $\alpha - \frac{1}{2}$ for the root-mean-square error. The threshold $\alpha > \frac{1}{2}$ is exactly the condition under which the stochastic convolution has finite variance, so it governs both the well-posedness of **(1)** and the convergence of its discretisation.*

Sketch. Let $\varepsilon_n = X(t_n) - X_n$. Subtracting the scheme from the exact Volterra identity splits the one-step error into a drift part and a diffusion part. The drift part is handled as in **Theorem 12**. For the diffusion part, the Itô isometry converts the frozen-kernel error into $\sum_j \int_{t_j}^{t_{j+1}} \big[(t_{n+1} - s)^{\alpha-1} - c_{j,n+1}\big]^2 \mathbb{E}|g|^2\, ds$, whose summability requires $2\alpha - 2 > -1$, i.e. $\alpha > \frac{1}{2}$, and yields a contribution of order $h^{2\alpha-1}$. Taking expectations, using the Lipschitz bounds and the discrete fractional Gronwall inequality closes the estimate and gives mean-square convergence at the stated rate; this is the rate established for the Euler-Maruyama scheme for Caputo stochastic equations in[21] and for their delayed version in.[23] □

Proposition 3. *The quadrature weights $b_{j,n+1}$ and $a_{j,n+1}$ are nonnegative for $\alpha \in (0, 1]$. Consequently the discrete total population $N_n = S_n + E_n + I_n + R_n$ obeys, in expectation, the same bound as its continuous counterpart up to the truncation error: there is $C > 0$ with*

$$\mathbb{E}\, N_n \le \max\Big\{N_0, \tfrac{\Lambda}{\mu}\Big\} + C\, h^{\min\{2,1+\alpha\}}, \qquad 0 \le n \le N.$$

Proof. Nonnegativity of $b_{j,n+1}$ is immediate, and that of $a_{j,n+1}$ for $1 \le j \le n$ follows from the convexity of $x \mapsto x^{\alpha+1}$; the endpoint weights are nonnegative by direct inspection. Summing the four discrete equations removes the control through $-uS + uS$ and leaves a discrete fractional recursion for N_n driven by $\Lambda - \mu N$ plus the mean-zero increments $\sigma I\,\Delta W$. Taking expectations annihilates the stochastic sum; the nonnegative weights make the resulting recursion a discrete comparison scheme for ${}^{C}D_t^{\alpha}\mathbb{E}N = \Lambda - \mu\,\mathbb{E}N$, whose solution is bounded by $\max\{N_0, \Lambda/\mu\}$. The defect is the quadrature error of **Theorem 12**. □

Remark 17. *The explicit Euler-Maruyama step does not preserve positivity at finite h: the most recent increment enters I_{n+1} with the weight $c_{n,n+1}\sigma I_n \Delta W_n/\Gamma(\alpha)$, so that a single increment with $\Delta W_n < -\alpha\Gamma(\alpha)h^{1-\alpha}/\sigma$ drives I_{n+1} below zero even when the exact solution is positive. The probability of such an increment in one step is $\mathbb{P}(\xi < -\alpha\Gamma(\alpha)/\kappa_h)$ with ξ standard normal and*

$$\kappa_h := \frac{\sigma\, h^{\alpha-\frac{1}{2}}}{\alpha\Gamma(\alpha)}, \tag{43}$$

*which tends to zero as $h \to 0$ for every $\alpha > \frac{1}{2}$, but slowly when α is close to $\frac{1}{2}$. The quantity κ_h is therefore the relevant step-size indicator for fractional stochastic simulations near extinction, where I is small and negative excursions matter; the experiments below keep κ_h below about 0.22 except where the effect of refinement is studied deliberately (**Table 2**).*

8.4. Verification of the convergence orders

Theorems 12 and **13** are checked on three test problems. The first is the linear equation ${}^{C}D_t^{\alpha}N = \Lambda - \mu N$ satisfied by the total population of the deterministic model, whose exact solution is the Mittag-Leffler formula of **Lemma 7** with $N(0) = 60$; here the error is measured against the closed form. The second is the deterministic delayed SEIR model with the baseline parameters of **Table 4**, $\sigma = 0$, $\tau = 2$ and the constant history $(98, 1, 1, 0)$, for which no closed form exists; the error is measured against a reference solution computed with the same scheme at $h_{\mathrm{ref}} = 2^{-9}$, on $[0, 20]$, in the maximum over the common grid points of the Euclidean norm of the state error. The third is the stochastic model with $\sigma = 0.2$, $\tau = 2$ and $M = 200$ Brownian paths, for which the coarse-grid increments are obtained by summing the fine-grid increments of a reference solution at $h_{\mathrm{ref}} = 2^{-5} \cdot 0.1$ on $[0, 10]$, and the root-mean-square error $\max_n(\mathbb{E}|X(t_n) - X_n|^2)^{1/2}$ is estimated from the sample. **Table 3** reports the errors and the observed orders $\log_2(e_h/e_{h/2})$, and **Figure 4** displays them.

Table 3. Errors and observed convergence orders of the scheme. Deterministic problems: maximum error over the grid; stochastic problem: root-mean-square error over 200 paths, sup over grid points. The theoretical orders are $\min\{2, 1+\alpha\}$ for the deterministic scheme on a smooth solution and $\alpha - \frac{1}{2}$ for the root-mean-square error of the stochastic scheme.

Linear test problem (error against the Mittag-Leffler solution)						
h	**0.5**	**0.25**	**0.125**	**0.0625**	**0.03125**	**observed order**
$\alpha = 0.6$	$1.51 \cdot 10^{-2}$	$7.53 \cdot 10^{-3}$	$3.56 \cdot 10^{-3}$	$1.63 \cdot 10^{-3}$	$7.33 \cdot 10^{-4}$	1.00, 1.08, 1.13, 1.15
$\alpha = 0.8$	$5.31 \cdot 10^{-3}$	$2.09 \cdot 10^{-3}$	$7.57 \cdot 10^{-4}$	$2.63 \cdot 10^{-4}$	$8.90 \cdot 10^{-5}$	1.34, 1.47, 1.53, 1.56
$\alpha = 0.9$	$4.65 \cdot 10^{-3}$	$1.22 \cdot 10^{-3}$	$3.25 \cdot 10^{-4}$	$8.71 \cdot 10^{-5}$	$2.34 \cdot 10^{-5}$	1.93, 1.91, 1.90, 1.90
$\alpha = 1.0$	$6.37 \cdot 10^{-3}$	$1.56 \cdot 10^{-3}$	$3.87 \cdot 10^{-4}$	$9.63 \cdot 10^{-5}$	$2.40 \cdot 10^{-5}$	2.03, 2.01, 2.01, 2.00
Delayed SEIR model, $\sigma = 0$ (error against the reference solution at $h_{\mathrm{ref}} = 2^{-9}$)						
$\alpha = 0.6$	$2.28 \cdot 10^{-1}$	$7.23 \cdot 10^{-2}$	$2.29 \cdot 10^{-2}$	$7.33 \cdot 10^{-3}$	$2.35 \cdot 10^{-3}$	1.66, 1.66, 1.65, 1.64
$\alpha = 0.8$	$2.75 \cdot 10^{-1}$	$7.37 \cdot 10^{-2}$	$2.02 \cdot 10^{-2}$	$5.63 \cdot 10^{-3}$	$1.58 \cdot 10^{-3}$	1.90, 1.87, 1.84, 1.83
$\alpha = 0.9$	$2.73 \cdot 10^{-1}$	$6.82 \cdot 10^{-2}$	$1.75 \cdot 10^{-2}$	$4.59 \cdot 10^{-3}$	$1.21 \cdot 10^{-3}$	2.00, 1.96, 1.93, 1.93
$\alpha = 1.0$	$2.59 \cdot 10^{-1}$	$6.09 \cdot 10^{-2}$	$1.47 \cdot 10^{-2}$	$3.62 \cdot 10^{-3}$	$8.96 \cdot 10^{-4}$	2.09, 2.05, 2.02, 2.02
Stochastic delayed SEIR model, $\sigma = 0.2$ (root-mean-square error, $M = 200$)						
h	0.2	0.1	0.05	0.025		observed order (theory)
$\alpha = 0.75$	$5.39 \cdot 10^{-1}$	$4.51 \cdot 10^{-1}$	$3.62 \cdot 10^{-1}$	$3.09 \cdot 10^{-1}$		0.26, 0.32, 0.23 (0.25)
$\alpha = 0.90$	$3.81 \cdot 10^{-1}$	$2.94 \cdot 10^{-1}$	$2.10 \cdot 10^{-1}$	$1.57 \cdot 10^{-1}$		0.37, 0.49, 0.41 (0.40)
$\alpha = 1.00$	$3.27 \cdot 10^{-1}$	$2.39 \cdot 10^{-1}$	$1.58 \cdot 10^{-1}$	$1.07 \cdot 10^{-1}$		0.45, 0.60, 0.56 (0.50)

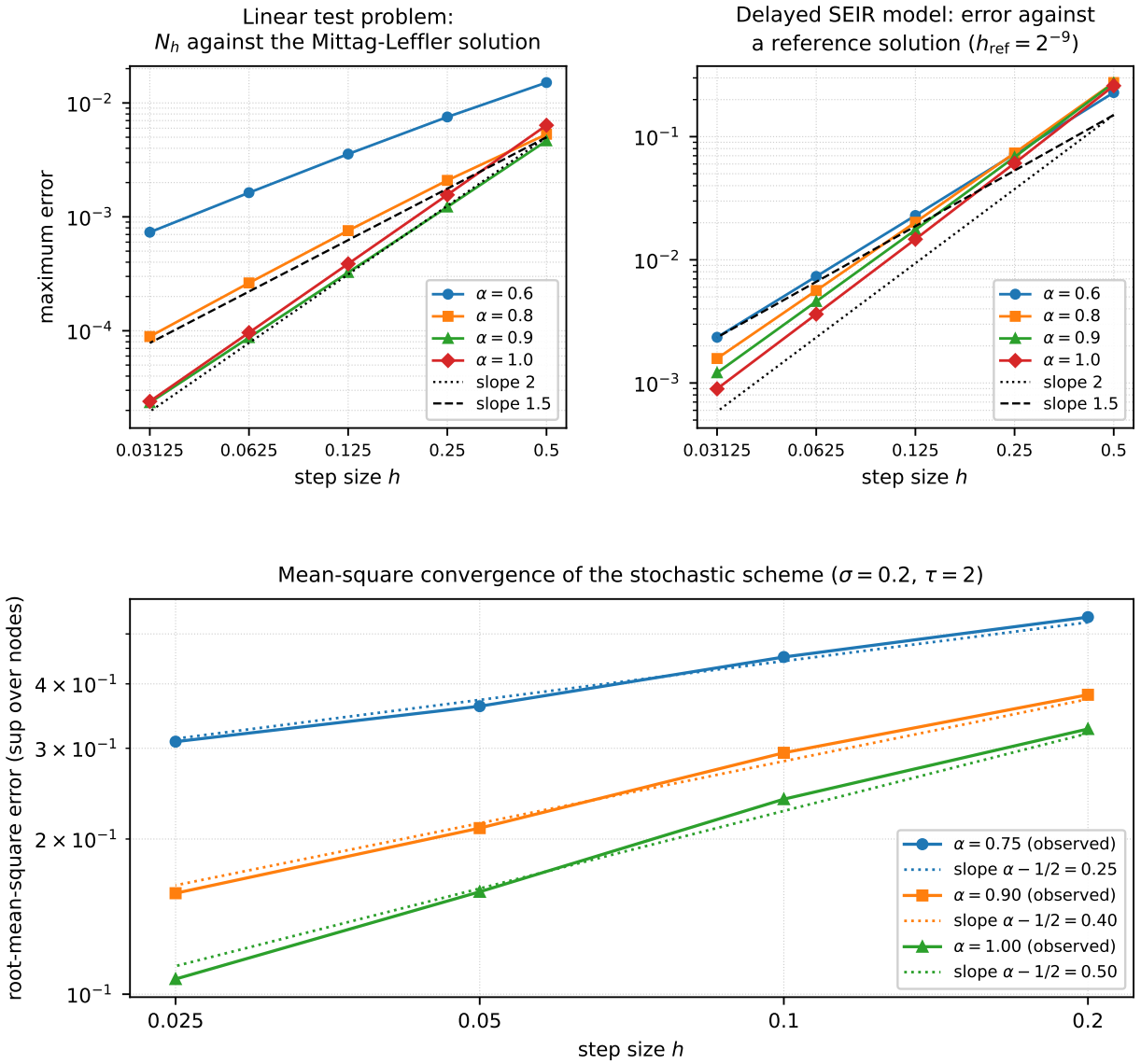


Figure 4. Convergence of the scheme. Top left: linear test problem against the Mittag-Leffler solution. Top right: delayed SEIR model against a reference solution. Bottom: root-mean-square error of the stochastic scheme, with the theoretical slopes $\alpha - \frac{1}{2}$.

On the delayed SEIR model the observed orders, between 1.64 and 1.66 for $\alpha = 0.6$, 1.83 and 1.90 for $\alpha = 0.8$, 1.93 and 2.00 for $\alpha = 0.9$, and 2.02 and 2.09 for $\alpha = 1$, match the rate $\min\{2, 1+\alpha\}$ of **Theorem 12** closely, in spite of the breaking point at $t = \tau$. On the linear problem, whose solution behaves like t^α at the origin and whose Caputo derivative is therefore not smooth there, the order drops to about 1.15 and 1.56 for $\alpha = 0.6$ and 0.8, close to 2α, while it stays near 2 for $\alpha \geq 0.9$; this is the reduction of order for solutions of limited smoothness analysed in,[51] and the absolute errors remain below $2 \cdot 10^{-3}$ for $h \leq 0.0625$ in every case. For the stochastic scheme the root-mean-square orders fluctuate around the theoretical values $\alpha - \frac{1}{2} = 0.25$, 0.40 and 0.50, as expected from a sample estimate with 200 paths, and the errors decrease monotonically under refinement. The scheme therefore delivers the accuracy claimed in **Theorems 12** and **13**, and the baseline step $h = 0.1$ used below produces errors of order 10^{-2} on the deterministic trajectories, well below the effects being studied.

8.5. Parameter values

Table 4 lists the baseline parameters. Because the incidence is of mass-action type, βSI, and the disease-free susceptible level $S_0 = \Lambda/\mu$ is large, the transmission coefficient is correspondingly small; the value $\beta = 0.02$ places the system in a clearly supercritical but realistic regime.

With these values $R_0 = \beta\Lambda\kappa/[\mu(\kappa+\mu)(\gamma+\mu)] = 4 > 1$, so by **Theorem 6** the endemic equilibrium exists and, by **(24)**-**(25)**, equals $(25, 15, 15, 45)$, with $N^* = 100 = \Lambda/\mu$ as it must. The history is the constant $(S, E, I, R) = (98, 1, 1, 0)$ on $[-\tau, 0]$,

so that $N(0) = 100$, and the step is $h = 0.1$ unless stated otherwise. Unless stated otherwise these values are used throughout; the experiments that probe other regimes announce their changes explicitly.

8.6. Baseline dynamics of the four compartments

Figure 5 shows the four compartments at the baseline parameters, for the deterministic skeleton and for the stochastic model with $\sigma = 0.2$ ($M = 2{,}000$ paths). Starting from a single exposed and a single infectious individual, the susceptible pool is depleted from 98 to a minimum of about 22 near $t = 28$ and then recovers towards $S^* = 25$; the exposed and infectious classes peak at 22.2 ($t \approx 18$) and 20.3 ($t \approx 22$) respectively and relax to 15; the recovered class saturates near 45. The sample mean of the noisy model is indistinguishable from the deterministic trajectory on the scale of the figure, in agreement with the fact that the noise has zero mean, while the one-standard-deviation envelope of the infectious class settles at ± 3.7 around I^*, that is, a coefficient of variation of about 25% for $\sigma = 0.2$. The recovered class inherits a wider envelope, because it accumulates the fluctuations of I through γI and is damped only by the slow rate μ. None of the 2,000 paths left the positive cone.

Table 4. Baseline parameters and derived quantities used in the simulations (rates in time$^{-\alpha}$, see **Remark 2**).

Parameter	Description	Value
Λ	Recruitment rate	10
β	Transmission coefficient	0.02
μ	Natural death rate	0.1
κ	Progression rate (E→I)	0.4
γ	Recovery rate	0.3
σ	Noise intensity	0.2
τ	Incubation delay	2
α	Fractional order	0.9
Derived: $S_0 = \Lambda/\mu = 100$, $R_0 = 4$, $\mathcal{E}^* = (S^*, E^*, I^*, R^*) = (25, 15, 15, 45)$.		

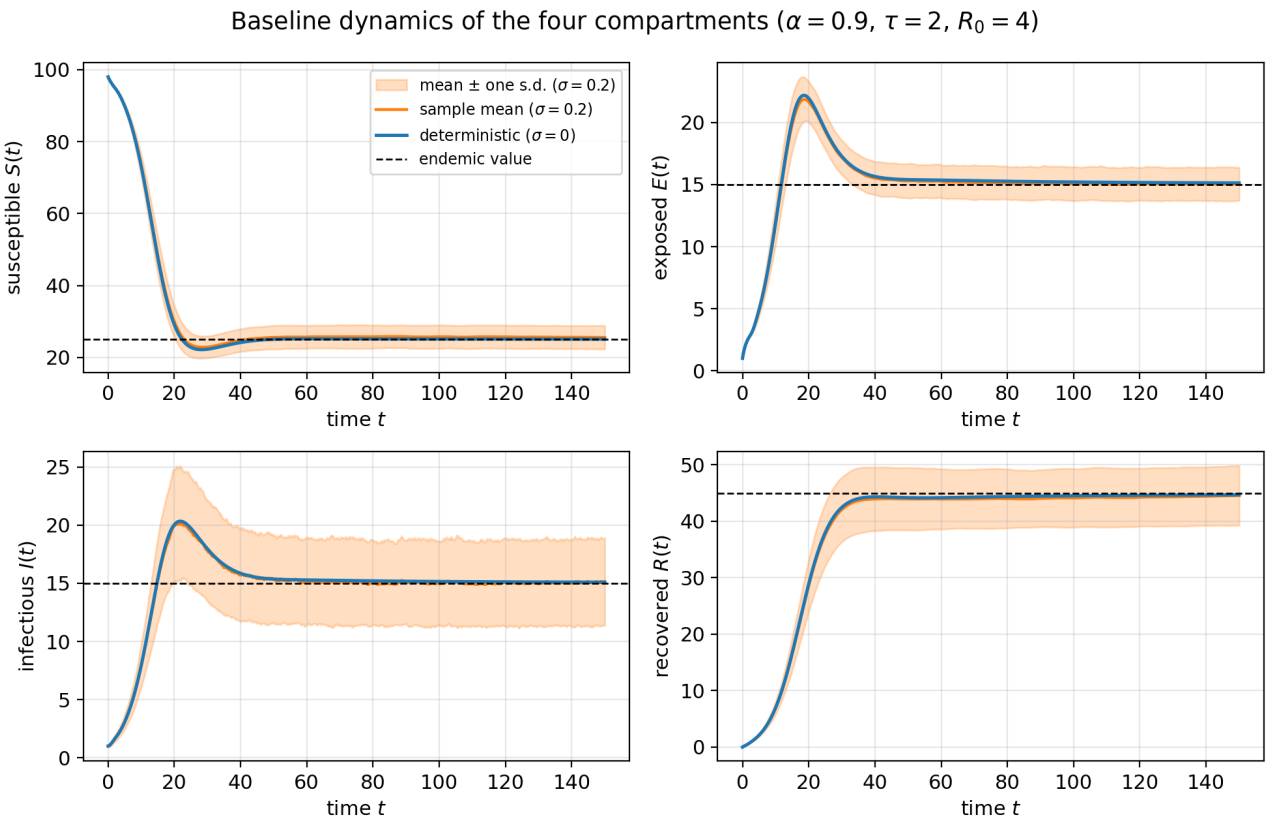


Figure 5. Baseline dynamics of S, E, I and R for the deterministic skeleton ($\sigma = 0$) and for the stochastic model ($\sigma = 0.2$, sample mean and one-standard-deviation envelope over 2,000 paths), with $\alpha = 0.9$, $\tau = 2$ and $R_0 = 4$. Dashed lines: endemic values.

8.7. Effect of the fractional order α

A point worth stressing at the outset is that the endemic equilibrium **(24)** is independent of α: the order shapes the transient, not the destination. **Figure 6** accordingly shows several values of α relaxing to the same endemic level. As α decreases, the memory kernel lengthens, the initial growth slows, the epidemic peak is lowered and delayed, and the approach to $\mathcal{E}^*$ becomes algebraic (Mittag-Leffler) rather than exponential. Quantitatively, the peak of I falls from 20.7 at $t = 19$ for $\alpha = 1$ to 20.3 ($t = 22$), 19.9 ($t = 26$), 19.4 ($t = 32$) and 18.9 ($t = 44$) for $\alpha = 0.9$, 0.8, 0.7 and 0.6; at $t = 150$ the deterministic trajectory is within 0.1 of I^* for $\alpha \geq 0.9$ but still 1.75 above it for $\alpha = 0.6$, which is the visible signature of the slow Mittag-Leffler relaxation $E_\alpha(-ct^\alpha) \sim t^{-\alpha}/(c\,\Gamma(1-\alpha))$. This is the quantitative meaning of the "stabilising memory" often invoked informally.

8.8. Effect of the delay and the absence of oscillations

Theorem 9 asserts that the delay cannot destabilise the endemic equilibrium. **Figure 2** confirms this for $\tau \in \{0, 2, 5, 10\}$: larger τ produces a slower rise and a lower, later peak, from 22.7 at $t = 14$ for $\tau = 0$ to 20.3 ($t = 22$), 18.3 ($t = 32$) and 16.6 ($t = 47$) for $\tau = 2$, 5 and 10, and every trajectory settles at $I^* = 15$ without any sustained oscillation; the overshoot above I^* decreases with τ rather than increasing, which is the opposite of what a delay-induced instability would produce. The small shoulders visible on the $\tau = 10$ curve at multiples of τ are the breaking points of the delay equation, where the delayed argument switches from the history to the computed solution. The delay does modify timing, and hence the value of early intervention (Section 8.12), but not the long-run outcome.

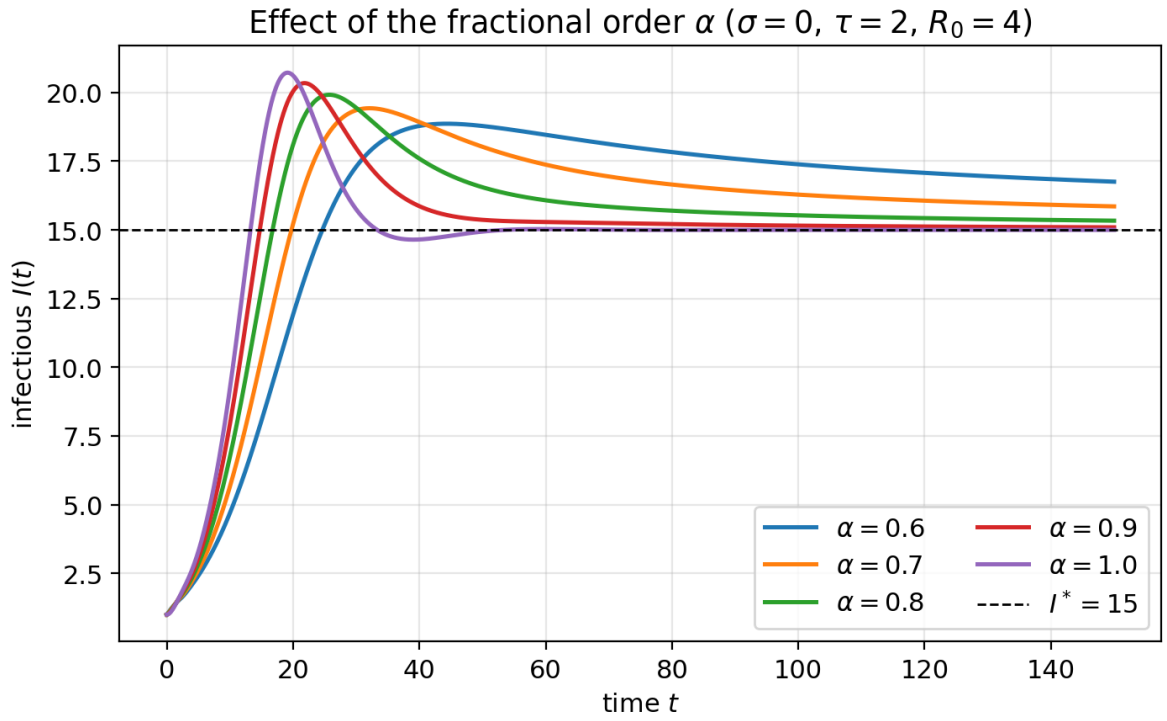


Figure 6. Effect of the fractional order α on the infectious population $I(t)$ for the deterministic skeleton ($\sigma = 0$, $\tau = 2$). The endemic level is common to all orders; only the transient differs.

8.9. Effect of the transmission rate β

Both the threshold $R_0 = \beta\Lambda\kappa/[\mu(\kappa+\mu)(\gamma+\mu)]$ and the endemic burden I^* increase with β. **Figure 7** traces $I(t)$ across a range of β straddling the critical value $\beta_c = \mu(\kappa+\mu)(\gamma+\mu)/(\Lambda\kappa) = 0.005$ at which $R_0 = 1$: below β_c the infection dies out, above it the system settles at an endemic level that grows with β. For $\beta = 0.004$ ($R_0 = 0.8$) the infectious class decays monotonically from 1 to 0.06 at $t = 150$, the slow tail again reflecting the Mittag-Leffler relaxation; for $\beta = 0.008$ ($R_0 = 1.6$) it rises without a pronounced peak to the endemic level 7.5; for $\beta = 0.02$ ($R_0 = 4$) and $\beta = 0.04$ ($R_0 = 8$) the peaks reach 20.3 and 26.7 and the endemic levels 15 and 17.5. The endemic level saturates as β grows, because $I^* = \kappa\Lambda(1 - 1/R_0)/[(\kappa+\mu)(\gamma+\mu)] \leq 20$, whereas the peak keeps increasing, so that contact reduction is most valuable for limiting the peak burden. This makes quantitatively visible why contact-reduction measures, which act directly on β, are so effective.

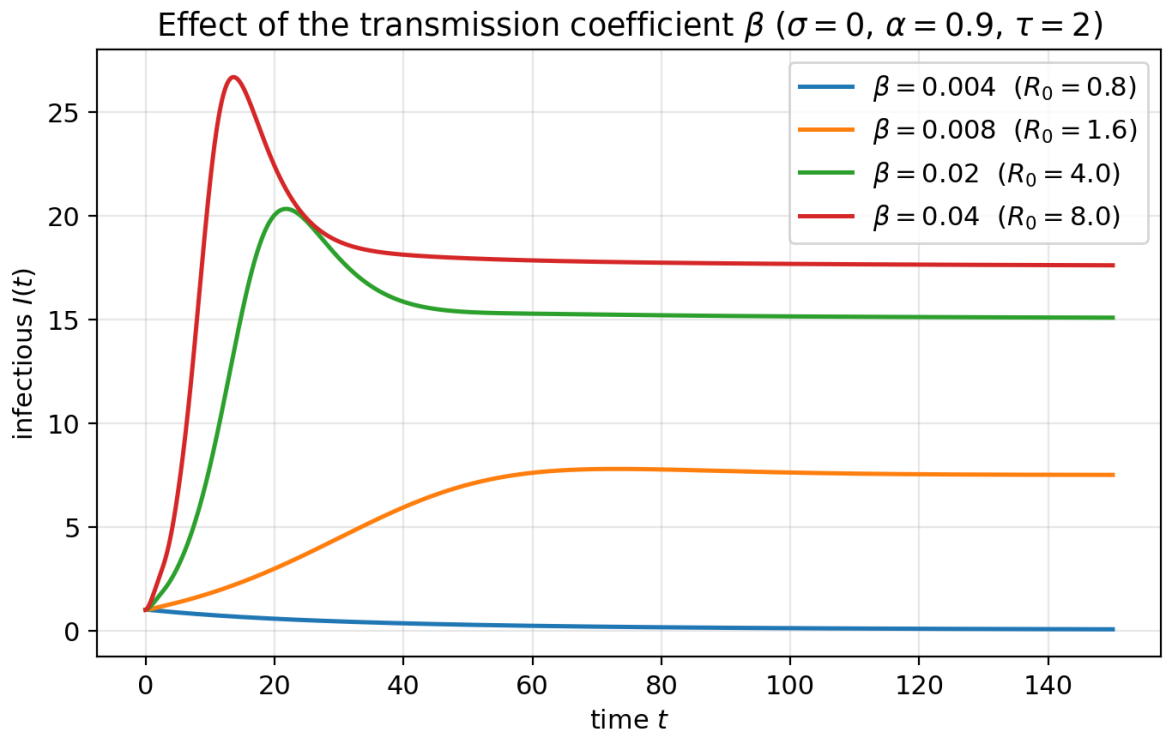


Figure 7. Effect of the transmission coefficient β on the infectious population of the deterministic skeleton ($\alpha = 0.9$, $\tau = 2$).

8.10. The total population and the balance law in expectation

Lemma 7 states that $N(t)$ fluctuates around the Mittag-Leffler mean $m(t)$ and is not conserved along paths. **Figure 8** illustrates this with $N(0) = 60$, $\sigma = 0.5$, $\alpha = 0.9$ and $\tau = 2$ ($M = 2{,}000$): individual paths of N wander with a standard deviation that reaches 17 at $t = 100$, whereas the sample mean follows $m(t)$ to within the Monte Carlo error: its deviation from $m(t)$ never exceeds 1.3, for a mean of order 100, and stays within about three standard errors over the whole horizon. This is the balance law in expectation of Section 3 and, at the same time, a check of the scheme's structure preservation (**Proposition 3**).

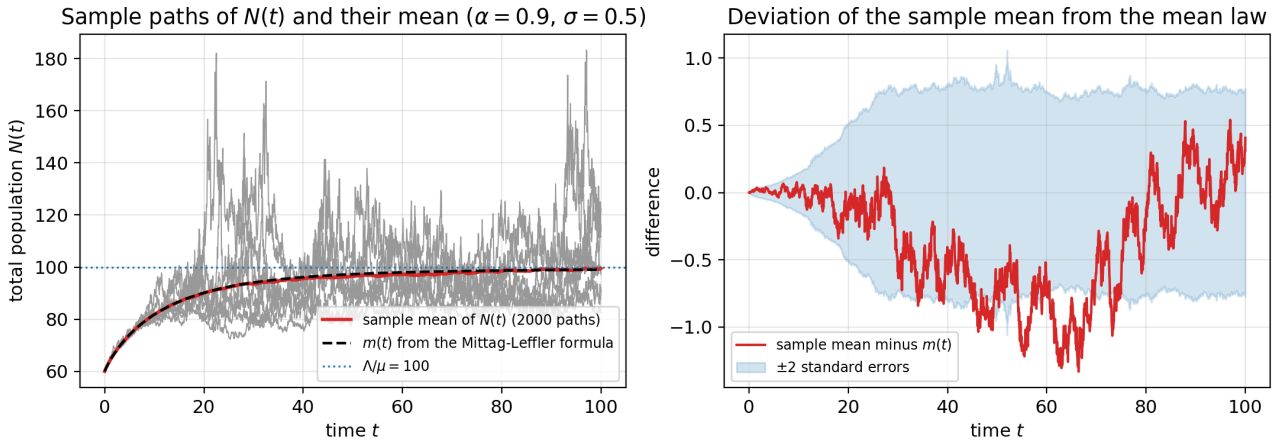


Figure 8. Left: sample paths of the total population $N(t)$, their sample mean over 2,000 paths and the Mittag-Leffler mean $m(t)$ of **Lemma 7** ($\alpha = 0.9$, $\sigma = 0.5$, $\tau = 2$, $N(0) = 60$). Right: deviation of the sample mean from $m(t)$ with a two-standard-error band.

8.11. Noise-induced extinction

To exhibit noise-induced extinction one must work near the persistence threshold, since in the baseline regime ($\beta S_0 = 2$) the extinction exponent of **Theorem 8** stays positive for any moderate σ, and the infection merely fluctuates about $\mathcal{E}^*$. We therefore lower the transmission to $\beta = 0.006$, giving $R_0 = 1.2$, $\beta S_0 = 0.6$ and $I^* = 10/3$, and we set $\alpha = 1$ so that **Theorem 8** applies. For $\tau = 0$ one has $c_0 = \beta S_0 - \gamma = 0.3 \geq 2\mu$, so **(28)** gives the critical intensity

$$\sigma_0^* = \frac{c_0}{\sqrt{2\mu}} = \frac{0.3}{\sqrt{0.2}} \approx 0.671,$$

and $\Theta_0 < 0$ exactly when $\sigma > \sigma_0^*$; for $\tau = 2$ one has $c_2 = 0.6e^{0.2} - 0.3 \approx 0.433$ and $\sigma_2^* \approx 0.968$.

Sample paths. **Figure 9** uses $\tau = 0$ and $\sigma \in \{0.2, 0.5, 0.9\}$ with $M = 2{,}000$ paths and $h = 0.005$. For $\sigma = 0.2$ ($\Theta_0 = 0.18$) the infection persists, the median of I at $t = 100$ being 2.44 against $I^* = 3.33$; for $\sigma = 0.5$ ($\Theta_0 = 0.075$) it persists with much larger fluctuations, the median falling to 0.40 with 1% of the paths already below 10^{-2}; for $\sigma = 0.9 > \sigma_0^*$ ($\Theta_0 = -0.044$) the median is $2.1 \cdot 10^{-3}$ and 58% of the paths have $E + I < 10^{-2}$ at $t = 100$. The mean of I, also shown, stays well above the median in the noisy cases because it is dominated by the few paths that happen to be large: extinction is a pathwise phenomenon and is invisible in the first moment, which is why Theorem 5 and Theorem 8 are statements of a different nature.

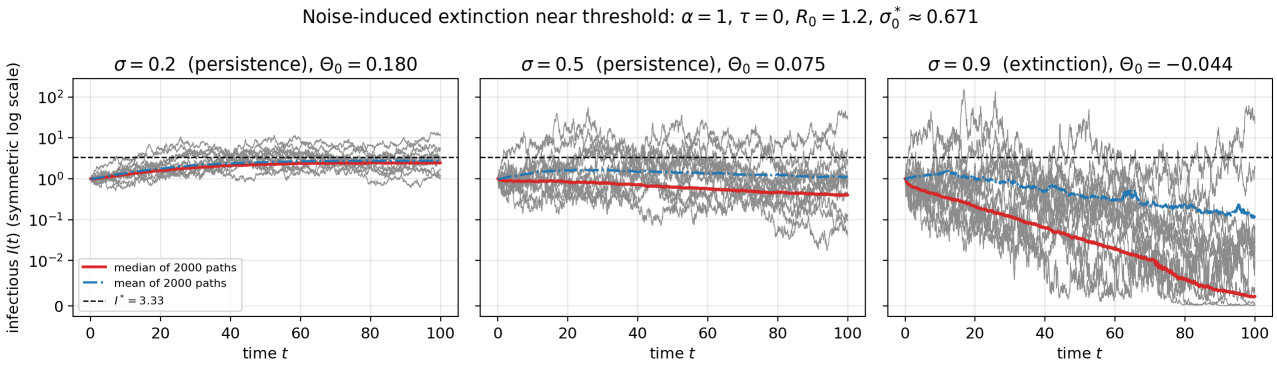


Figure 9. Effect of the noise intensity σ on the infectious population in the near-critical regime ($\alpha = 1$, $\tau = 0$, $R_0 = 1.2$): twelve sample paths, median and mean over 2,000 paths, on a symmetric logarithmic scale. Extinction sets in once σ exceeds the threshold $\sigma_0^* \approx 0.671$ of **Theorem 8**.

Lyapunov exponents. **Theorem 8** bounds the exponential rate of decay of $E + I$. **Figure 10** plots the sample exponents $t^{-1} \ln[(E(t) + I(t))/(E(0) + I(0))]$ up to $t = 1{,}000$ ($M = 1{,}000$ paths, $h = 0.01$) for $\tau = 0$, $\sigma = 0.9$ and for $\tau = 2$, $\sigma = 1.2$, together with the bounds $\Theta_0 = -0.044$ and $\Theta_2 = -0.035$. In both cases the median exponent at $t = 1{,}000$, -0.052 and -0.050 respectively, lies below the bound, and the 5%-95% band narrows like $t^{-1/2}$, as the martingale term $M(t)/t$ of the proof requires; the fraction of paths whose sample exponent still exceeds the bound at $t = 1{,}000$ is 24% and 5%, down from 32% and 18% at $t = 200$, in keeping with the asymptotic nature of the statement. The bound is conservative, as it must be, since it is obtained by maximising the drift of $\ln V$ over all values of the ratio I/V.

Extinction probability across the threshold. **Figure 11 (left)** shows the fraction of paths with $E(T) + I(T) < 10^{-2}$ at $T = 300$ as a function of σ, for $\tau = 0$ and $\tau = 2$ ($M = 2{,}000$ paths, $h = 0.005$). For $\tau = 0$ the fraction rises from 0.3% at $\sigma = 0.4$ to 34% at $\sigma = 0.6$, 68% at $\sigma = 0.7$, 89% at $\sigma = 0.8$ and 99% at $\sigma = 1$: the transition is centred on σ_0^* and is smeared by the finite horizon, since a path with a sample exponent slightly below zero needs a long time to fall below 10^{-2}. For $\tau = 2$ the curve is shifted to the right, the fraction being 45% at $\sigma = 0.8$ and 83% at $\sigma = 1$, but the shift is much smaller than the gap between σ_0^* and σ_2^*: the delay does make extinction slightly harder, because infections seeded before a downward fluctuation keep arriving for one latent period, and the factor $e^{\mu\tau}$ of **Theorem 8** overestimates this effect. The right panel compares, for $\tau = 0$, the median and the mean of $E(T) + I(T)$ at $T = 150$ for $\alpha = 1$ and $\alpha = 0.9$ ($M = 300$ paths and $h = 0.02$ for the fractional runs, $\kappa_h = 0.22$ at $\sigma = 1$): the medians decrease monotonically with σ for both orders, from 5.1 and 5.5 at $\sigma = 0.2$ to $5 \cdot 10^{-4}$ and 0.22 at $\sigma = 0.9$, whereas the means, which are carried by a few large paths, are noisier; the fractional

median exceeds the classical one by a factor that grows from 1.1 at $\sigma = 0.2$ to more than 400 at $\sigma = 0.9$, because the fractional decay is algebraic. The noise therefore suppresses the infection for $\alpha = 0.9$ in the same monotone way as for $\alpha = 1$, but the exponential extinction of **Theorem 8** is replaced by a slower, Mittag-Leffler-type decay; a rigorous threshold for this regime is the open problem stated in **Remark 11**.

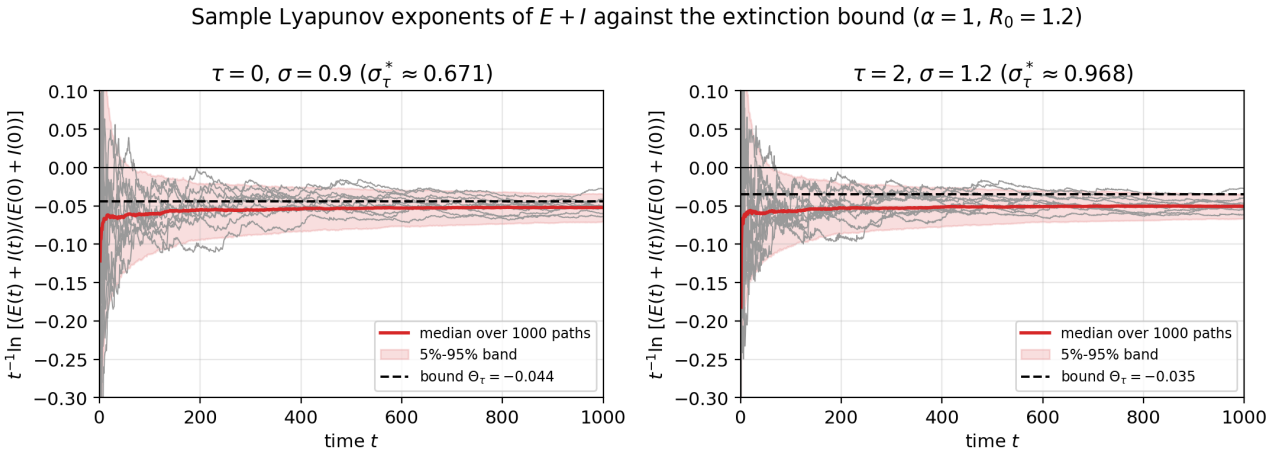


Figure 10. Sample Lyapunov exponents of the infected mass $E + I$ for $\alpha = 1$ and $R_0 = 1.2$: ten paths, median and 5%-95% band over 1,000 paths, and the bound Θ_τ of **Theorem 8**. Left: $\tau = 0$, $\sigma = 0.9$. Right: $\tau = 2$, $\sigma = 1.2$.

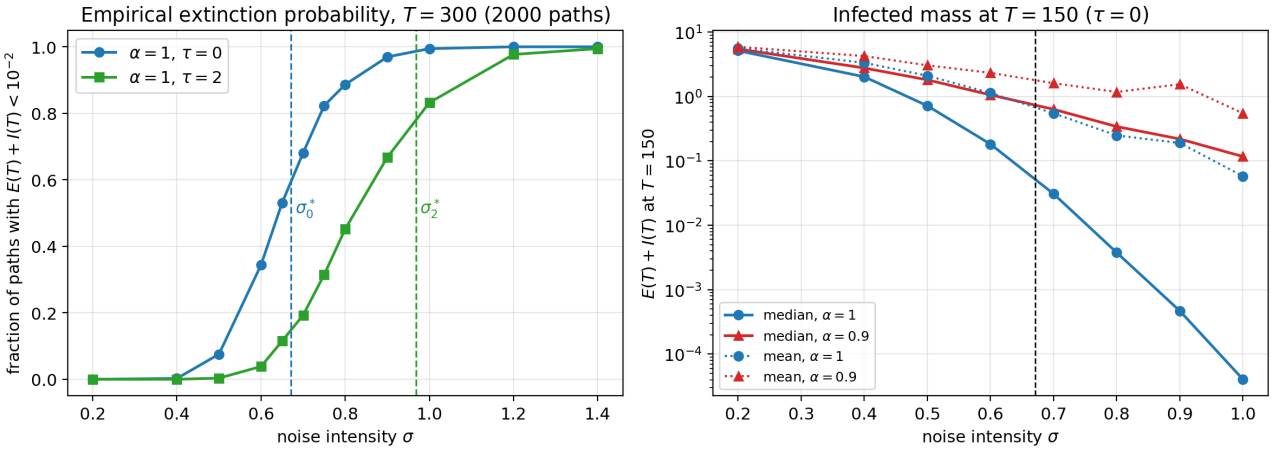


Figure 11. Left: empirical extinction probability at $T = 300$ as a function of σ for $\alpha = 1$ with $\tau = 0$ and $\tau = 2$ (2,000 paths per point); the dashed lines mark σ_0^* and σ_2^*. Right: median and mean of the infected mass $E(T) + I(T)$ at $T = 150$ for $\alpha = 1$ and $\alpha = 0.9$, $\tau = 0$.

Fractional memory near the threshold. **Figure 12** shows twelve paths, the median and the mean of I for $\alpha = 0.9$, $\tau = 0$ and $\sigma \in \{0.5, 0.9\}$ ($M = 300$, $h = 0.02$). The picture is qualitatively the same as in **Figure 9**: for $\sigma = 0.5$ the infection persists with a median of 0.87 at $t = 100$, for $\sigma = 0.9$ the median has fallen to 0.11, but the decay is visibly slower than for $\alpha = 1$ and the paths are smoother, the memory averaging out part of the noise. No path left the cone in either case at this step size, for which the indicator of **Remark 17** is $\kappa_h = 0.20$ at $\sigma = 0.9$; **Table 2** shows what happens when κ_h is allowed to grow.

Excursions out of the cone and mesh refinement. **Remark 17** predicts that negative values of I produced by the explicit scheme become rarer as h decreases, at a rate governed by κ_h. **Table 2** reports, for the near-critical regime with $\tau = 0$, the proportion of 300 paths on $[0, 60]$ in which I becomes negative, for $\alpha \in \{0.9, 0.8, 0.7\}$,

$\sigma \in \{0.5, 0.9\}$ and $h \in \{0.05, 0.02, 0.01\}$, together with κ_h. For $\alpha = 0.9$ and $\sigma = 0.5$ no excursion occurs at any step size ($\kappa_h \le 0.16$); for $\sigma = 0.9$ the proportion is 9.7% at $h = 0.05$ ($\kappa_h = 0.28$) and zero at $h = 0.02$ and $h = 0.01$ ($\kappa_h \le 0.20$). For $\alpha = 0.8$ and $\sigma = 0.9$ the proportion falls from 99% to 61% and 11% as κ_h decreases from 0.39 to 0.30 and 0.24, and for $\alpha = 0.7$ and $\sigma = 0.5$ from 36% to 12% and 2.3% as κ_h decreases from 0.30 to 0.25 and 0.22; the combination $\alpha = 0.7$, $\sigma = 0.9$ keeps $\kappa_h \ge 0.39$ in the range of steps considered and every path leaves the cone, which shows that the rule of **Remark 17** is a necessary one. In every case the proportion of excursions decreases with κ_h for a fixed pair (α, σ), and it tends to zero as $h \to 0$, slowly when α is small; the proportion also depends on the number of steps taken, so that equal values of κ_h do not give identical proportions across different pairs. These observations are the numerical evidence referred to in **Remark 6**: the excursions are a finite-step artefact of the explicit noise treatment, they disappear under refinement, and they never occur in the endemic regime, where I stays away from zero (no exits in 2,000 paths at the baseline parameters for any $\alpha \in \{0.6, \dots, 1\}$ with $\sigma = 0.2$).

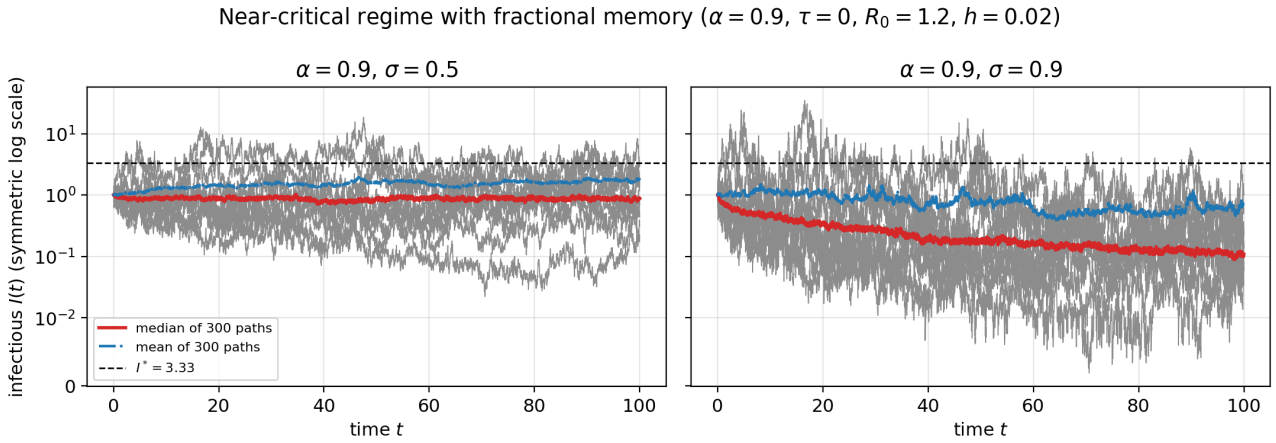


Figure 12. Near-critical regime with fractional memory ($\alpha = 0.9$, $\tau = 0$, $R_0 = 1.2$, $h = 0.02$): twelve sample paths, median and mean of I over 300 paths for $\sigma = 0.5$ (left) and $\sigma = 0.9$ (right), on a symmetric logarithmic scale.

8.12. Impact of the optimal vaccination control

The optimality system couples the forward state equations **(1)** to the backward adjoint equations **(35)**-**(38)** through the characterisation **(40)**. We solve the certainty-equivalent system of the deterministic skeleton by the forward-backward sweep: the state is integrated forward with the current control by the scheme **(41)**-**(42)**; the adjoint is integrated backward from $p(T) = 0$ by the same scheme applied in the reversed time $s = T - t$, in which the right-sided kernel $k(s - t)$ becomes a left-sided one and the advanced argument $p(t + \tau)$ becomes a delayed one with zero history, so that the indicator in **(37)** is implemented automatically; the control is then updated by **(40)** with the relaxation $u \leftarrow 0.8\, u + 0.2\, u_{\text{new}}$, and the sweep is iterated until the maximum change of u falls below 10^{-6}, which takes between 54 and 63 iterations in the cases reported. The horizon is $T = 50$, the step $h = 0.1$, and the weights are $A = 1$, $B = 50$ unless stated otherwise.

Figure 13 contrasts the controlled and uncontrolled infectious trajectories and displays the optimal profile $u^*(t)$. Without control the infectious class peaks at 20.3 and the cumulative infection $\int_0^{50} I\, dt$ is 702; under the optimal policy the peak is 2.4 and the cumulative infection 71, a reduction of about 90%, while the quadratic infection cost falls from 11,555 to 104. The control starts at $u^*(0) = 0.88$, when the susceptible pool and the marginal value p_1 of protecting it are largest, decreases to about 0.3 by $t = 20$, and relaxes to zero over the last latent period before the horizon, where the advanced term of **(37)** is switched off and vaccinating no longer pays. The total cost is $J = 328$, of which 224 is vaccination effort.

Figure 14 shows the adjoint processes and the dependence of the policy on the cost weight. The adjoint p_4 vanishes identically, as **Remark 14** predicts; p_2 and p_3 are large and decreasing; and p_1 is small but positive, its product with S shaping the control. Lowering B to 10 makes vaccination cheap: the control saturates at its upper bound

for the first few time units, the peak of I drops to 1.25 and the cumulative infection to 45, at a total cost $J = 113$. Raising B to 200 makes it expensive: the control starts at 0.60, the peak of I rises to 4.3, the cumulative infection to 112 and the total cost to 851. In every case the shape of the policy is the same, most intense at the outset and tapering towards the horizon.

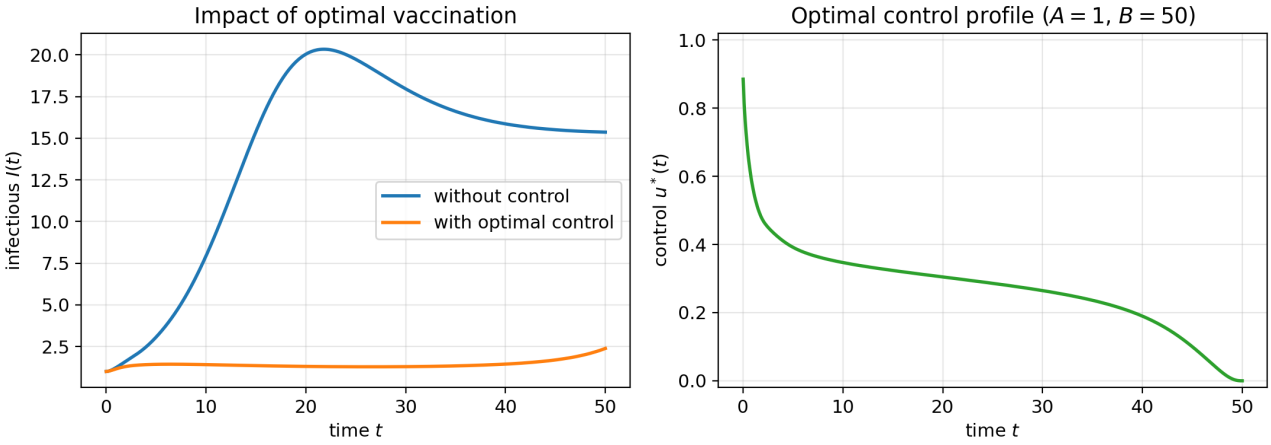


Figure 13. Comparison of infectious trajectories with and without optimal control ($\alpha = 0.9$, $\tau = 2$, $A = 1$, $B = 50$, $T = 50$), together with the optimal control profile

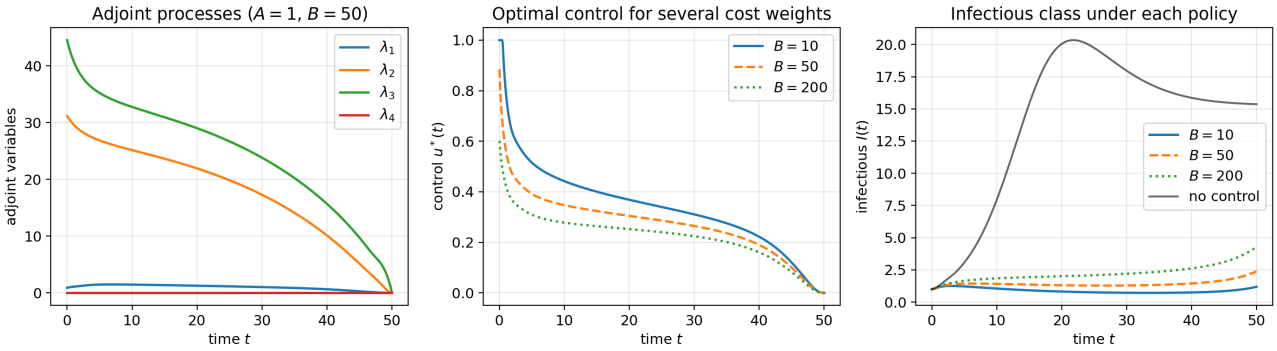


Figure 14. Left: adjoint processes for $A = 1$, $B = 50$. Middle and right: optimal control and controlled infectious class for $B \in \{10, 50, 200\}$, with the uncontrolled trajectory for comparison.

Figure 15 examines the influence of the fractional order on the policy. For $\alpha \in \{0.7, 0.9, 1\}$ the initial control values are similar (0.86, 0.88 and 0.86), but the memory changes the balance of the cost: the optimal total cost is 422, 328 and 288, with infection costs 165, 104 and 80, so that a longer memory makes the infection harder to suppress within the horizon, because the slow Mittag-Leffler relaxation keeps the infectious class from decaying quickly once the control is relaxed. The controlled peaks are 2.85, 2.39 and 2.23.

Finally, **Table 5** evaluates the open-loop policy computed on the skeleton when it is applied to the stochastic model, by averaging the infection cost over $M = 1{,}000$ noisy paths. For $\sigma = 0.2$ the expected infection cost under the policy is 112 against 12,001 without control, and the mean peak of I is 2.8 against 29.6; for $\sigma = 0.5$ the corresponding figures are 174 against 15,066 and 5.1 against 57.2. The policy thus retains more than 98% of its benefit under noise, although the dispersion of the realised cost grows with σ; the expectation in **(40)** would adjust the schedule to this dispersion, and the certainty-equivalent policy is a reliable approximation for the noise levels considered.

8.13. Phase portrait

Figure 16 shows trajectories in the (S, I) plane from several initial conditions. Consistent with **Theorems 7** and **9**, all interior trajectories spiral into the endemic point $(S^*, I^*) = (25, 15)$ without forming a closed orbit; the stochastic path fluctuates in a neighbourhood whose size scales with σ.

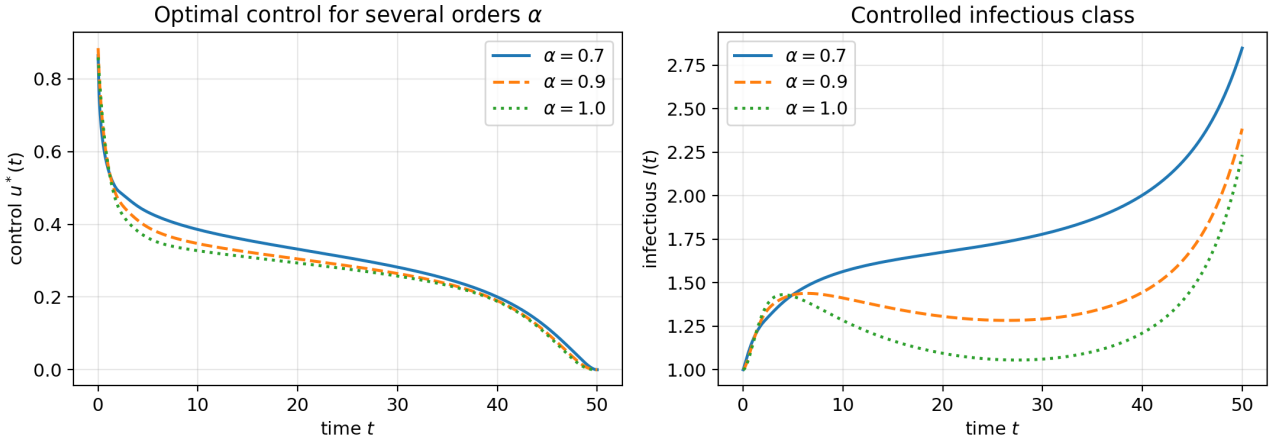


Figure 15. Optimal control (left) and controlled infectious class (right) for $\alpha \in \{0.7, 0.9, 1\}$, with $\tau = 2$, $A = 1$, $B = 50$

Table 5. Performance of the optimal vaccination policy ($A = 1$, $B = 50$, $T = 50$, $\alpha = 0.9$, $\tau = 2$). Infection cost $\int_0^T AI^2 dt$ and peak of I; for $\sigma > 0$ the values are means (and standard deviations of the cost) over 1,000 paths.

	Without control		**With u^***	
	Infection cost	**Peak of I**	**Infection cost**	**Peak of I**
$\sigma = 0$	11,555	20.3	104	2.39
$\sigma = 0.2$	12,001 (2,573)	29.6	112 (60)	2.78
$\sigma = 0.5$	15,066 (11,450)	57.2	174 (404)	5.06

8.14. Sensitivity analysis of R_0

The normalised forward sensitivity index of R_0 with respect to a parameter p is $\Upsilon_p = (\partial R_0/\partial p)(p/R_0) = \partial \ln R_0/\partial \ln p$. Differentiating **(16)** gives the exact indices

$$\Upsilon_\beta = 1, \qquad \Upsilon_\Lambda = 1, \qquad \Upsilon_\kappa = \frac{\mu}{\kappa+\mu},$$
$$\Upsilon_\gamma = -\frac{\gamma}{\gamma+\mu}, \qquad \Upsilon_\mu = -1 - \frac{\mu}{\kappa+\mu} - \frac{\mu}{\gamma+\mu}.$$

Observe that Υ_μ is not simply -1: the mortality rate appears in three places in **(16)**, and the chain rule collects a contribution from each. At the baseline values ($\mu = 0.1$, $\kappa = 0.4$, $\gamma = 0.3$), the indices evaluate to the values listed in **Table 6**.

Table 6. Normalised sensitivity indices of R_0 at the baseline parameters.

Υ_β	Υ_Λ	Υ_κ	Υ_γ	Υ_μ
1	1	0.20	−0.75	−1.45

A unit relative increase in β or Λ raises R_0 by the same relative amount; an increase in the progression rate κ raises it weakly (faster progression to infectiousness), while increases in γ and with μ lower it, μ having the strongest effect because of its threefold appearance. **Figure 17** displays the indices and, alongside, the level sets of R_0 in the (β, γ) plane, where the curve $R_0 = 1$ separates the extinction region from the endemic one: at the baseline recovery rate the critical transmission coefficient is $\beta_c = 0.005$, a fourfold reduction of the baseline value, whereas a recovery rate above $\gamma = 1.5$, five times the baseline value, would be needed to bring the baseline $\beta = 0.02$ below threshold; contact reduction is therefore the more effective lever in this parameter regime, in agreement with the indices.

Remark 18. *The transmission and recruitment rates carry the largest positive elasticities, so interventions that curb contact (lowering β) or, less obviously, that hasten recovery (raising γ) are the most efficient levers on R_0; this is consistent with the strong effect of the optimal vaccination policy seen in **Figure 13**, which acts on the susceptible pool that multiplies β.*

8.15. Summary of the numerical findings

The simulations corroborate the analysis on every point and quantify several of them. The scheme attains the predicted orders, $\min\{2, 1+\alpha\}$ on the delayed model and $\alpha - \frac{1}{2}$ in root mean square for

the noisy model, and it preserves the mean balance law to within Monte Carlo error. The fractional order reshapes transients without moving the equilibrium, lowering and delaying the peak by up to 9% and 25 time units between $\alpha = 1$ and $\alpha = 0.6$, and slowing the relaxation to an algebraic rate. The delay lowers and postpones the peak but never destabilises the endemic equilibrium, exactly as **Theorem 9** predicts. The transmission rate governs the threshold and the endemic burden through R_0, with the peak growing without bound with β while the endemic level saturates at 20. The environmental noise lowers the median infection and, past the explicit threshold σ_τ^*, extinguishes it almost surely for $\alpha = 1$, with sample Lyapunov exponents below the bound of **Theorem 8**; for $\alpha = 0.9$ the suppression is of the same monotone type but slower. Finally, the optimal vaccination policy reduces the peak and the cumulative infection by about 90% at the baseline weights, keeps more than 98% of this benefit when applied to the noisy model, and is most intense at the outset in every case examined.

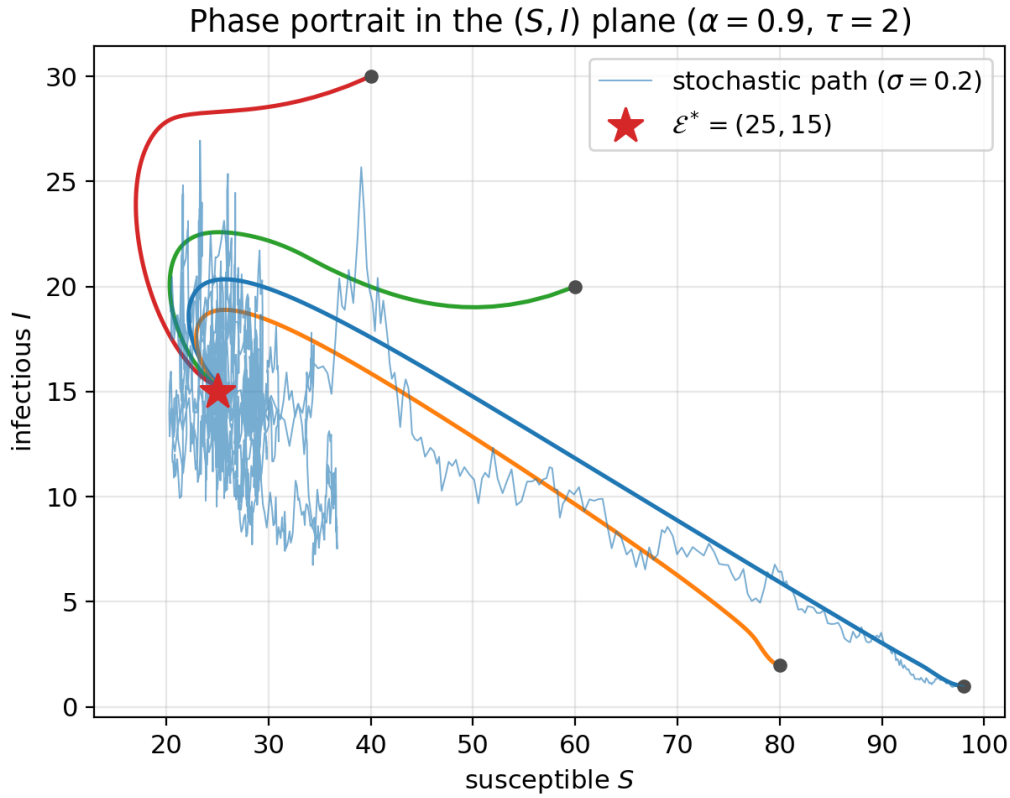


Figure 16. Phase portrait of the epidemic dynamics in the (S, I) plane ($\alpha = 0.9$, $\tau = 2$): four deterministic trajectories and one stochastic path with $\sigma = 0.2$

9. Discussion

This work analysed a Caputo fractional-order SEIR model that simultaneously carries three features rarely treated together with the same care: a latency delay in transmission, multiplicative environmental noise, and a vaccination control. The analytical results and the numerical experiments illuminate each other, and it is worth drawing the two strands together.

Memory and randomness require careful modelling. The stochastic convolution against the singular kernel $(t - s)^{\alpha-1}$ has finite variance only for $\alpha > \frac{1}{2}$, and this single inequality recurs throughout the paper: it underlies the well-posedness of the model (**Theorem 1**), the finiteness of the second moments (**Theorem 3**) and the convergence of the numerical scheme (**Theorem 13**), and its numerical trace is the root-mean-square order $\alpha - \frac{1}{2}$ of **Table 3**, which degrades towards zero as α approaches $\frac{1}{2}$. A related subtlety is that, with the noise placed in the infectious compartment, the total population is itself stochastic, so the demographic balance holds in expectation rather than pathwise; the resolvent representation of **Lemma 7** makes this precise, and **Figure 8** shows individual paths of N drifting by as much as 17 individuals around a mean that follows the Mittag-Leffler law to within Monte Carlo error. A third subtlety concerns positivity: the vanishing of the diffusion

coefficient at $I = 0$ guarantees positivity for the classical order, where the explicit formula **(12)** is available, but not by itself for $\alpha < 1$, where the memory of past increments persists at the boundary. The evidence of **Table 2** is that the negative values observed in simulations are produced by the explicit noise step at finite h and disappear under refinement as the indicator κ_h of **(43)** decreases; the hypothesis (H) is thus well supported, and the step-size rule $\kappa_h \lesssim 0.2$ is a practical guideline for fractional stochastic simulations near extinction.

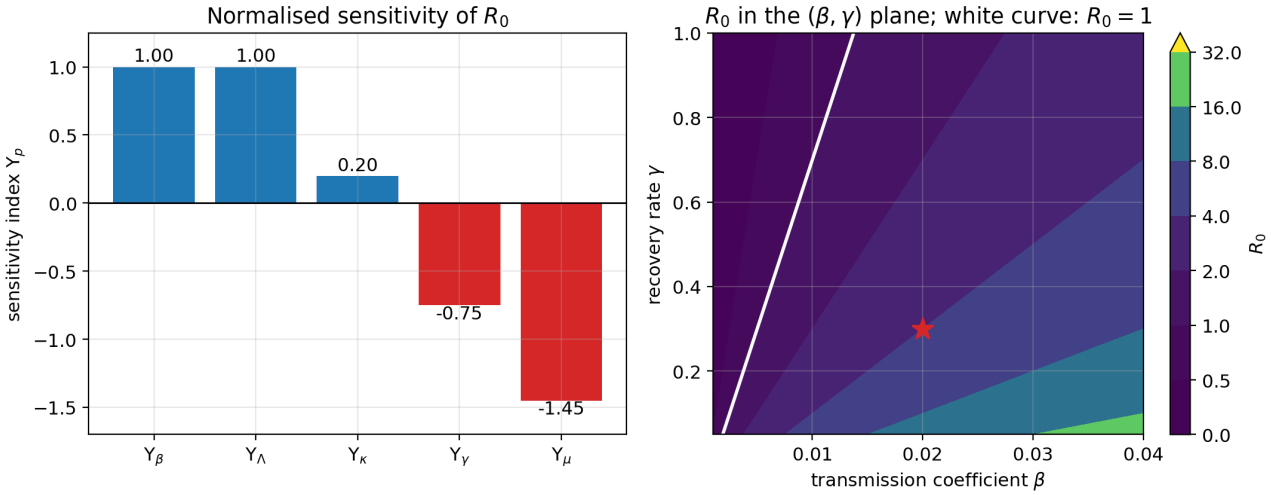


Figure 17. Left: normalised sensitivity indices of R_0 at the baseline parameters. Right: level sets of R_0 in the (β, γ) plane; the white curve is $R_0 = 1$ and the star marks the baseline.

The threshold R_0 organises the mean behaviour. Below unity the infected classes vanish in the mean for every delay, every order and every noise intensity (**Theorem 5**), which for the deterministic skeleton is the global asymptotic stability of the disease-free equilibrium; above unity a unique endemic equilibrium appears and is globally asymptotically stable in the absence of delay (**Theorem 7**). **Figure 7** displays both sides of the threshold, and **Figure 17** shows how far each parameter is from it. The fractional order does not alter these equilibria; it slows the approach to them and converts exponential relaxation into the slower Mittag-Leffler decay, which is visible in **Figure 6** as a peak lowered by up to 9% and delayed by up to 25 time units, and as a residual excess of 1.75 infectious individuals above I^* at $t = 150$ for $\alpha = 0.6$. This is the precise content of the frequently cited "stabilising" role of memory: slower transients and damped overshoots, at the price of a longer approach to the endemic state.

The most instructive outcome is negative. The characteristic quasi-polynomial at the endemic equilibrium satisfies a modulus inequality, $|P| > |Q|$ throughout the closed right half-plane, which rules out imaginary-axis crossings and hence any Hopf bifurcation: the endemic state is locally asymptotically stable for all delays (**Theorem 9**). This is a structural property of an SEIR cascade whose only delay sits in the incidence, and it holds already in the integer-order case. **Figure 2** illustrates it: delays of 2, 5 and 10 time units lower the peak from 22.7 to 20.3, 18.3 and 16.6 and postpone it from $t = 14$ to $t = 22$, 32 and 47, but every transient is damped and the overshoot decreases with the delay. The result cautions against the common expectation that a discrete delay must eventually destabilise an epidemic equilibrium; to obtain oscillations one needs a richer feedback, such as a delayed nonlinear removal term, two delays, waning immunity, or distributed kernels acting on several classes, as in the models cited in **Remark 12**.

Environmental fluctuation is not merely a nuisance. Beyond the explicit intensity σ_τ^* of **Theorem 8** the infection is extinguished almost surely for the classical order, even when the deterministic system would sustain it. The threshold is sharp enough to be used predictively: in the near-critical experiment of **Figure 9** the median infectious population at $t = 100$ drops by three orders of magnitude between $\sigma = 0.2$ and $\sigma = 0.9$, the sample Lyapunov exponents of **Figure 10** settle below the bounds Θ_0 and Θ_2, and the empirical extinction probability of **Figure 11** rises steeply across σ_0^*. The delay makes extinction slightly harder,

because infections seeded before a downward fluctuation keep arriving for one latent period, but the shift observed numerically is much smaller than the factor $e^{\mu\tau}$ of the sufficient condition, which leaves room for a sharper delayed criterion. For the fractional order the noise suppresses the infection in the same monotone fashion, but the decay is algebraic rather than exponential, and the mean threshold of **Theorem 5**, which is independent of σ, is the only rigorous statement currently available; the almost-sure fractional threshold is an open problem whose numerical signature is documented in **Figures 11** and **12**. The two notions of extinction should not be confused: the mean of I in **Figure 9** stays well above the median, because it is carried by a few large paths, so that first-moment statements and pathwise statements answer different questions.

Vaccination is most valuable early. The optimal vaccination problem, treated through a maximum principle whose adjoint is a backward Volterra equation with a time-advanced term, yields a control that is most aggressive at the outset and tapers towards the horizon (**Figure 13**). At the baseline weights the policy reduces the peak of the infectious class from 20.3 to 2.4 and the cumulative infection by about 90%; cheaper vaccination saturates the control at its upper bound for the first time units, dearer vaccination lowers its initial level but not its shape (Figure 14); a longer memory makes the infection harder to suppress within the horizon, the infection cost doubling between $\alpha = 1$ and $\alpha = 0.7$ (**Figure 15**); and the policy computed on the deterministic skeleton keeps more than 98% of its benefit when applied to the noisy model (**Table 5**). Because the diffusion coefficient is control-free, the optimal policy retains the projected linear form **(40)**, which keeps the optimality system tractable by the forward-backward sweep, and the vanishing of the recovered-class adjoint reduces the policy to a function of the susceptible adjoint alone.

The numerical scheme. Compared with the explicit fractional Euler method commonly used for fractional epidemic simulations, the predictor-corrector scheme raises the deterministic order from α to $\min\{2, 1+\alpha\}$ at the cost of one additional drift evaluation per step, and **Table 3** shows that this order is attained on the delayed problem in spite of the breaking point at $t = \tau$; the nonnegativity of its weights makes it a discrete comparison scheme that preserves the balance law in expectation (**Proposition 3**); the treatment of the stochastic convolution by subinterval averages of the kernel gives the root-mean-square order $\alpha - \frac{1}{2}$ established for Euler-Maruyama-type schemes in;[21,23] and the reversed-time implementation of the adjoint reuses the same weights for the optimality system. Its limitations are the quadratic cost in the number of steps, which is inherent to the memory integral and restricts the number of Monte Carlo paths for small h, and the loss of positivity at finite step size discussed above, which an implicit or positivity-preserving treatment of the noise term would remove.

Several limitations frame these results and suggest extensions. The model uses a single discrete delay and mass-action incidence; saturating or behaviour-dependent incidence, distributed delays, and the noise-in-transmission formulation that preserves the population balance are all worth analysing, and the last two may restore oscillatory regimes. The stochastic stability statements are either in the mean or, for the almost-sure threshold, restricted to the classical order; an almost-sure and a mean-square analysis in the fractional setting, where no elementary Itô formula is available, remain open, as does the proof of the positivity hypothesis (H). The optimal control is computed in its certainty-equivalent form, and an implementation of the stochastic adjoint **(39)** would quantify the value of accounting for the noise in the schedule. Moreover, the parameters here are illustrative rather than fitted; calibrating the model to incidence data, with identifiability of α, σ and τ, is the necessary next step before the control conclusions can guide policy.

10. Conclusion

This paper has developed and analysed a Caputo fractional-order SEIR model that brings together, within a single framework, three features that most often appear in isolation; hereditary memory through the fractional derivative, environmental randomness through a multiplicative noise on the infectious class, and a latent period through a discrete delay in transmission, while also admitting a vaccination control. Rather than treat these ingredients as cosmetic additions, each has been followed to its analytical consequences, and the picture that emerges is coherent and, in places, contrary to the expectations that the separate literatures might suggest.

The mathematical core of the work is a set of statements that hold together. The model is well posed when the fractional order exceeds one half, the same inequality that gives the stochastic memory integral a finite variance and that governs the convergence of the numerical scheme; below it the model is not merely difficult but ill posed. Global

existence follows from the delayed structure, which makes every equation linear on each latent window, and the total population admits a Mittag-Leffler resolvent representation from which the balance law in expectation and the second-moment bounds follow. The basic reproduction number organises the mean behaviour: extinction of the infected classes in the mean when $R_0 < 1$, for every delay, order and noise intensity (under the positivity hypothesis when $\alpha < 1$), and a unique endemic equilibrium when $R_0 > 1$, globally attracting without delay. The delay, which one might expect to destabilise that endemic state, does not: the endemic equilibrium is locally asymptotically stable for every delay, so latency alone cannot produce a Hopf bifurcation in this structure. Randomness, by contrast, is far from inert: for the classical order, beyond an explicit threshold on its intensity that depends on the delay, it extinguishes the infection almost surely at an exponential rate, even in regimes where the deterministic model would sustain it. Against this backdrop the optimal vaccination policy, characterised through a maximum principle whose adjoint is a backward Volterra equation with a time-advanced term, is most aggressive early in the outbreak and relaxes as the horizon approaches.

The computations quantify these statements. The fractional predictor-corrector scheme attains the order $\min\{2, 1+\alpha\}$ on the delayed model, with observed orders between 1.6 and 2.1 for α between 0.6 and 1, and the root-mean-square order $\alpha - \frac{1}{2}$ on the noisy model, and it preserves the mean balance law to within Monte Carlo error. Lowering the order from 1 to 0.6 lowers the epidemic peak by 9% and delays it by 25 time units without changing the endemic level; increasing the delay from 0 to 10 lowers the peak from 22.7 to 16.6 and postpones it from $t = 14$ to $t = 47$ without producing oscillations. In the near-critical regime $R_0 = 1.2$ the median infectious population at $t = 100$ falls by three orders of magnitude as the noise intensity increases from 0.2 to 0.9 across the threshold $\sigma_0^* \approx 0.67$, the sample Lyapunov exponents settle below the analytical bounds, and the empirical extinction probability rises steeply across the threshold, with a modest shift to the right when the delay is present. The optimal vaccination policy reduces the peak of the infectious class from 20.3 to 2.4 and the cumulative infection by about 90% at the baseline weights, and it retains more than 98% of this benefit when applied to the stochastic model with noise intensities up to 0.5.

Relative to the schemes commonly used for fractional epidemic simulations, the predictor-corrector method offers one order more accuracy than the fractional Euler method for one additional drift evaluation per step, handles the delay and the breaking point at $t = \tau$ without loss of order, treats the stochastic convolution with the optimal Euler-Maruyama rate, preserves the balance law through the nonnegativity of its weights, and solves the adjoint system with the same weights in reversed time. Its costs are the quadratic memory and the need to keep the step-size indicator κ_h of **Remark 17** small near extinction, where the explicit noise step can produce negative values that disappear under refinement.

Beyond the specific model, the contribution to be emphasised is methodological. The treatment clarifies four points at which intuition or earlier practice can mislead: the well-posedness threshold that the noise places on the fractional order; the fate of the total population once that noise is confined to a single compartment, where boundedness survives only in the mean; the question of whether a transmission delay must be destabilising, which here it is not; and the distinction between extinction in the mean, which is independent of the noise, and almost-sure extinction, which the noise promotes. Several avenues invite further study: saturating or behaviour-dependent incidence, distributed rather than discrete delays, and the population-conserving placement of noise in the transmission rate would each enrich the dynamics and might, unlike the present model, admit oscillatory regimes; a proof of positivity for the noisy compartment when $\alpha < 1$, and almost-sure and mean-square stability theories in the fractional setting, remain open; the stochastic adjoint could be implemented to assess the value of noise-aware vaccination schedules; and the calibration of the model, with identifiable fractional order, noise intensity and delay, to incidence data is the natural next step toward fractional stochastic epidemic models that are at once realistic and analytically secure.

Acknowledgments

The author extends the appreciation to the Deanship of Postgraduate Studies and Scientific Research at Majmaah University for funding this research work through the project number (R-2026-521).

Fundings

The author extends the appreciation to the Deanship of Postgraduate Studies and Scientific Research at Majmaah University for funding this research work through the project number (R-2026-521).

Conflict of interest

The authors declare they have no competing interests.

Author contributions

This is a single authored article.

Availability of data

None.

AI tools statement

Author confirms that no AI tools were used in the preparation of this manuscript.

References

1. Podlubny I. *Fractional Differential Equations*. San Diego: Academic Press; 1999.
2. Kilbas AA, Srivastava HM, Trujillo JJ. *Theory and Applications of Fractional Differential Equations*. Amsterdam: Elsevier; 2006.
3. Diethelm K. *The Analysis of Fractional Differential Equations*. Lecture Notes in Mathematics, Vol 2004. Berlin: Springer; 2010. https://doi.org/10.1007/978-3-642-14574-2
4. Diethelm K. A fractional calculus based model for the simulation of an outbreak of dengue fever. *Nonlinear Dyn.* 2013;71(4):613-619. https://doi.org/10.1007/s11071-012-0475-2
5. Almeida R. Analysis of a fractional SEIR model with treatment. *Appl Math Lett.* 2018;84:56-62. https://doi.org/10.1016/j.aml.2018.04.015
6. Rihan FA, Al-Mdallal QM, AlSakaji HJ, Hashish A. A fractional-order epidemic model with time-delay and nonlinear incidence rate. *Chaos Solitons Fractals.* 2019;126:97-105. https://doi.org/10.1016/j.chaos.2019.05.039
7. Naik PA, Zu J, Owolabi KM. Global dynamics of a fractional order model for the transmission of HIV epidemic with optimal control. *Chaos Solitons Fractals.* 2020;138:109826. https://doi.org/10.1016/j.chaos.2020.109826
8. Gacem I, Kouche M, Ainseba B. Stability analysis of a fractional-order SEIR epidemic model with general incidence rate and time delay. *Math Methods Appl Sci.* 2023;46(9):10947-10969. https://doi.org/10.1002/mma.9161
9. Xu S, Hu Y. Dynamic analysis of a Caputo fractional-order SEIR model with a general incidence rate. *Sci Rep.* 2025;15:17561. https://doi.org/10.1038/s41598-025-01400-9
10. Suganya S, Parthiban V, Shangerganesh L, Hariharan S. Transmission dynamics of fractional order SVEIR model for African swine fever virus with optimal control analysis. *Sci Rep.* 2024;14:27185. https://doi.org/10.1038/s41598-024-78140-9
11. Zhang J, Xue Y, Hu G. Analysis of fractional order SVEIR infectious disease model with fear effect and secondary vaccination. *Nonlinear Dyn.* 2025;113(24):34047-34065. https://doi.org/10.1007/s11071-025-11752-6
12. El Bechir AJ, Elemine Vall MS, Mohamed Y. Optimal control and stability investigation of a fractional SEIJR approach with a generalized nonlinear transmission rate. *J Appl Math Comput.* 2026;72(1):19. https://doi.org/10.1007/s12190-025-02669-9
13. Yazhini M, Samidurai R, Shang Y. Event-triggered synchronization of fractional-order complex-valued BAM neural networks with application to image encryption. *Chaos Solitons Fractals.* 2026;203:117666. https://doi.org/10.1016/j.chaos.2025.117666
14. Allen LJS. An introduction to stochastic epidemic models. In: Brauer F, van den Driessche P, Wu J, eds. *Mathematical Epidemiology*. Lecture Notes in Mathematics, Vol 1945. Berlin: Springer; 2008:81-130. https://doi.org/10.1007/978-3-540-78911-6_3
15. Mao X. *Stochastic Differential Equations and Applications*. 2nd ed. Chichester: Horwood Publishing; 2007.
16. Gray A, Greenhalgh D, Hu L, Mao X, Pan J. A stochastic differential equation SIS epidemic model. *SIAM J Appl Math.* 2011;71(3):876-902. https://doi.org/10.1137/10081856X
17. Liu Q, Jiang D, Shi N, Hayat T, Ahmad B. Stationary distribution and extinction of a stochastic SEIR epidemic model with standard incidence. *Physica A.* 2017;476:58-69. https://doi.org/10.1016/j.physa.2017.02.028
18. Sakthivel R, Revathi P, Ren Y. Existence of solutions for nonlinear fractional stochastic differential equations. *Nonlinear Anal.* 2013;81:70-86. https://doi.org/10.1016/j.na.2012.10.009
19. Anh PT, Doan TS, Huong PT. A variation of constant formula for Caputo fractional stochastic differential equations. *Stat Probab Lett.* 2019;145:351-358. https://doi.org/10.1016/j.spl.2018.10.010
20. Son DT, Huong PT, Kloeden PE, Tuan HT. Asymptotic separation between solutions of Caputo

fractional stochastic differential equations. *Stoch Anal Appl.* 2018;36(4):654-664. https://doi.org/10.1080/07362994.2018.1440243

21. Doan TS, Huong PT, Kloeden PE, Vu AM. Euler-Maruyama scheme for Caputo stochastic fractional differential equations. *J Comput Appl Math.* 2020;380:112989. https://doi.org/10.1016/j.cam.2020.112989

22. Huong PT, The NT. Well-posedness and regularity for solutions of Caputo stochastic fractional delay differential equations. *Stat Probab Lett.* 2023;195:109768. https://doi.org/10.1016/j.spl.2022.109768

23. Huong PT. Euler-Maruyama schemes for Caputo stochastic fractional delay differential equations. *Random Oper Stoch Equ.* 2025;33(2):223-234. https://doi.org/10.1515/rose-2025-2013

24. Sabbar Y, Din A, Kiouach D. Influence of fractal-fractional differentiation and independent quadratic Lévy jumps on the dynamics of a general epidemic model with vaccination strategy. *Chaos Solitons Fractals.* 2023;171:113434. https://doi.org/10.1016/j.chaos.2023.113434

25. Ren G, Yu Y, Xu W, Li F, Wu J. A fractional stochastic SPEIQR epidemic model in switching network for COVID-19. *Chin J Phys.* 2024;89:290-301. https://doi.org/10.1016/j.cjph.2024.03.001

26. Tamimi H, Saadati R, Ghaemi MB. Application of nonlinear stochastic fractional systems in the generalized SEIR model. *Chaos.* 2025;35(8):083109. https://doi.org/10.1063/5.0279918

27. Kuang Y. *Delay Differential Equations with Applications in Population Dynamics*. Boston: Academic Press; 1993.

28. Ruan S. Delay differential equations in single species dynamics. In: Arino O, Hbid ML, Ait Dads E, eds. *Delay Differential Equations and Applications*. NATO Science Series II, Vol 205. Dordrecht: Springer; 2006:477-517. https://doi.org/10.1007/1-4020-3647-7_11

29. Rihan FA. *Delay Differential Equations and Applications to Biology*. Singapore: Springer; 2021. https://doi.org/10.1007/978-981-16-0626-7

30. Matignon D. Stability results for fractional differential equations with applications to control processing. In: *Computational Engineering in Systems Applications*. Vol 2. Lille: IMACS/IEEE-SMC; 1996:963-968.

31. Deng W, Li C, Lü J. Stability analysis of linear fractional differential system with multiple time delays. *Nonlinear Dyn.* 2007;48(4):409-416. https://doi.org/10.1007/s11071-006-9094-0

32. Cooke KL, van den Driessche P. Analysis of an SEIRS epidemic model with two delays. *J Math Biol.* 1996;35(2):240-260. https://doi.org/10.1007/s002850050051

33. Huang C, Cao J, Xiao M, Alsaedi A, Hayat T. Bifurcations in a delayed fractional complex-valued neural network. *Appl Math Comput.* 2017;292:210-227. https://doi.org/10.1016/j.amc.2016.07.029

34. Majee S, Jana S, Kar TK, Bhunia B. Complex dynamics of a fractional-order delayed epidemic model incorporating waning immunity and optimal control. *Eur Phys J Spec Top.* 2025;234(8):1823-1850. https://doi.org/10.1140/epjs/s11734-024-01221-3

35. Madhusudanan V, Naik PA, Murthy BSN, Guerrini L, Srinivas MN, Chada L. Modeling tuberculosis transmission with kernel functions: effects of vaccination and time delay. *Eur Phys J Plus.* 2026;141(1):76. https://doi.org/10.1140/epjp/s13360-026-07309-0

36. Kheiri H, Jafari M. Optimal control of a fractional-order model for the HIV/AIDS epidemic. *Int J Biomath.* 2018;11(7):1850086. https://doi.org/10.1142/S1793524518500869

37. Sweilam NH, AL-Mekhlafi SM, Baleanu D. Optimal control for a fractional tuberculosis infection model including the impact of diabetes and resistant strains. *J Adv Res.* 2019;17:125-137. https://doi.org/10.1016/j.jare.2019.01.007

38. Agrawal OP. A general formulation and solution scheme for fractional optimal control problems. *Nonlinear Dyn.* 2004;38(1-4):323-337. https://doi.org/10.1007/s11071-004-3764-6

39. Jarad F, Abdeljawad T, Baleanu D. Fractional variational optimal control problems with delayed arguments. *Nonlinear Dyn.* 2010;62(3):609-614. https://doi.org/10.1007/s11071-010-9748-9

40. Peng S. A general stochastic maximum principle for optimal control problems. *SIAM J Control Optim.* 1990;28(4):966-979. https://doi.org/10.1137/0328054

41. Yong J, Zhou XY. *Stochastic Controls: Hamiltonian Systems and HJB Equations*. New York: Springer; 1999. https://doi.org/10.1007/978-1-4612-1466-3

42. Chen L, Wu Z. Maximum principle for the stochastic optimal control problem with delay and application. *Automatica.* 2010;46(6):1074-1080. https://doi.org/10.1016/j.automatica.2010.03.005

43. Øksendal B, Sulem A, Zhang T. Optimal control of stochastic delay equations and time-advanced backward stochastic differential equations. *Adv*

Appl Probab. 2011;43(2):572-596.
https://doi.org/10.1239/aap/1308662493

44. Yong J. Backward stochastic Volterra integral equations and some related problems. *Stoch Process Appl.* 2006;116(5):779-795.
https://doi.org/10.1016/j.spa.2006.01.005

45. Yong J. Well-posedness and regularity of backward stochastic Volterra integral equations. *Probab Theory Relat Fields.* 2008;142(1-2):21-77.
https://doi.org/10.1007/s00440-007-0098-6

46. Agram N, Øksendal B. Malliavin calculus and optimal control of stochastic Volterra equations. *J Optim Theory Appl.* 2015;167(3):1070-1094.
https://doi.org/10.1007/s10957-015-0753-5

47. Wang T. Linear quadratic control problems of stochastic Volterra integral equations. *ESAIM Control Optim Calc Var.* 2018;24(4):1849-1879.
https://doi.org/10.1051/cocv/2017002

48. Hamaguchi Y. On the maximum principle for optimal control problems of stochastic Volterra integral equations with delay. *Appl Math Optim.* 2023;87(3):42.
https://doi.org/10.1007/s00245-022-09958-w

49. Hamaguchi Y. Global maximum principle for optimal control of stochastic Volterra equations with singular kernels: an infinite dimensional approach. *J Differ Equ.* 2025;446:113618.
https://doi.org/10.1016/j.jde.2025.113618

50. Diethelm K, Ford NJ, Freed AD. A predictor-corrector approach for the numerical solution of fractional differential equations. *Nonlinear Dyn.* 2002;29(1):3-22.
https://doi.org/10.1023/A:1016592219341

51. Diethelm K, Ford NJ, Freed AD. Detailed error analysis for a fractional Adams method. *Numer Algorithms.* 2004;36(1):31-52.
https://doi.org/10.1023/B:NUMA.0000027736.85078.be

52. Bhalekar S, Daftardar-Gejji V. A predictor-corrector scheme for solving nonlinear delay differential equations of fractional order. *J Fract Calc Appl.* 2011;1(5):1-9.

53. Li C, Zeng F. *Numerical Methods for Fractional Calculus.* Boca Raton: CRC Press; 2015.
https://doi.org/10.1201/b18503

54. Shang Y. A Lie algebra approach to susceptible-infected-susceptible epidemics. *Electron J Differ Equ.* 2012;2012(233):1-7.

55. Shang Y. Lie algebra method for solving biological population model. *J Theor Appl Phys.* 2013;7(1):67.
https://doi.org/10.1186/2251-7235-7-67

56. Shang Y. Analytical solution for an in-host viral infection model with time-inhomogeneous rates. *Acta Phys Pol B.* 2015;46(8):1567-1577.
https://doi.org/10.5506/APhysPolB.46.1567

57. Shang Y. Lie algebraic discussion for affinity based information diffusion in social networks. *Open Phys.* 2017;15(1):705-711.
https://doi.org/10.1515/phys-2017-0083

58. Odibat ZM, Shawagfeh NT. Generalized Taylor's formula. *Appl Math Comput.* 2007;186(1):286-293.
https://doi.org/10.1016/j.amc.2006.07.102

59. Kaczorek T. *Selected Problems of Fractional Systems Theory.* Lecture Notes in Control and Information Sciences, Vol 411. Berlin: Springer; 2011.
https://doi.org/10.1007/978-3-642-20502-6

60. Abi Jaber E, Larsson M, Pulido S. Affine Volterra processes. *Ann Appl Probab.* 2019;29(5):3155-3200.
https://doi.org/10.1214/19-AAP1477

61. van den Driessche P, Watmough J. Reproduction numbers and sub-threshold endemic equilibria for compartmental models of disease transmission. *Math Biosci.* 2002;180(1-2):29-48.
https://doi.org/10.1016/S0025-5564(02)00108-6

62. Vargas-De-León C. Volterra-type Lyapunov functions for fractional-order epidemic systems. *Commun Nonlinear Sci Numer Simul.* 2015;24(1-3):75-85.
https://doi.org/10.1016/j.cnsns.2014.12.013

63. Aguila-Camacho N, Duarte-Mermoud MA, Gallegos JA. Lyapunov functions for fractional order systems. *Commun Nonlinear Sci Numer Simul.* 2014;19(9):2951-2957.
https://doi.org/10.1016/j.cnsns.2014.01.022

64. Huo J, Zhao H, Zhu L. The effect of vaccines on backward bifurcation in a fractional order HIV model. *Nonlinear Anal Real World Appl.* 2015;26:289-305.
https://doi.org/10.1016/j.nonrwa.2015.05.014

65. Gallegos JA, Duarte-Mermoud MA. On the Lyapunov theory for fractional order systems. *Appl Math Comput.* 2016;287-288:161-170.
https://doi.org/10.1016/j.amc.2016.04.039

66. Beretta E, Kuang Y. Geometric stability switch criteria in delay differential systems with delay dependent parameters. *SIAM J Math Anal.* 2002;33(5):1144-1165.
https://doi.org/10.1137/S0036141000376086

Jameelah Alotaibi *is an Assistant Professor in the Department of Mathematics, College of Science, Majmaah University, Saudi Arabia. Her research interests include applied mathematics, fractional differential equations, mathematical modeling, stochastic systems, and stability analysis.*
https://orcid.org/0009-0003-6600-1073

An International Journal of Optimization and Control: Theories & Applications (https://accscience.com/journal/ijocta)



This work is licensed under a Creative Commons Attribution 4.0 International License. The authors retain ownership of the copyright for their article, but they allow anyone to download, reuse, reprint, modify, distribute, and/or copy articles in IJOCTA, so long as the original authors and source are credited. To see the complete license contents, please visit http://creativecommons.org/licenses/by/4.0/.